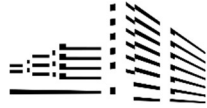




UNIVERSITAT
POLITÈCNICA
DE VALÈNCIA



IIS La Fe



*The use of human induced
pluripotent stem cell-derived atrial
cardiomyocytes for studying
arrhythmia mechanisms*

PhD in Technologies for Health and Well-Being

Author: Marilù Casini

Supervisors: Pilar Sepulveda Sanchis and Imelda Ontoria Oviedo

Tutor: Andreu Martínez Climent

January 2024

“Don’t be a drag. Just be a queen.”

Lady Gaga

Acknowledgements

*Thanks to the researchers I had the pleasure to meet during this long path,
those who taught me the beauty and the sadness of science,
those who showed their humanity without any fear,
those who believed in me when I didn't.*

*Thanks to the scientific pioneers who dedicate to more inclusive research,
those who were not afraid to speak up for themselves and others,
those who had the audacity of being open and fight,
those who opened the doors for people like me.*

*Thanks to my biological and chosen families for their continuous support,
no words can describe how sincerely grateful I am.*

*Thanks to my virtual community of science passionate and PhDisagiati,
for giving me the reason of believing in a more inclusive science.*

Thanks.

Index

Abbreviations.....	10
Summary.....	13
Resumen.....	14
Resum.....	15
Introduction	17
1.1 Background on PersonalizeAF project	18
1.2 Atrial fibrillation	21
1.2.1 Clinical aspects of atrial fibrillation	21
1.2.2 Atrial remodeling	26
1.2.2.1 Electrophysiological remodeling.....	27
1.2.2.2 Structural remodeling	29
1.2.2.3 Immune remodeling	33
1.2.3 Therapies for AF	35
1.2.3.1 Antiarrhythmic drugs.....	36
1.2.3.2 Catheter ablation.....	38
1.2.4 Experimental models to study AF	38
1.3 hiPSC in cardiac research.....	41
1.3.1 Types of stem cells.....	41
1.3.2 Human induced pluripotent stem cells discovery.....	44
1.3.3 hiPSC reprogramming.....	45
1.3.4 hiPSC differentiation into cardiomyocytes.....	47
1.3.5 Subtypes specific differentiations of hiPSC	51
1.3.6 hiPSC for arrhythmia studies	53

1.4	Cardiac optogenetics	56
1.4.1	Optogenetic actuators in cardiac research	57
1.4.2	Applications in arrhythmia studies.....	60
1.5	Summary and Outlook	63
	Hypothesis	68
	Aims	70
	Material and methods	73
3.1	Cell culture	74
3.1.1	Selection of hiPSC lines.....	74
3.1.2	hiPSC maintaining	75
3.1.3	hiPSC subtype differentiation	77
3.1.4	hiPSC-CM disaggregation	81
3.2	Analysis of cardiac markers	83
3.2.1	RNA extraction and retro transcription	83
3.2.2	Real-time quantitative polymerase chain reaction.....	84
3.2.3	Flow cytometry	87
3.2.4	Immunostaining	88
3.2.5	Transfection of hiPSC-aCM.....	88
3.3	Electrophysiological and mechanical analysis	90
3.3.2	Patch Clamp for action potential recordings	90
3.3.3	Sharp electrode for optogenetics experiments	91
3.3.4	Nanoindentation for mechanical studies.....	92
3.3.5	Optical mapping experiments	94
3.3.6	Optical contraction measurements.....	96
3.4	RNA-seq	97

3.5	Statistical analysis.....	98
	Results	101
4.1	Characterization of hiPSC differentiation.....	102
4.2	Characterization of hiPSC-vCM and hiPSC-aCM	108
4.2.1	Molecular characterization of hiPSC-vCM and hiPSC-aCM	108
4.2.2	Functional characterization of hiPSC-vCM and hiPSC-aCM	112
4.2.3	Mechanical characterization of hiPSC-vCM and hiPSC-aCM....	115
4.3	hiPSC-aCM as <i>in-vitro</i> model of AF	118
4.3.1	Spontaneous in-vitro atrial fibrillation in hiPSC-aCM.....	118
4.3.2	hiPSC-aCM in fibrillation undergo gene expression changes....	122
4.4	Perturbation of AP with optogenetics	130
4.4.1	HcCKR1 and HcKCR2 alter AP properties of hiPSC-aCM.....	130
4.4.2	WiChR efficiently inhibits the activity of hiPSC-aCM	136
	Discussion	141
5.1	hiPSC as a valuable model for atrial cells.....	142
5.1.1	Comparison of hiPSC-aCM differentiatiton protocols.....	142
5.1.2	Comparison of hiPSC-aCM with adult atrial cardiomyocytes	145
5.2	hiPSC-aCM recapitulate basic AF mechanisms	149
5.3	Comparison with other AF models	156
5.4	Optogenetic to study arrhythmia mechanisms.....	159
	Conclusions	166
	Limitations and future prospectives	167
	Contributions	170
	Trainings.....	172
	Secondments.....	173

Abbreviations

AAD : Antiarrhythmic drugs

AF : atrial fibrillation

Ang II : Angiotensin II

AP : action potential

APD : Action potential duration

ArchT : Halobrum sp TP009

AT1-R : Type 1 angiotensin receptor

ATRA : All-trans retinoic acid

CACNA1 : Calcium Voltage-Gated Channel Subunit Alpha 1 A

CaMKII : Calmodulin-dependent protein kinase type II

CDH1 : E-cadherin

ChR : Channelrhodopsin

ChR2 : Channelrhodopsin 2

CTGF : Connective tissue growth factor

CXCL12 : CXC Chemokine 12

CXCL8 : CXC Chemokine 8

Cxs : Connexins

DADs : delayed afterdepolarization

EADs : early afterdepolarization

EB : Embryonic bodies

ECM : Extracellular matrix

ESC : Embryonic stem cells

GJA1 : Gap Junction Protein Alpha 1

HcKCR1 : Kalium channelrhodopsin 1 from *Hyphochytrium catenoides*

HcKCR2: Kalium channelrhodopsin 2 from *Hyphochytrium catenoides*

HEY2 : Hairy/enhancer-of-split related with YRPW motif protein 2

hiPSC : Human induced pluripotent stem cells

hiPSC-aCM : Human induced pluripotent stem cell-derived atrial cardiomyocytes

hiPSC-CM : Human induced pluripotent stem cell-derived cardiomyocytes

ICAM : Intercellular Adhesion Molecule 1

ICa,L : L-type Ca²⁺ current

IK1 : Inward-rectifier K⁺ current

IL1 : Interleukine 1

IL11 : Interleukine 11

IL6 : Inteleukine 6

IL16 : Interleukine 16

IL18 : Interleukine 18

iPSC : Hnduced pluripotent stem cells

IRX4 : Iroquois homebox 4

IWP2 : Inhibitor of WNT production-2

IWP4 : Inhibitor of WNT production-4

KCNA5 : Potassium voltage-gated channel subfamily A member 5

KCNJ3 : Potassium inwardly rectifying channel subfamily J member 3

KCR : K⁺-selective channel

MAPK : Mitogen-activated protein kinase

MIF : Macrophage migration inhibitory factor

MMP1 : Metalloproteinase 1

MMPs : Metalloproteinases

MYH7 : Myosin heavy chain 7

MYL2 : Myosing light chain 2

MYL4 : Myosin light chain 4

MYL7 : Myosin light chain 7

NKX2-5 : NK2 transcription factor related locus 5

NpHR : Natronomonas pharaonis

NPPA : natriuretic peptide A

NR2F1 : Nuclear receptor subfamily 2 group F member 1

NR2F1 : Nuclear receptor subfamily 2 group F member 2

OCT4 : Octamer-binding transcription factor 4

PAC : Photoactivated adenylyl cyclase

PDGF- α : Platelet-derived growth factor

PKC : Protein kinase C

RMP : Resting membrane potential

RyR : Ryanodine receptor

SDC4 : Syndecan-4

SERCA2a : Sarco(endoplasmic)reticulum Ca²⁺-ATPase subisoform 2a

SR : Sarcoplasmic reticulum

TBX5 : T-box transcription factor 5

TGF β : Transforming growth factor β

TIMPs : Tissue inhibitor of metalloproteinase

TNF α : Tumor necrosis factor- α

TNNT2 : Troponin T2, Cardiac Type

WiChR : Kalium channelrhodopsin from *Wobblia lunata*

WP : Work package

Summary

Each year hundreds of thousands of new cases worldwide are annually diagnosed with atrial fibrillation (AF), estimating that approximately 33.5 million of people worldwide live with this complex disease. However, it became clear that AF is not only a prevalent cardiac arrhythmia but also a multifaceted and progressive one. Thus, the development of new experimental models that recapitulate this complex mechanism is required.

For this reason, this thesis has navigated through the intricate landscape of AF remodeling under an electrophysiological, structural and immunological point of view using an *in vitro* model of human induced pluripotent stem cell-derived atrial cardiomyocytes (hiPSC-aCM). The model showed to be able to recapitulate re-entry mechanisms as well as genetic remodeling correlated to electrophysiological, structural and immunological changes similar to those observed in AF patients, demonstrating its value as model for studying initiation arrhythmia mechanisms. Furthermore, the thesis explored innovative optogenetic approaches for action potential perturbation in hiPSC-aCM, demonstrating their possible use for arrhythmia termination.

In conclusion, this PhD thesis makes a significant contribution to the development and testing of a new human atrial *in vitro* model of AF, providing a strong basis for future improvements of therapeutic target and drugs.

Resumen

Cada año, cientos de miles de nuevos casos en todo el mundo son diagnosticados anualmente con fibrilación auricular, estimándose que aproximadamente 33.5 millones de personas viven con esta compleja enfermedad. Sin embargo, se hizo evidente que la fibrilación auricular es una enfermedad multifacética y progresiva. Por lo tanto, se requiere el desarrollo de nuevos modelos experimentales que recapitulen este complejo mecanismo.

Por esta razón, esta tesis ha navegado a través del intrincado panorama del remodelado de la fibrilación auricular desde un punto de vista electrofisiológico, estructural e inmunológico, utilizando un modelo in vitro de cardiomiocitos atriales derivados de células madre pluripotentes inducidas humanas (hiPSC-aCM). El modelo demostró ser capaz de recapitular mecanismos de reentrada, así como remodelados genéticos correlacionados con cambios electrofisiológicos, estructurales e inmunológicos similares a los observados en pacientes con fibrilación auricular, demostrando su valor como modelo para estudiar los mecanismos de iniciación de la arritmia. Además, la tesis exploró enfoques optogenéticos innovadores para la perturbación del potencial de acción en hiPSC-aCM, demostrando su posible uso para la terminación de la arritmia.

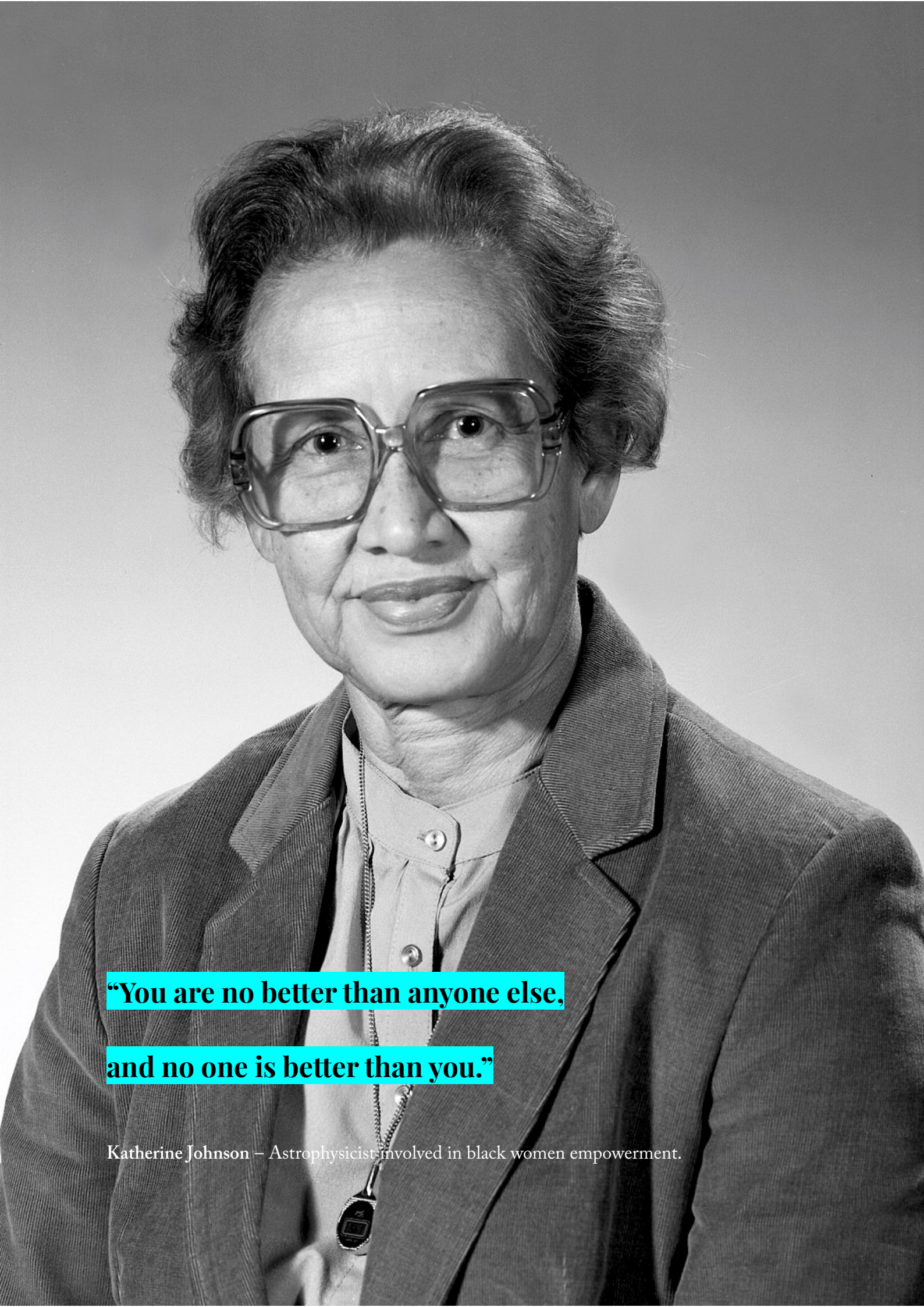
En conclusión, esta tesis de doctorado realiza una contribución significativa al desarrollo y prueba de un nuevo modelo in vitro de fibrilación auricular en atrios humanos, proporcionando una base sólida para futuras mejoras en los objetivos terapéuticos y medicamentos.

Resum

Cada any, centenars de milers de nous casos a tot el món són diagnosticats anualment amb fibril·lació auricular, estimantse que aproximadament 33.5 milions de persones viuen amb aquesta complexa malaltia. No obstant això, es va fer evident que la fibril·lació auricular és una malaltia multifacètica i progressiva. Per tant, es requereix el desenvolupament de nous models experimentals que recapitulen aquest complex mecanisme.

Per aquesta raó, aquesta tesi ha navegat a través del intrincat panorama del remodelat de la fibril·lació auricular des d'un punt de vista electrofisiològic, estructural i immunològic, utilitzant un model in vitro de cardiomiòcits atrials derivats de cèl·lules mare pluripotents induïdes humanes (hiPSC-aCM). El model va demostrar ser capaç de recapitular mecanismes de reentrada, així com remodelats genètics correlacionats amb canvis electrofisiològics, estructurals i immunològics similars als observats en pacients amb fibril·lació auricular, demostrant el seu valor com a model per estudiar els mecanismes d'iniciació de l'arítmia. A més, la tesi va explorar enfoc optogenètics innovadors per a la pertorbació del potencial d'acció en hiPSC-aCM, demostrant el seu possible ús per a la terminació de l'arítmia.

En conclusió, aquesta tesi de doctorat realitza una contribució significativa al desenvolupament i prova d'un nou model in vitro de fibril·lació auricular en atris humans, proporcionant una base sòlida per a futures millores en els objectius terapèutics i medicaments.



**“You are no better than anyone else,
and no one is better than you.”**

Katherine Johnson – Astrophysicist involved in black women empowerment.

Introduction

1.1 Background on PersonalizeAF project

This doctoral thesis is part of the PersonalizeAF project, an initiative under the Marie Skłodowska-Curie Innovative Training Networks funded by the European Commission. The aim of PersonalizeAF is to develop 15 doctoral theses, involving biologists, engineers, and clinicians working collaboratively to advance knowledge and personalize treatments for atrial fibrillation. This project brings together a diverse group of institutions, fostering a multidisciplinary environment for cutting-edge research in this field. For detailed information about the project and participating institutions, you can visit the PersonalizeAF website (www.personalizeAF.net).

Delving into the depths of AF pathophysiology and pharmacology, it becomes evident that for developing new treatment strategies scientific community has to individualize the characterization of AF substrate. By applying a more personalized approach, we would be able to take into account the interpatient variability and select the most efficient therapy.

For this reason, this thesis takes part of an innovative multinational, multisectoral and multidisciplinary research and training programme called PersonalizeAF. The PersonalizeAF consortium, indeed, had the ambition to integrate knowledge from *in vitro*, *in silico*, *ex vivo*, *in vivo* and human models in order to improve the atrial state characterization during AF remodeling and develop new diagnostic methods with the final goal of improving AF patient management.

To do so, PersonalizeAF merged a scientific community of 11 academic universities, 6 academic hospitals and 5 biomedical companies that worked in a collaborative manner in three scientific interdependent work packages (WP) that involved: atrial state characterization (WP1), treatment improvement (WP2) and decision support (WP3). The interplay and correlation among the three WP is represented in Figure 1.1. The work of this particular thesis used an *in vitro* model of hiPSC-aCM to contribute to the genetic and electrophysiological modification during AF (WP1) and to the testing of new tools for optogenetic termination of AF (WP2).

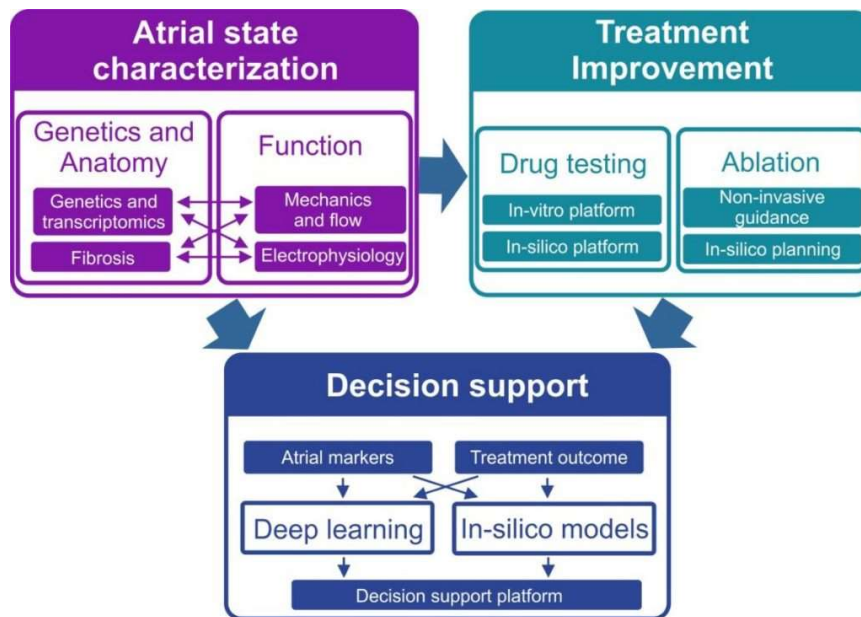


Figure 1.1 Interplay between the three different working packages (WP) of the PersonalizeAF network. Atrial state characterization (WP1) centered on advancing novel technologies and improving the current ones to delineate the atrial substrate that fosters the initiation and maintenance of AF. Treatment improvement (WP2) focused on devising toolboxes and workbenches for the analysis of novel and existing treatments, aiming to identify the particular AF phenotype targeted by each therapeutic alternative. Decision support (WP3) has the goal to integrate the data collected for providing the best diagnostic and therapeutic option for the hospital environment.

Thanks to the PersonalizeAF consortium, each research section of this thesis was performed in different laboratories specialized in the specific field of interest. The establishment of the hiPSC-aCM differentiation and its molecular was performed at *La Fe Health Research Institute* (Valencia, Spain) under the supervision of Professor Pilar Sepulveda, Doctor Andreu Climent and Doctor Imelda Ontoria Oviedo. The functional and mechanical characterization of hiPSC-aCM was performed at *Universitäts-Herzzentrum Freiburg • Bad Krozingen* (Freiburg, Germany) under the supervision of Professor Ursula Ravens and Doctor Remi Peyronnet. After the characterization was performed, the establishment of the *in vitro* model of AF in hiPSC-aCM was performed and analyzed at La Fe Health Research Institute in collaboration with the *ITACA Institute* of the Polytechnic University of Valencia (Valencia, Spain), while the transcriptomic analysis took place at *GenomeScan* company (Leiden, Netherlands) under the supervision of Doctor Sander Tuit. Finally, the functional characterization of optogenetic tools for AP termination was performed at *Universitäts-Herzzentrum Freiburg • Bad Krozingen* (Freiburg, Germany) under the supervision of Professor Ursula Ravens and Doctor Franziska Scheider-Warme.

Thanks to this opportunity, each section of this research work could gain value from specialized professionals who shared and transmit their knowledge with the common goal of pursuing a more multidisciplinary point of view for AF characterization and treatment.

1.2 Atrial fibrillation

1.2.1 Clinical aspects of atrial fibrillation

Each year hundreds of thousands of new cases worldwide are annually diagnosed with atrial fibrillation (AF) (1). It is estimated that approximately 33.5 million of people worldwide live with this complex disease, ranking it as is one of the most common arrhythmias (2). Based on data from the Framingham Heart Study, the incidence is suspected to increase twice in the next 50 years (3). Its characteristic of irregular and rapid heart rate usually leads to other adverse diseases such as heart failure and tachycardia-related cardiomyopathy, causing a significant morbidity and mortality (4). Such a scenario is mainly due to the extremely complex pathophysiology of AF that, once it is initiated, undergo to a progressive and self-sustaining maintenance, progression and stabilization of the disease (5,6).

Under a clinical point of view, there are three different stages of AF conditions: paroxysmal AF, persistent AF and permanent AF (7). The difference among those three conditions is mainly the frame time in which AF episodes are faced. Paroxysmal AF is described as arrhythmia episodes that last less than 7 days (8), persistent AF last more than 7 days, while permanent AF is the case when the normal sinus rhythm is not restored any longer (9). Patients can present the first episode of AF in a paroxysmal or persistent condition already. However, if this clinical condition is maintained over time, AF is likely to progress to the more severe clinical condition due to its self-sustaining characteristic (10). The common

characteristic of each patient is that AF initiation requires a trigger on a vulnerable substrate. The vulnerability can be influenced and determined by rare or common mutations and gene variants (11,12), but as well as by common comorbidities such as hypertension, heart failure and cardiac valve disease (13). Consequently, the onset of this complex disease typically occurs in the later stages of life. It is indeed estimated that among the 70% of AF patients, we can find people between 65 and 85 years old (14). The life of those patients is strongly limited by AF symptoms that comprehend fatigue, shortness of breath, palpitations and dizziness (15).

The complexity of AF stands in its evolution and progression of the disease, as represented in Figure 1.1 (10). Indeed, AF vulnerability is strongly connected to the substrate severity remodeling. A condition that can be due to age/disease-related remodeling, but as well as the AF condition itself, causing a self-sustaining and progression mechanisms. Patients with genetic predisposition, may have the first AF episodes a relatively young age (16). Subsequently, the remodeling due to AF itself helps to maintain the arrhythmic state, as well as to progress it (Figure 1.2 A). Nevertheless, only a small number of patients possess a genetic substrate that confers significant susceptibility to AF (17,18). Most of the patients, for example, for the initiation of paroxysmal AF episodes require additional disease-related remodeling that increase their vulnerability. Such condition, if not controlled, may progress to longer-lasting persistent AF forms (Figure 1.2 B) (19). Finally, because of their age/disease-related remodeling and substrate vulnerability, some patients have a first episode that may progress to permanent AF (Figure 1.2 C).

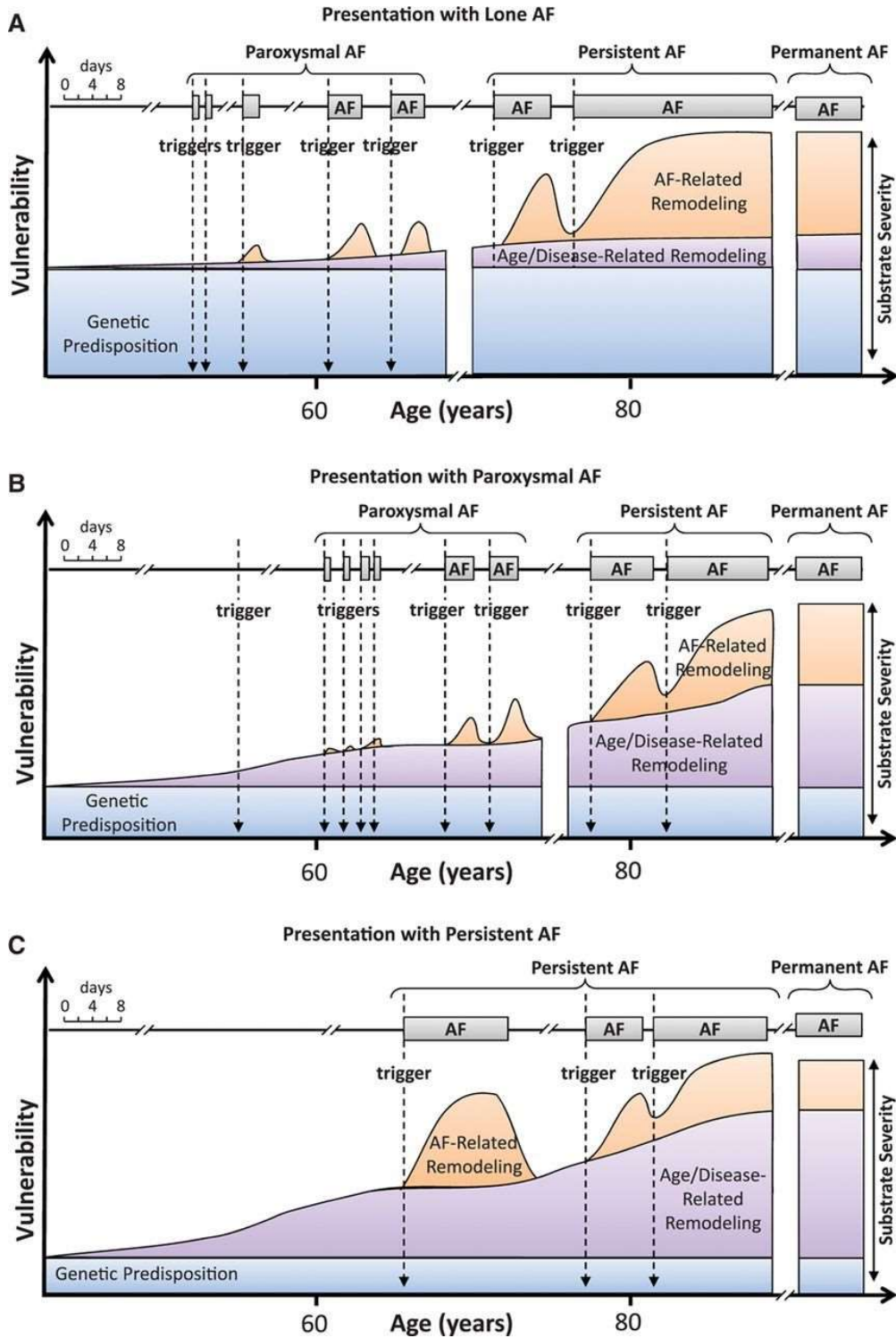


Figure 1.2 Conceptual framework of atrial fibrillation (AF) initiation, maintenance, and progression. The figure represents the three main scenario of patients that can undergo to AF iniization and progression depending on their genetic predisposition and age/disease-related remodeling. Figure modified by Heijman et al., 2014.

Despite the large scientific interest on AF because of its economic and clinical implications, there are still debates about the exact mechanisms of AF initiation and maintenance (20). Scientific community did not reach a single a common theory. Instead, there is a possibility that different several mechanisms of AF initiation might co-exist (21). So far, there are three main fundamental mechanisms that have been identified: ectopic (triggered) activity, anatomical re-entry and functional re-entry (Figure 1.3).

Focal ectopic activity is mediated by early afterdepolarization (EADs), delayed afterdepolarizations (DADs) or atrial automaticity (22). Respectively promoted by prolonged repolarization of the action potential (AP), Ca^{2+} -handling abnormalities and spontaneous diastolic depolarization to a threshold value (23). Anatomical re-entry occur around an anatomic obstacle such as fibrosis or scar tissue, forming a circuit of abnormal electrical conduction patterns in the atrial tissue (24). Such phenomenon occurs when, along the conduction pathway of the re-entry, each cell has sufficient time to recover and be excited by the arrival of the consequent impulse. Finally, functional re-entry occurs when premature impulses conduct unidirectionally around a region that is characterized by partially refractory period or slower conduction (25,26). The unidirectional pathway and the peculiar properties of this region contribute to the formation of a loop, resulting in a phenomenon known as a “spiral wave” (27). As these spiral waves intensify and rotate at high rates, they generate electrical turbulence, akin to a whirlwind of signals. It is important to state that ectopic firing and re-entry are correlated among

themselves. Indeed, initiation of a re-entry usually requires a premature ectopic activity as trigger.

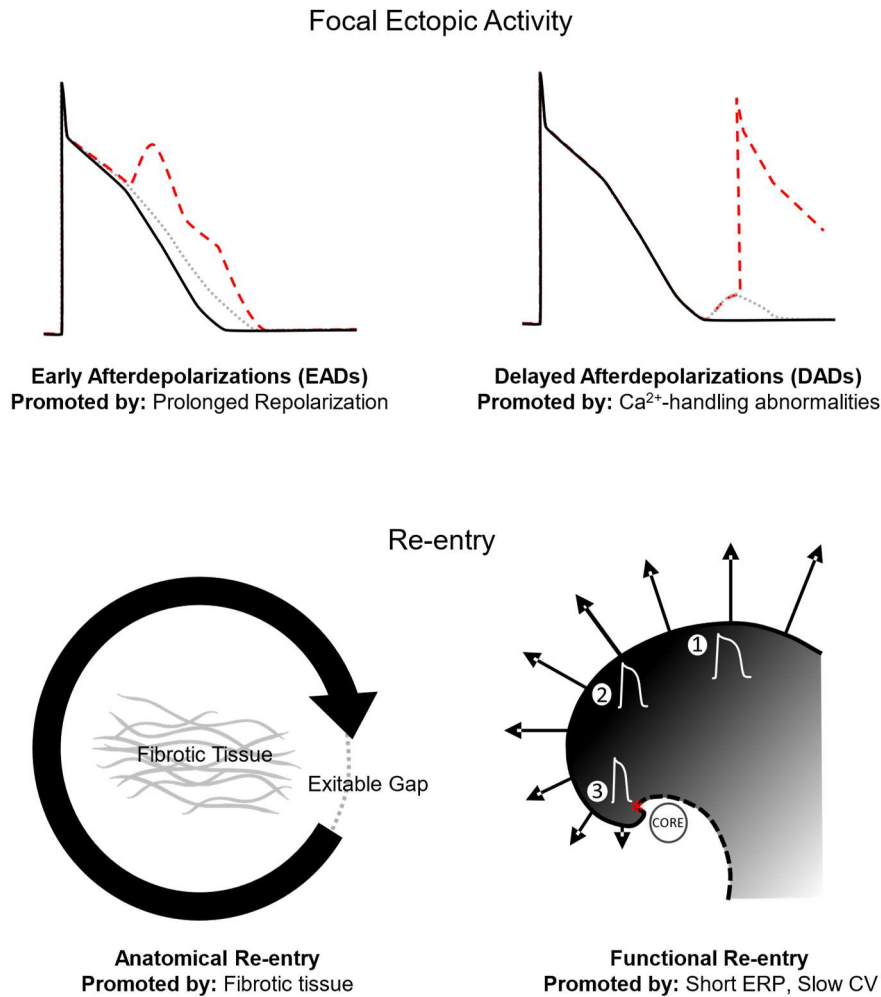


Figure 1.3 Major arrhythmogenic mechanisms including focal ectopic activity and re-entry mechanisms. On the top part of the figure are represented focal ectopic activities mediated by early (left) and delayed (right) afterdepolarizations, which are promoted by prolonged repolarization and Ca²⁺-handling abnormalities respectively. On the bottom part of the figure are represented the anatomical and functional re-entries. ERP = effective refractory period, CV = conduction velocity.

Overall, the initiation and maintenance of AF require that a triggering event intersects with a vulnerable substrate (28). Once it is initiated, AF itself modifies atrial electrical properties promoting arrhythmia maintenance, this process is called ‘atrial remodeling’.

1.2.2 Atrial remodeling

Atrial remodeling refers to the changes that occur in the atrial tissue over time as a result of the persistent and irregular electrical activity associated with AF (29). Overall, remodeling in AF is a complex and multifaceted process characterized by alterations across various levels, such as electrophysiological (30,31), structural (32,33), neural (34), and immunological (35). These modifications give rise to a self-perpetuating cycle, amplifying the persistence and complexity of AF management over time. Given the thesis's specific focus, the subsequent paragraphs will focus on three distinct types of remodeling: electrophysiological, structural, and immunological. Despite this necessary distinction among the different type of remodeling, it is crucial to acknowledge the intricate interplay and mutual influence among the aforementioned remodeling processes (36). Finally, this thesis focuses mainly on the remodeling faced by cardiomyocytes during AF, however, it is important to underlying that this complex mechanism takes into account other cells types of the heart such as fibroblasts and immune cells (37–39).

1.2.2.1 Electrophysiological remodeling

One of the mechanisms that maintain, and progress AF pathophysiology is the electrical remodeling of atrial cardiomyocytes. The rapid atrial activation caused by AF has been demonstrated to alter various mechanisms that orchestrate action potential (AP) formation and its conduction among the atrial tissue (22). Among those, we can find alterations of the Ca^{2+} -induced Ca^{2+} release system, increase of inward rectifier K^+ currents and alteration of the gap junction functions (Figure 1.4).

Ca^{2+} handling abnormalities

Rapid atrial activation caused by AF itself provoke a Ca^{2+} unwarranted loading, activating the Ca^{2+} /calmodulin system that indirectly reduces the transcription of Cav1.2 (40). One of the principal L-type Ca^{2+} channel subunit. Such mechanisms initiate a self-sustain mechanisms that leads to an increased Ca^{2+} abnormalities (41). In parallel, increased atrial rate can lead to a phosphorylation-induced disfunction of ryanodine receptor (RyR) and/or sarcoplasmic reticulum (SR) Ca^{2+} overload (42). Such altered calcium handling can also be accentuated by the activation of Ca^{2+} calmodulin-dependent protein kinase type II (CaMKII) and hyperphosphorylation of phospholamban (43,44).

Increased K⁺ currents

Inward rectifier currents such as I_{K1} and $I_{K,Ach}$ are fundamental contributors to AF maintaining due to their role in action potential duration (APD) and hyperpolarization of the membrane potential (45). Both mechanisms that sustain and accelerate re-entry mechanisms. I_{K1} increase in AF pathophysiology is associated to an increased expression of the Kir2.1 subunit (46) as result of reduced levels of Kir2.1-inhibitory miRNAs (47). On the other hand, increased $I_{K,Ach}$ seems to be associated to the alteration of the protein kinase C (PKC) regulation (48).

Gap junction function

In the heart, gap junctions are composed of connexins (Cxs) and form intercellular connections that are responsible for electrical coupling of cardiomyocytes (49). Among the various Cxs isoform, the atria is mainly composed by the three isoform Cx40, Cx43 and Cx45 (50). While expression changes of Cx40 and Cx43 AF are still under debate, different studies agreed on the Cx lateralization phenomenon (51,52). A consequence of Cx40 and Cx43 spatial remodeling is an enhanced lateral conduction velocity, favouring re-entry formation and maintenance (53). However, it is still unclear the mechanism by which the Cx location is modulated. A contribution to this process seems to be the intracellular remodeling of the site where Cxs are oligomerized, the golgi apparatus (54). Nevertheless, further in deep studies needs to be done.

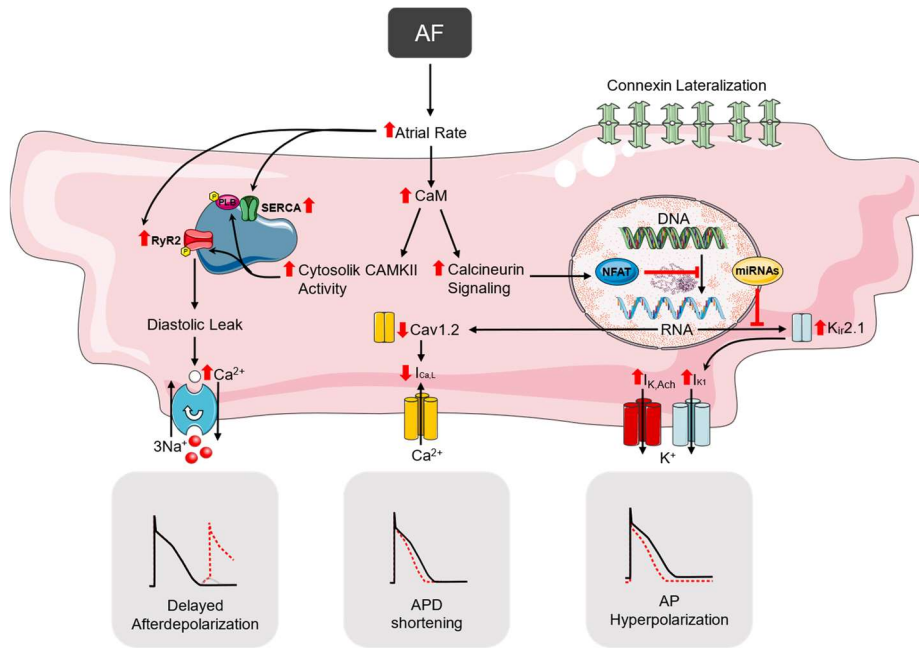


Figure 1.4 Representation of electrophysiological remodeling mechanisms. Alteration of Ca²⁺-handling can lead to delayed afterdepolarization and APD shortening through the NCX exchanged and L-type Ca²⁺ channel alteration, respectively. While alteration of K⁺ currents lead to hyperpolarization of the membrane potential. Altogether, those changes sustain AF and promote the remodeling. CaM = calmodulin, CAMKII = Ca²⁺/calmodulin-dependent protein kinase II, SERCA = Sarco-Endoplasmic Reticulum Calcium ATPase, RyR= Ryanodine Receptor, NFAT = Nuclear factor of activated T-cells.

1.2.2.2 Structural remodeling

In addition to the electrophysiological remodeling previously explained, atrial tissue changes during AF are also associated to adaptive alterations in morphology (55). The adaptive changes are mainly correlated to degeneration of endothelial cells and cardiomyocytes with fibrosis replacement, as well as cardiomyocytes dedifferentiation and hypertrophy.

Fibrosis mechanisms

Fibrosis is the mechanism by which normal and healthy cardiac tissue is replaced by fibrous connective tissue (56). Such replacement comes as response to damage that can be caused by chronic inflammation, hypertension and/or chronic arrhythmia. The main protagonist of fibrosis mechanisms are cardiac fibroblasts (37). Indeed, upon profibrotic stimuli, fibroblasts produce an array of extracellular matrix (ECM) proteins along with proteolytic enzymes that alter these proteins (57). Additionally, they have the capability to transform into myofibroblasts, which are contractile cells with an enhanced capacity for ECM protein synthesis (58). This transformation disrupts the balance between ECM synthesis and degradation, ultimately resulting in an arrhythmogenic atrial substrate (59). ECM is composed by collagens, proteoglycans, glycoprotein, metalloproteinases (MMPs) and tissue inhibitor of metalloproteinases (TIMPs). Among these, collagen is the main constituent providing tensile strength, regulating cell adhesion and cell migration (60). ECM modulation is a constantly changing and well-regulated procedure, finely tuned by the activity of proteolytic enzymes and their inhibitors (32). Within these enzymes, the MMP family holds particular significance. These enzymes are capable not only of breaking down nearly all ECM proteins but also influencing the levels of cytokines, growth factors, and various other molecules, thereby impacting ECM synthesis (61).

Another strong stimulator of collagen synthesis is the transforming growth factor β (TGF β) (Figure 1.5). Its binding to the receptors T β R-I, -II and -III lead

to an increased expression of genes involved in the fibrosis process by activation of the Smad complex (62). Furthermore, as shown in Figure 1.5 both Angiotensin II (Ang II) and TGF β seem to orchestrate the expression of connective tissue growth factor (CTGF) (63), a fundamental modulator of different pathogenesis mechanisms related to ECM deposition, cell mobility and cell adhesion. In an AF context and cardiac remodeling, ECM alteration and consequent fibrosis lead to a separation and uncouple of cardiomyocytes slowing conduction velocity and promoting re-entrant arrhythmia generation (64).

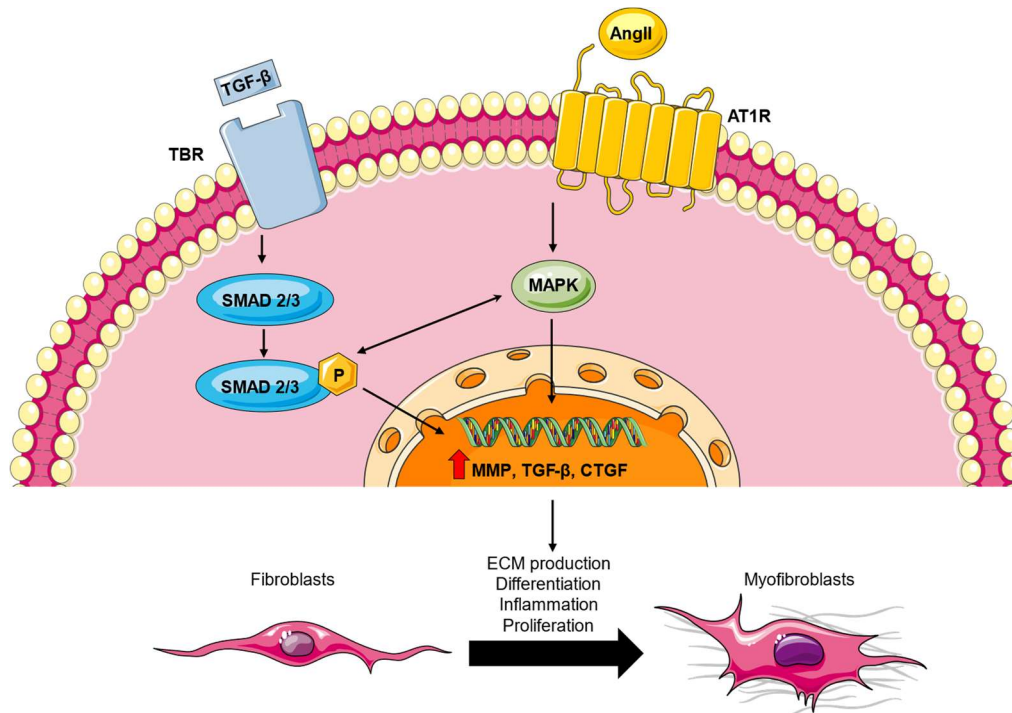


Figure 1.5 Representation of structural remodeling mechanisms. Both TGF β and AngII are connected to the release of factors involved in fibroblast differentiation, ECM production, inflammation and proliferation. TBR = Transforming Growth Factor Beta Receptor, SMAD = Suppressor of Mothers Against Decapentaplegic 2/3, AT1R = Angiotensin II Receptor Type 1, MAPK = mitogen-activated protein kinase.

Cardiomyocytes dedifferentiation

The first evidence of human atrial cardiomyocytes dedifferentiation during AF dates back to the 2002 (65). The authors demonstrated that in cardiac specimens of AF patients, myolytic cardiomyocytes showed characteristics of dedifferentiated cells with re-expression of α -smooth muscle actin and β -myosin heavy chain. Both proteins are characteristic of the fetal cardiomyocyte state and provoke a more disorganized cytoskeleton and contraction of the cardiomyocyte. Together with those changes, dedifferentiated cardiomyocyte underwent a sarcomere replacement with glycogen (66). So far, dedifferentiated cardiomyocytes from atrial tissue of AF patients have not been functionally characterized. However, it is known that fetal cardiomyocytes have a more depolarized resting membrane potential (RMP), a faster APD and less efficient excitation-contraction coupling (67). Therefore, those structural and functional changes might contribute to the AF remodeling of atrial tissue. Nevertheless, more research needs to be done to better understand the complex mechanism behind cardiomyocytes dedifferentiation and their implications in AF remodeling.

Cardiomyocyte hypertrophy

During AF, the atria is affected by enlargement with consequent cellular stretch and hypertrophy. Studies on tissue samples from AF patients demonstrated how atria remodeling influenced not only the amount of connective tissue, but also the wall thickness and cardiomyocytes volume (68). The cellular mechanisms by which

cardiomyocytes hypertrophy is regulated are disparate. Among those, we can find the Ang II and the TGF β signaling pathways (69).

In studies on tissues from AF patients an increased expression of Ang II has been found (70). Ang II has the ability of regulating fibroblast proliferation and cardiac hypertrophy by stimulation of the mitogen-activated protein kinase (MAPK) through the type 1 angiotensin receptor (AT1-R). Another molecule correlated to myocardial hypertrophy and remodeling is aldosterone (71), whose release is stimulated by Ang II in the adrenal cortex (72). Interestingly, Ang II has been shown to increase the expression of TGF β , an important protagonist of cardiac hypertrophy (73), cardiomyocyte apoptosis (74) and mediator between fibroblasts and cardiomyocytes (69). However, the exact molecular mechanisms by which TGF β is responsible for the hypertrophic response is still unknown.

1.2.2.3 Immune remodeling

The concept that the immune system contributes to the remodeling of the heart during AF is quite recent (35) and in this chapter the main mechanisms will be explained (Figure 1.6). In the last years new studies demonstrated how immune cell activation and immune molecular secretion are alternated during development and progression of AF (75,76). Such promotion of inflammatory response, however, leads to an enhancement of atrial remodeling. Among the inflammatory factors that are released during AF we can find tumor necrosis factor- α (TNF α), macrophage

migration inhibitory factor (MIF), interleukin 1 (IL1) and interleukin 6 (IL6). Altogether, those inflammatory factors can directly and indirectly affect cardiomyocyte's electrophysiological function. More specifically, TNF α , MIF, IL1 and IL6 increase RyR2 expression and phosphorylation, reduce sarco(endo)plasmic reticulum Ca²⁺-ATPase subisoform 2a (SERCA2a) expression and function, and alter expression and distribution of Cx43 (77,78). The consequent effect is enhanced arrhythmia susceptibility by spontaneous Ca²⁺ release and conduction velocity reduction.

Furthermore, numerous studies demonstrated an active participation of immune cells and secreted cytokines to the fibrotic process. TNF α , for example, can increase MMPs secretion by modulating TGF β signaling pathway (79). Additionally, there is a strong interplay between immune cells and fibroblasts activation. The release of Human platelet-derived growth factor (PDGF- α), TGF β , TNF α , CXC chemokine 8 (CXCL8), IL11 and CXC chemokine 12 (CXCL12) by macrophages, neutrophil and T-cells have been demonstrated to directly affect fibroblast differentiation and their ECM deposition (38,80).

In conclusion, electrophysiological and structural changes that atria tissue undergo during AF are strongly affected by the activation of inflammatory responses.

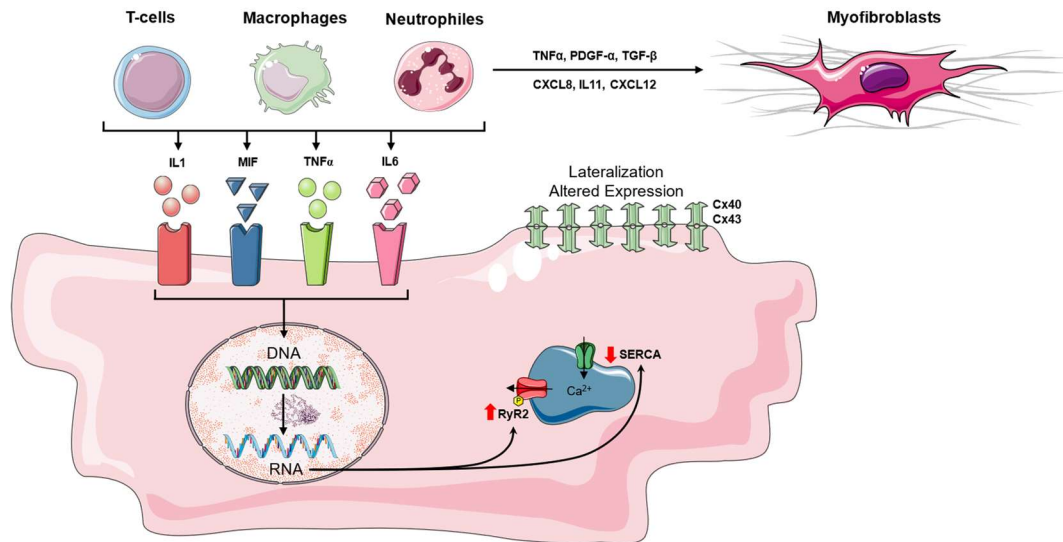


Figure 1.6 schematic representation of immune remodeling in AF. T-cells, macrophages and neutrophils influence cardiomyocytes and myofibroblast activity releasing cytokines such as IL1, MIF, TNF α , IL8, PDGF α , TGF β , CXCL8 and CXCL12. IL1 = Interleukin 1, MIF = Macrophage Migration Inhibitory Factor, TNF α = Tumor Necrosis Factor Alpha, IL8 = Interleukin 8, PDGF α = Platelet Derived Growth Factor Alpha, TGF β = Transforming Growth Factor Beta, CXCL8 = CXC Motif Chemokine Ligand 8, CXCL12 = CXC Motif Chemokine Ligand 12, SERCA = Sarco-Endoplasmic Reticulum Calcium ATPase, RyR2 = Ryanodine Receptor 2, Cx40 and Cx43 = Connexin 40 and 43.

1.2.3 Therapies for AF

In the last European society of cardiology guidelines, the management of AF advocate for the ABC pathway: anticoagulation/avoid stroke (A), better symptom control (B) and comorbidities/cardiovascular risk factor management (C) (81). For better symptom control medical doctors refers to a correct assessment of the AF symptoms, quality of life and patients' preference for treatment strategies. The latter can be divided into antiarrhythmic drugs (AAD) or ablation (82).

1.2.3.1 Antiarrhythmic drugs

The most used antiarrhythmic drugs for AF treatment belong are either potassium channel blockers prolonging the effective refractory period (dofetilide and sotalol) (83,84) or sodium channel blockers reducing excitability and, therefore conduction velocity of the AP propagation (amiodarone, dronedarone, flecainide, propafenone) (85). Following the Sing/Vaughan-Williams classification (Table 1.1) (86), the mentioned drugs can be identified as class III and class I, respectively. While class II and IV are more recommended in persistent AF patients in order to control the ventricular rate (87). However, it is important to consider that most of them have actions of more than one class. Following the European Society of Cardiology guidelines, the recommended drug depends on AF severity and other concomitant heart diseases of the patient (88). Indeed, despite AAD therapies aims to reduce symptoms related to AF, their effectiveness in maintaining sinus rhythm is moderate and drug-induced proarrhythmic or extracardiac side-effects are frequent (89).

CLASS	EXAMPLES	MECHANISM
IA	Quinidine Procainamide	Na ⁺ channel blockers (intermediate association/dissociation)
IB	Lidocaine	Na ⁺ channel blockers (fast association/dissociation)
IC	Flecainide Propafenone	Na ⁺ channel blockers (slow association/dissociation)
II	Propranolol Metoprolol	β-blockers (propranolol shows some class I action)
III	Amiodarone Sotalol	K ⁺ channel blockers (sotalol shows beta blocker activity, while amiodarone has Class I, II, III and IV activity)
IV	Verapamil Diltiazem	Ca ²⁺ channel blockers
V	Adenosine Digoxin	Unkown mechanisms (direct nodal inhibition?)

Table 1.1 Singh-Vaughan Williams classification of antiarrhythmic drugs. Antiarrhythmic drugs are divided in five major groups. The first one, composed by the subgroups Ia, Ib and Ic comprehend Na⁺ channel blockers. Group II is formed by β-blockers. While group III by K⁺ channel blockers and group IV by Ca²⁺ channel blockers. Group V is a group that involves drugs whose mechanism is not part of previous groups or is unknown.

1.2.3.2 Catheter ablation

Catheter ablation for has the goal to reduce symptoms and improve quality of life of those patients who failed to respond to AAD (90). The strong limit of such procedure is the requirement of a highly specialised equipment and medical team. Furthermore, it should be taken into consideration that ablation procedure has major risk factors for AF recurrence, leading to the high possibility of repeated ablation procedures (91). However, the recent CAPTAF randomized clinical trial demonstrated that ablation procedure, compared to AAD medication, lead to an improved quality of life and reduction in AF burden, which translated into a reduction of hospitalization (92).

1.2.4 Experimental models to study AF

As explained in the previous paragraph, unfortunately the available therapies for AF treatment are far from optimal. In parallel, for the development of new pharmacological therapies for AF, scientific community need to improve the understanding of AF molecular mechanisms, with particular interest to those correlated to AF-sustained remodeling (93). To do so, experimental models that sophisticatedly resemble the complex clinical conditions of AF patients are needed. To effectively study the underlying mechanisms of AF, it is critical to reproduce the propagation patterns of cardiac potentials in both healthy and arrhythmic

conditions of the human heart (93), as well as to recapitulated and perpetuate the intricate mechanisms of atrial remodeling in a systematic and controllable way.

So far, a range of experimental models, including *in silico*, *in vivo*, *ex vivo*, and *in vitro* approaches, is employed in the investigation of atrial arrhythmias (94). Each model offers its own advantages and disadvantages. *In silico* models have a great potential for a rapid and low-cost testing (95,96), but their capability to reproduce intricate and complex biological and structural properties of the heart is still limited (97). *In vivo* and *ex vivo* animal models reflect the most physiological conditions, however, there are strong ethical concerns (98) and interspecies differences that push for a use limitation of those models (99). Furthermore, despite small animal models like rabbits, rats and mice provided great information about fibrosis and inflammation in AF (100–102), they have different repolarizing currents, with consequent difficulties for results interpretation (103). On the other hand, large animal models like dogs, pigs and sheep are great for remodeling studies, but they are expensive and lack of providing information about initial occurrence of AF (104). A way to overcome species differences and ethical concerns is the use of *ex vivo* human models. However, tissue and cell samples from patients have high patient variability, require highly specialized procedures and permit measurements only for a very short period of time.

On the other hand, *in vitro* models comprehend immortalized cell lines of cardiomyocytes such as AC10 (human) (105) and H9C2 (rat) (106) and HL1 (mouse) (30). The first two mentioned lines have the major disadvantage of absent

contraction properties, limiting their use for functional studies. On the other hand, HL1 are atrial cardiomyocytes that show contraction properties, but because of its mouse origin, express different functional properties compared to human models.

The advent of human induced pluripotent stem-cell (hiPSC) derived atrial cardiomyocytes opened a new chapter providing an unlimited source of human atrial-like cardiomyocytes for single cells, monolayer and 3D studies. Despite they do not have the ability to re-create the complex three-dimensional and multicellular architectures of the heart, their suitability for drug responses (107,108) and genetic modifications (109) make of them a great tool for studying AF initiation and progression under a molecular point of view.

1.3 hiPSC in cardiac research

1.3.1 Types of stem cells

Stem cells are characterised by the ability to self-renew and the capacity to differentiate into other specialised cell types in an unlimited manner (110). More specifically, stem cells, after dividing, can maintain their stem cell properties or enter a differentiation programme to differentiate into other specialised cell types. Depending on their differentiation potential and capacity, stem cells can be classified into four categories (111) (Figure 1.7).

Totipotent stem cells

Totipotent stem cells are cells capable of differentiating into all embryonic and extra-embryonic tissues. These cells are therefore capable of giving rise to a complete organism. Only the zygote and the cells obtained after their first divisions (blastomeres) have this potential.

Pluripotent stem cells

These cells can differentiate into cells of the three germ layers but cannot produce extra-embryonic tissues. Among pluripotent stem cells, we can find the cells from the inner cell mass of blastocysts, also called embryonic stem cells (ESC), and induced pluripotent stem cells (iPSC).

Multipotent stem cells

Multipotent stem cells present in adult tissues and can give rise to different cell types within a specific lineage. For example, haematopoietic stem cells, which can differentiate into the different blood cell types, or mesenchymal stem cells, which can differentiate into osteocytes and adipocytes, among other cell types.

Unipotent stem cells

These cells are only able to differentiate into one cell type. For example, spermatogonia, which differentiate to give rise to spermatozoa, or skeletal muscle satellite cells, which can differentiate into osteocytes, chondrocytes and adipocytes, among other cell types.

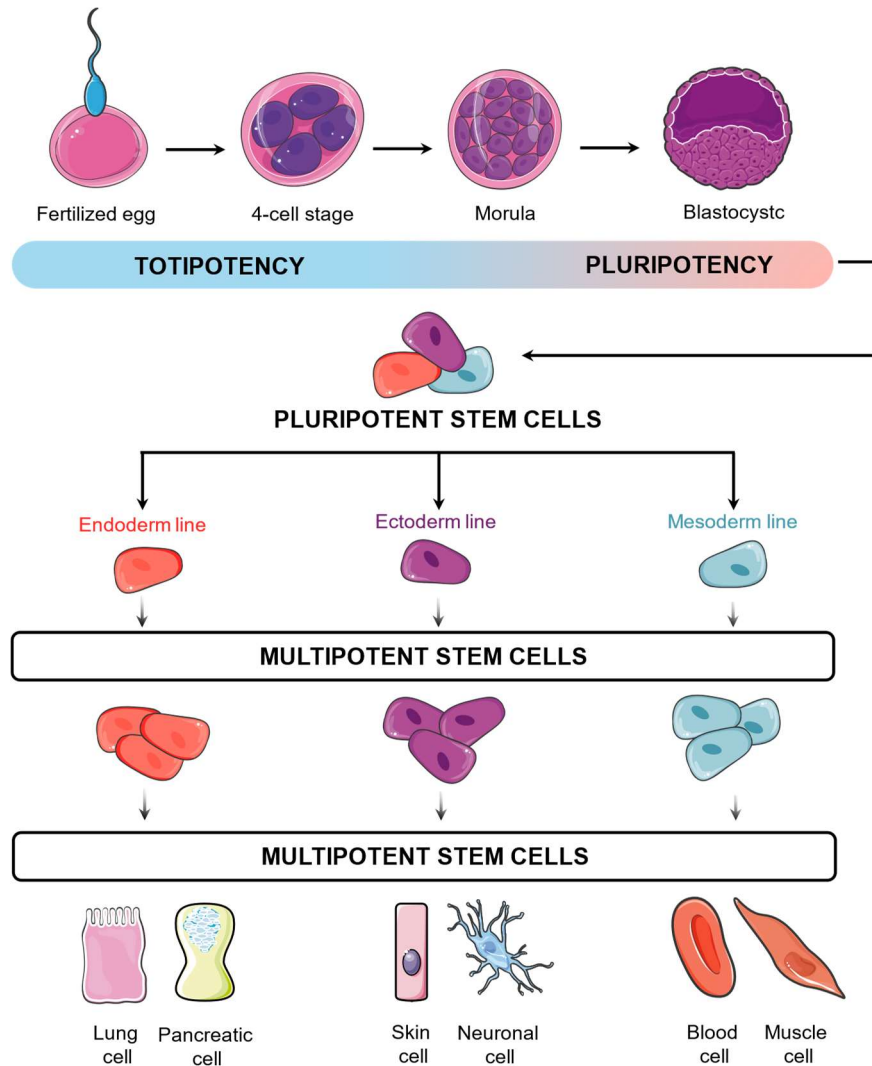


Figure 1.7. Different stem cell types. Totipotent stem cells exhibit the utmost potential by generating all cell types within the body. Pluripotent stem cells, on the other hand, display a slightly higher level of specialization, as they differentiate into cells originating from the three germ layers—ectoderm, endoderm, and mesoderm—resulting in the formation of diverse tissues and organs. In contrast, multipotent stem cells possess a more restricted potential compared to totipotent and pluripotent counterparts, differentiating into various cell types within a specific lineage or tissue. Unipotent stem cells, with the most confined potential, specialize in differentiating into a singular mature cell type specific to a particular tissue or organ. Induced pluripotent stem cells (iPSCs) undergo genetic reprogramming, acquiring characteristics akin to pluripotent stem cells, and demonstrating the ability to differentiate into various cell types throughout the body.

1.3.2 Human induced pluripotent stem cells discovery

The first iPSC were generated by Yamanaka and Takahashi in 2006 (112). In their study, they used adult mouse fibroblasts modified in order to express a resistance gene under the *Fbxo15* locus, an ESC-specific gene. To identify transcriptional factors capable of reprogramming adult cells to pluripotent cells, they overexpressed, using retroviral vectors, a set of 24 pluripotency-associated factors that could activate the resistance gene. The combination of factors allowed the activation of *Fbxo15* and the formation of resistant colonies with ESC-like morphology. Successive rounds of elimination of individual factors identified the minimum combination of factors that could induce pluripotency, later called the Yamanaka factors: *Klf4*, *Sox2*, *c-Myc* and *Oct4*. These iPSC generated by *Fbxo15* selection expressed pluripotency markers such as *SSEA-1* and *Nanog* on their surface. At the same time, the obtained iPSC were able to generate teratomas in mice and to contribute to embryo formation after injection into blastocysts. In 2007, for the first time human induced pluripotent stem cells (hiPSC) were produced from human adult fibroblasts (113). The discovery of hiPSC has been one of the major breakthroughs in the field of biology and medicine. Indeed, unlike ESCs, hiPSC do not have the ethical problem associated with the destruction of embryos (114), allowing them to be for basic and translational research with fewer restrictions. In addition, the fact that patient-specific hiPSC can be derived favours their use for

both regenerative medicine, patient-specific disease modeling, drug discovery and testing (115).

1.3.3 hiPSC reprogramming

The first iPSC generated used retroviral vectors that were stably integrated into the genome of the cells to induce the expression of c-Myc, Klf4, Oct3/4 and Sox2 (116). Retroviral transgenes were usually silenced towards the end of reprogramming (117). However, this process was incomplete and ended up producing partially reprogrammed cells that continue requiring the expression of exogenous factors because of their lack of ability in activating the expression of endogenous genes (118). Furthermore, the reactivation of retroviral transgenes in iPSC can impede their capacity for differentiation and frequently results in tumor formation within animal chimeras (116). This problem is much greater when using lentiviral vectors that express the reprogramming factors constitutively (119).

Different approaches have been taken to obtain transgene-free iPSCs to avoid the potential detrimental effects of uncontrolled transgene expression and insertional mutagenesis. One of the ways to iPSCs without transgene integration is to use vectors that do not integrate into the genome of the host cells. The first integration-free iPSC was obtained from mouse hepatocytes using non-integrating adenoviral vectors (117). In addition, virus-free iPSCs have been obtained from mouse embryonic fibroblasts using plasmids (120). Human fibroblasts have also

been reprogrammed in a non-integrative manner using Sendai virus. Since Sendai virus remains in the cytoplasm after infection, it has a high rate of transduction and reprogramming, and its copies are diluted after multiple passages, yielding virus-free iPSC (121,122). The efficiency of reprogramming using non-integrating methods is much lower than that achieved with integrating vectors, but they avoid the integration of transgenes into the iPSC genome and are therefore preferred for use in research and in the clinic. Other non-integrative systems that increase the safety of iPSC use non-viral systems. These include DNA-based systems, such as the use of circular vectors expressing Yamanaka factors (123,124).

Although the most common reprogramming techniques are DNA-based and achieve effective and efficient reprogramming of somatic cells (Figure 1.8), they are considered less safe. Indeed, even in non-integrative systems the DNA fragments used in reprogramming can end up being inserted into the genome (125). For this reason, some groups have focused on the search for reprogramming methods that do not use non-DNA reprogramming methods based on the use of mRNA (126,127), miRNA (128) recombinant proteins (129) or even small chemical molecules (130).

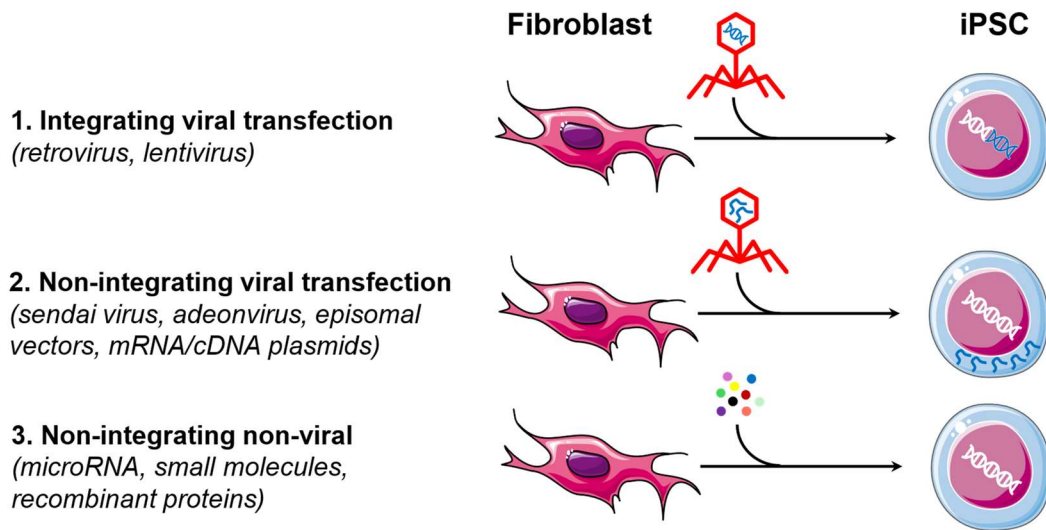


Figure 1.8. Different methodologies for delivering reprogramming factors. The first method was the application of viral systems for delivering transcription, but this approach posed drawbacks due to the inclusion of their genetic material. To overcome this limitation, innovative techniques, such as non-integrating vectors, self-excising vectors, and non-integrating non-viral vectors, have emerged as progressive enhancements over the initial method.

1.3.4 hiPSC differentiation into cardiomyocytes

Generation of hiPSC-derived cardiomyocytes (hiPSC-CM) is of growing interest for their potential as *in vitro* model of cardiac studies. Indeed, their ability to generate hiPSC-CM from patients provides unprecedented opportunities for regenerative medicine, disease modelling and drug screening (131). The first established protocol to differentiate hiPSC into cardiomyocytes was published in 2011 (132). In the same year, many other protocols have been established, testing different pluripotency media, as well as substrate culture, disaggregation reagents and cytokines for direct differentiations (133–135). Indeed, for hiPSC differentiation

into cardiomyocytes there are three fundamental steps that need to be accomplished: formation of mesoderm cells, formation of cardiac mesoderm cells and, finally cardiomyocytes maturation(136). Indeed, the formation of the heart undergoes a constantly changing process, intricately regulated by the sequential activation of various signal transduction proteins and transcription factors operating in a collaborative fashion. Several signaling pathways and growth factors play a role in shaping cardiac cells, with notable emphasis on Wnt/Nodal, bone morphogenetic protein (BMP), fibroblast growth factor (FGF) (137–139). The role and effects of cardiogenesis of each pathway is explained in Table 1.2. Given that these factors exhibit optimal functionality within specific time frames and occasionally hinder cardiogenesis in alternate periods, precise optimization of the timing for their introduction is essential to effectively steer pluripotent stem cells toward the desired path of differentiation.

PATHWAY	GENERAL EFFECTS ON CARIOGENESIS
WNT	Early activation of Wnt/ β -catenin essential for cardiac mesoderm while its inhibition or transient activation is fundamental for heart differentiation from mesoderm.
BMP	Involved in the early development of the heart by promoting mesoderm over endoderm, as well as at later stage for cardiac specification of mesoderm.
NODAL	Promote cardiac mesoderm formation and seems to have a possible role in mesoderm-to-cardiac differentiation.
FGF	Synergizes with nodal/activin A signaling for mesoderm formation and with BMPs for mesoderm-to-cardiac differentiation.
NOTCH	Promotes cardiovascular mesoderm to cardiomyocytes.

Table 1.2 Summary of signaling pathways involved in heart development. The involvement of the listed pathways in cardiac differentiation has been discovered by experimental studies on different models such as drosophila, mouse, zebrafish, hPSC, ESC, Xenopus and chick. BMP = bone morphogenetic protein; FGF = fibroblast growth factor (133,140–143).

For recapitulating cardiac differentiation *in vitro* with hiPSC, different approaches and protocols have been used so far. Each of them includes a different time sequence and concentration of various growth factors that affect the previously explained pathways. Among those, we can find the commonly used molecules CHIR99021 as GSK3 inhibitor, Inhibitor of WNT Production-2 and -4 (IWP2 and IWP4) both Wnt inhibitors, BMP, FGF and Activin A (144). The concentration and time point of those molecules can vary depending on the method used. So far, the three prevalent cardiac differentiation methods that have been established are: embryoid bodies (EB), monolayers under guided differentiation and inductive co-culture.

Embryoid bodies

This method allows to obtain three-dimensional cell aggregates facilitating the differentiation process towards cardiomyocytes. Upon dissociating hiPSC cultures into individual cells and aggregating them, typically through the hanging drop method, they transformed into spherical structures comprising an inner layer resembling ectoderm-like cells and a singular outer layer of endoderm. The formed structures, akin to early post-implantation embryos, represent the EB. Cardiac differentiation is then induced by addition of differentiation media containing the grow factors and signaling molecules listed before. Subsequently, the EB are then transferred to coated culture dishes for adherence and cardiomyocytes maturation (132,145,146).

Monolayers under guided differentiation

An alternative approach for differentiation of hiPSC is represented by cells grown as monolayers. In this case, hiPSC are cultured in a feeder-free culture system and cardiac differentiation is induced by addition of the specific grow factors listed before. After the differentiation is accomplished, cardiomyocytes are then dissociated and replated at desired densities for further maturation before the experiments (147–149).

Inductive co-culture

In this case the protocol take advantage of the signaling cues from other cell types that naturally promote cardiac differentiation. A common approach is, for example, co-culturing hiPSC with endodermal, mesodermal or END-2 cell types, which provide essential signals for cardiomyocyte specification. However, this type of has low purity of cardiomyocytes (150).

1.3.5 Subtypes specific differentiations of hiPSC

HiPSC discovery introduced a great source for cardiac research studies. However, for advancing our understanding on chamber-specific diseases, it is fundamental to direct hiPSC differentiations into subtype specific cardiomyocytes. Indeed, human atrial cardiomyocytes exhibit different molecular, mechanical, and physiological properties compared to ventricular cardiomyocytes. For instance, adult ventricular cardiomyocytes are enriched of the myosin heavy chain 7 (*MYH7*) (151) and myosin light chain-2 (*MYL2*) (152), as well as of the transcription factors Iroquois homeobox 4 (*IRX4*) (153) and Hairy/enhancer-of-split related with YRPW motif protein 2 (*HEY2*) (154). While atrial cardiomyocytes express mainly the myosin isoform myosin light chain 7 (*MYL7*) (155) and myosin light chain 4 (*MYL4*) (156), and the transcription factor natriuretic peptide A (*NPPA*) (157). Those molecular differences are also followed by specific electrophysiological features for the two chamber-specific cell types. For example, human atrial

cardiomyocytes exhibit a shorter APD compared to ventricular cardiomyocytes, as well as slower conduction velocity resulting from variations in gap junction distribution and expression (158). Additionally, atrial cardiomyocytes demonstrate different calcium handling capacity (159), characterized by faster calcium release and uptake in comparison to ventricular cardiomyocytes.

In 2011, Zhang et al. explored for the first time the possibility to differentiate human embryonic stem cells into ventricular and atrial cardiomyocytes subtypes by modulating the retinoic acid signal (160). The significance of the regulatory factor retinoic acid (ATRA) in the specification of cardiomyocyte subtypes arises from its role in modulating key transcription factors that are critical for atrial development. Including NK2 transcription factor related locus 5 (NKX2-5), T-Box Transcription Factor 5 (TBX5), Nuclear Receptor Subfamily 2 Group F Member 1 (NR2F1), and Nuclear Receptor Subfamily 2 Group F Member 2 (NR2F2). The latter two transcription factors possess direct binding affinity to the regulatory DNA sequences of ion channel genes Potassium Voltage-Gated Channel Subfamily A Member 5 (KCNA5) and Potassium Inwardly Rectifying Channel Subfamily J Member 3 (KCNJ3), thereby imparting distinctive electrophysiological properties to atrial cells (161). Many of the aforementioned functional properties have been selected as readouts from those laboratories that in recent years wanted to investigate the role of ATRA in atrial subtype differentiation of hiPSC (162–165). Interestingly, despite the slightly different protocols and selected readouts, all these studies have in common the result that atrial specification is mediated by

ATRA signaling during the mesoderm stage of development (166). Altogether, the establishment and improvement of atrial-subtype differentiation protocols of hiPSC opened a new chapter for the study of chamber-specific diseases and drug screening.

1.3.6 hiPSC for arrhythmia studies

Despite hiPSC-derived atrial cardiomyocytes (hiPSC-aCM) being an attractive source for arrhythmia studies and personalized medicine, the number of studies that used this cells source for arrhythmia investigations is still limited. The first study was performed in 2017 from Marczenke et al. using genetically engineered hiPSC-aCM. Their goal was to model a hereditary form of AF correlated to the mutation of *KCNA5* (167). Atrial Kv1.5-deficient cardiomyocytes, differently to ventricular Kv1.5-deficient cardiomyocytes, revealed alterations in functional features. For the first time, hiPSC-aCM have been demonstrated to recapitulate specific arrhythmia mechanisms, mimicking clinical conditions. Furthermore, the different behaviour of the two cardiomyocytes subtype underlined the importance of using chamber-specific cardiomyocytes for disease model.

So far, only two studies used rapid pacing on multicellular sheets to study re-entries mechanisms in atrial arrhythmias. The first one by Laksman et al. used an EB-based differentiation protocol of hESC to atrial cardiomyocytes (168), while the second one by Thorpe et al., used a guided differentiation protocol on hiPSC

monolayers (169). Electrophysiological features of the differentiated atrial cardiomyocytes of the two protocols did not exhibit major differences (APD₉₀ 247 ± 37 ms in hESC-aCM and 264 ± 37 ms in hiPSC-aCM). However, since the two studies focused on different aspects of rotors behaviour, it is difficult to perform a direct comparison. While the first work focused on conduction velocity (CV = 3.0 ± 0.9 cm/s) and cycle length (CL = 312 ± 30 ms) of rotors, the second one focused on the stability and duration of rotors (22,000 ± 0 ms) and wavefronts (61.5 ± 90 ms). Nevertheless, both studies demonstrated how hiPSC-aCM can be used to study basic electrophysiological mechanisms involved in arrhythmia. Another study on 2019 by Goldfracht et al., experimented the use of engineered heart tissues (EHT) of hiPSC-aCM for disease modeling and drug testing (170). The authors underlined only that atrial and ventricular EHT had different electrophysiological and mechanical characteristics, but also that such a model can be used for investigating pharmacological effects of flecainide and vernakalant, as well as electrical cardioversion for arrhythmia termination. However, due to the fact that the generation of a single EHT requires almost 0.5 million of cardiomyocytes, the cost-effectiveness of this method might have some difficulties for a large-scale scenario (171).

Interestingly, in another study it has been tested whether hiPSC-aCM could be used to mimic specific areas of the heart such as the junction between the pulmonary vein and the left atrium (172), known to be an important mechanism of AF initiation and maintenance (173). In this model the authors found that electrical

conduction could be modulated depending on the geometrical patterning as well as on the cell heterogeneity between hiPSC-aCM and human atrial fibroblasts. Increasing the percentage of fibroblasts led to slower conduction even with low pacing frequencies without rotor formation. However, we need to take into account that this model does not consider the electrophysiological differences that atrial cardiomyocytes and pulmonary vein cardiomyocyte face.

Finally, an combined approach of optogenetics and hiPSC-aCM revealed that 3 Hz chronic tachypacing (7 days) induced an electrical remodeling that led to a decrease of RMP, a shortening of the APD as well as to an increased amplitude of inward-rectifier K^+ current (I_{K1}) and decrease of L-type Ca^{2+} current ($I_{Ca,L}$) (174). This study demonstrated for the first time the ability of hiPSC-aCM to undergo electrophysiological remodeling similar to AF patients.

Overall, hiPSC-aCM held a strong potential for atrial arrhythmia *in vitro* modeling thanks to their possibility of generating chamber-specific cardiomyocytes obtained from patients for personalized disease modeling and drug screening (94). Regrettably, the widespread use of hiPSC-aCM as a model for studying arrhythmia mechanisms, has been hindered by challenges. These challenges include the immaturity (175) and cell heterogeneity (176) of obtained hiPSC-aCM, as well as limitations such as cost-effectiveness and scalability. Additionally, the necessity for optimizing each stem cell line and the notable variability observed between differentiations of the same line have constrained the practical application of hiPSC-aCM models in the investigation of human disease.

1.4 Cardiac optogenetics

As explained in the paragraph “1.1.3 Therapies for AF” the current available treatments for AF have a modest efficacy and high risk of cardiac and not cardiac side-effects. Since AF is characterized by rapid and irregular rhythm and self-sustained remodeling, future therapies need to visualize, perturb and control cardiac activity before AF-induced remodeling reaches irreversible points. Optogenetics synergizes optical and genetic engineering strategies to facilitate for example the light-driven sensing and manipulation of electrical activity, delivering unmatched spatiotemporal precision and functionality. Interestingly, the expression of optogenetic proteins in targeted cells and their light-induced activation gives us the ability to perturb and monitor biological functions in a no-invasive way and with a spatiotemporal resolution that has never been matched by other approaches (electrical, mechanical or chemical) (177). The first application of optogenetic tools for rhythm control of the heart belongs to the 2010 (178). Since then, the field grown with an impressive interest over the past decade. Interestingly, the application of optogenetics to hiPSC offered immediate translational opportunities for high-throughput systems that enable swift testing and exploration of novel drugs and therapies (179) (107)(180). In a clinical prospective, optogenetics opened a new chapter for possible cardiac rhythm control tools in patients, as well as for a precise autonomic neuromodulation, and painless defibrillation. However, for such

translational applications, challenges like safe delivery, cell-specific expression and opsins with light deep within the tissue still need to be overcome (177).

1.4.1 Optogenetic actuators in cardiac research

Among the light-activated effector proteins, also called optogenetic actuators, we can find four different types: light-driven pump, channelrhodopsin (ChR), light-activated K^+ conductance silencer and K^+ -selective channel (KCR). Each one with differences concerning their origin, ion selectivity and kinetics. The aim of this particular section is to elucidate the characteristic of each channel type also represented in Figure 1.9.

Light-driven ion pumps

Light-driven ion pumps are microbial rhodopsins that, upon light activation, induce an active transport of ions against the transmembrane gradient. More specifically, light-driven ion pumps can be categorized in three types: light-driven proton, sodium and chloride pumps. The light-induced activation of the first two types leads to an outward transport of protons and sodium respectively. While the light-driven pumps drive inward transport of chloride anions. Thanks to their mechanism of action, when expressed in excitable cells such as cardiomyocytes, the light activation of those pumps causes hyperpolarization of the cell membrane with consequent AP inhibition (181,182). Among the light-driven ion pumps that have been tested in

cardiac research we can find the halorhodopsin chloride pump from *Natronomonas pharaonis* (NpHR) (183,184) and the archaerhodopsin proton pump from *Halorubrum sp TP009* (ArchT) (185).

Channelrhodopsins

Channelrhodopsins, also abbreviated as ChR, are microbial rhodopsins that, differently from the ion pumps, upon light activation mediate a passive ion flux along the electrochemical gradient. ChR can be separated in two different groups: cation ChR and anion ChR. In the case of cation-selective ChR, their light-induced activation leads to a conduction of protons, sodium, potassium, calcium, and magnesium ions (186). As result, their activation provokes a depolarizing effect on resting membrane potentials. Among those we can find the Channelrhodopsin-2 (ChR2) from the green alga *Chlamydomonas reinhardtii* (187,188) and ReaChR (189,190). On the other hand, anion-selective ChR mainly conduct chloride ions under physiological conditions leading to membrane to levels of Cl^- reversal potential. Among those we can find a subgroup of engineered channels such as iChloC and iC+++ and another subgroup of naturally occurring channels such as CtACR1 and GtACR2 from *Guillardia theta* (191–193).

Light-activated K^+ conductance silencer

The light-activated K^+ conductance silencer is a dual-element optical silencer system that consists of photoactivated adenylyl cyclase (PAC) and the compact cyclic

nucleotide-gated potassium channel SthK. Initiating the 'PAC-K' silencer through short bursts of low-intensity blue light demonstrated to induce a strong and reversible suppression of excitation in cardiomyocytes (194). Despite their minor consequences on resting membrane potential on cardiomyocytes, the use of this tool is limited by its slow kinetics. Indeed, with a short light pulse of 10 ms AP in primary cardiomyocytes was inhibited for an extended time periods of 283 ± 43 s.

K⁺-selective channel

The K⁺-selective channel (KCR) is a new class of natural occurring Kalium Rhodopsin with higher selectivity to K⁺. The first ones that have been discovered are the KCR from *Hyphochytrium catenoides* KCR1 and KCR2 (*HcKCR1* and *HcKCR2*, respectively) (195). Both channels upon light activation demonstrated a pronounced preference for K⁺ over Na⁺. However, *HcKCR1* showed a larger current amplitude and higher K⁺ selectivity compared to *HcKCR2*. Another naturally occurred KCR channel is WiChR channel from *Wobbia Lunata* (196). WiChR, together with *HcKCR1* and *HcKCR2*, is a K⁺ selective channel that induce an outward current in physiological conditions. However, previous studies from our collaborators on human embryonic kidney (HEK) cells highlighted the differences concerning photocycle kinetics and membrane hyperpolarization (196), indicating an improved K⁺ selectivity and light sensitivity of WiChR compared to both *HcKCR* channels. So far, none of these three channels have been tested in cardiomyocytes.

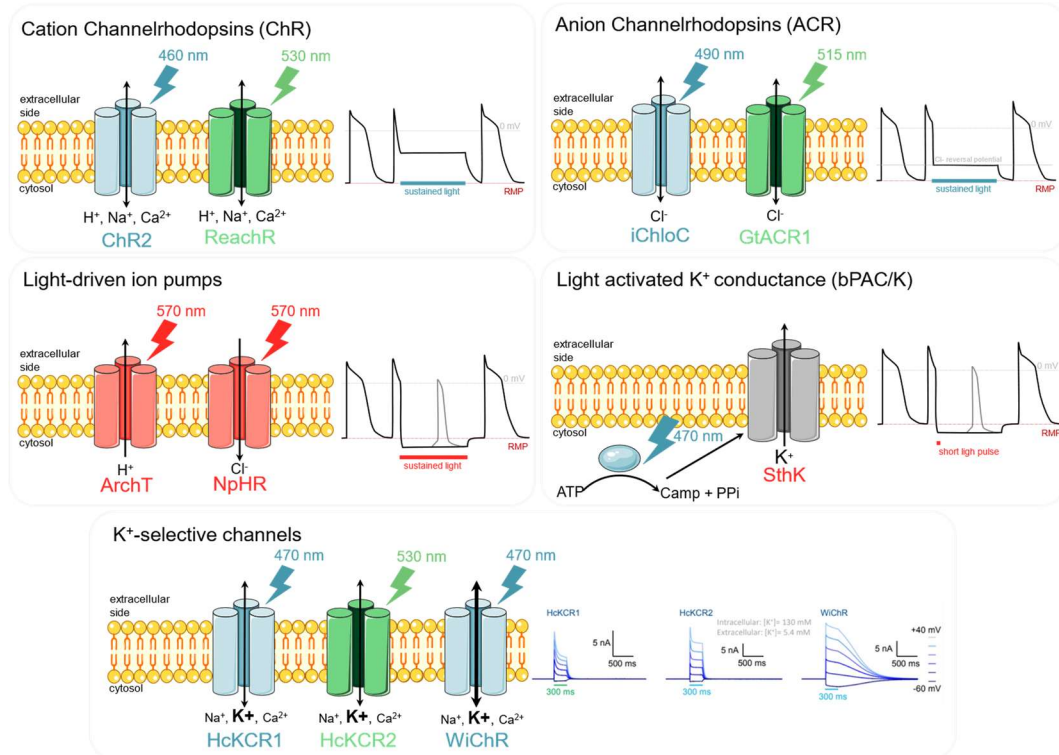


Figure 1.9. Representation of different optogenetic actuators and their effect on cardiomyocytes. Comparison of cation channelrhodopsins, anion channelrhodopsins, light-driven ion pumps and light-activated K^+ conductance (bPAC/K) and their effect on membrane potential in cardiomyocytes.

1.4.2 Applications in arrhythmia studies

The potential of optogenetic approaches relies on its ability to target specific locations and cell types in the heart with a highly precise and sensitive mechanisms of action. The resulting depolarization or hyperpolarization provoked by the light-induced ion flux offers a great therapeutic potential for optical pacing and optical defibrillation for arrhythmia termination (197,198).

Optical pacing

Among the various optogenetic actuators, ChR2 is the one that has been the most extensively used for optical pacing. Indeed, its light-induced depolarization on genetically engineered cardiomyocytes offered a great opportunity to triggers and control AP. Previous studies on hiPSC and 3D-engineered heart tissues demonstrated how ChR2 opening allowed intermittent tachypacing in a long-term stimulation (199). Its application permitted to overcome the strong limitations of electrical tachypacing due to electrodes oxidations and radical generation over prolonged activation periods. However, ChR2 showed strong desensitization properties when activated at high frequencies (199). Such limitation has been overcome by the use of the Channelrhodopsin variant f-Chrimson, allowing a 3 Hz tachypacing over one week to study electrophysiological remodeling in hiPSC-derived atrial cardiomyocytes (174). Another application for ChR2-induced optical pacing has been cardiotoxicity screenings (200).

Optical defibrillation

Optogenetic tools possess the capability to terminate atrial arrhythmia, contributing to an enhanced comprehension of arrhythmic mechanisms within the scientific community. This advancement also facilitates the refinement of defibrillation therapy through the optimization of location, geometries, and light levels in a minimally invasive approach. So far, the use of ChR2-induced depolarization in cardiomyocytes has been used in different protocols to stop arrhythmic re-entries.

Such mechanisms were possible by using longer light pulses that lead to a suppression of effective repolarization and thereby extending the period of Na⁺ channel inactivation (201). The different approaches combined different light levels, geometries and locations. A first study demonstrated how illumination of the whole epicardial surfaces of ChR2-expressing mouse heart could stop ventricular tachycardia (202). Afterwards, it has been demonstrated how a protocol of three-barrier patterns had the capacity of terminating tachycardia, but with the advantage of using a much lower irradiation energy (203). Subsequent studies showed that arrhythmia termination was feasible in the atrium too (204,205). Interestingly, another study explored the ability to terminate arrhythmia by pacing the excitable region between re-entry wavefronts. While Biasci et al., demonstrated for the first time how sub-threshold depolarization by low-intensity illumination led to cardiac alternans with consequent re-entry termination (206).

1.5 Summary and Outlook

As we embark on this investigative journey, it becomes clear that AF is not only a prevalent cardiac arrhythmia but also a multifaceted one, with significant clinical implications. This thesis has navigated through the intricate landscape of AF, from its clinical manifestation and epidemiology to the complex interplay of electrophysiological, structural, and immune remodeling processes that underpin its pathophysiology.

The prevalence of AF, affecting millions globally and poised to double in incidence over the coming decades, underscores the urgency in advancing our understanding of this condition. We delved into the diverse stages of AF – paroxysmal, persistent, and permanent – each characterized by distinct patterns and durations of arrhythmic episodes and highlighted the crucial role of genetic predispositions and comorbidities in the disease's onset and progression.

This introduction further explored the molecular and cellular mechanisms at play in AF, shedding light on the pivotal contributions of ion channel dysfunctions, gap junction remodeling, and the complex interactions between cardiomyocytes, fibroblasts, and immune cells. The nuances of these interactions not only facilitate the perpetuation of AF but also complicate its therapeutic management.

In addressing therapeutic strategies, we reviewed the current state of antiarrhythmic drugs and catheter ablation techniques, acknowledging their limitations and the need for more targeted and effective treatments. This need has led to the exploration of innovative approaches, notably the utilization of human induced pluripotent stem cells (hiPSC) and optogenetics in cardiac research. These cutting-edge methodologies offer unprecedented opportunities for personalized medicine, disease modeling, and the development of novel therapeutic interventions.

As we move forward in this thesis, we aim to build upon this foundation, delving deeper into the mechanistic intricacies of AF and exploring the potential of hiPSC and optogenetics as transformative tools in the quest to decipher and ultimately conquer atrial fibrillation. By bridging gaps in our current understanding and harnessing the power of these emerging technologies, we endeavor to contribute to a future where the burden of AF is significantly alleviated, both clinically and socially.

Hypothesis & Aims

Hypothesis

HiPSC represents a great tool for disease modelling and pre-clinical testing of new possible therapies. The interest in hiPSC for atrial arrhythmia studies broadly increased thanks to the establishment of new protocols to differentiate hiPSC into chamber-specific cardiomyocytes, such as hiPSC-aCM. As demonstration, initial studies showed how hiPSC-aCM were able to recapitulate some specific arrhythmia mechanisms, with particular interest in electrophysiological remodeling. However, none of the studies performed so far with hiPSC-aCM focused on the initiation of molecular remodeling that cardiomyocytes undergo during AF. Furthermore, differentiated hiPSC-aCM offer a great opportunity to study molecular remodeling mechanisms of cardiomyocytes in a controlled manner, without interferences from other cell types present in atrial tissue. A condition that is essential to understand the participation of each specific cell type, cardiomyocytes in this case, to AF initiation.

For these reasons, **the first hypothesis of this study is that monolayers of hiPSC-aCM under fibrillatory activity recapitulate properties of AF patients, allowing us to study the molecular remodeling that occurs during AF initiation and maintaining.** Such phenomenon would allow us to understand whether fibrillatory cardiomyocytes, without the presence of fibroblasts and immune cells, were a sufficient condition to modify molecular pathways related to structural and immune remodeling.

Additionally, thanks to its ability to overcome problems related to electrical pacing, since its discovery optogenetics quickly became an extraordinary tool for control and perturbation of cardiomyocytes. A series of studies, indeed, explored the possibility of these tools to terminate arrhythmia. Their success opened a new chapter for future applications of optogenetic tools as alternative options to ablation therapies and cardioverter defibrillators. However, further in deepen characterization of optogenetic actuators in pre-clinical models still need to be carefully performed. Among the last optogenetic actuators that have been discovered we can find the light-gated K^+ selective channels *HcKCR1*, *HcKCR2* and *WiChR*. Three tools that, thanks to their K^+ selectivity, could serve as potent tools for arrhythmia termination, counteracting the Na^+ inward currents and establishing a new equilibrium without major changes in resting membrane potential. Their ability to perturbate AP shape and propagation, however, has not been studied yet.

For these reasons, **the second hypothesis of this thesis is that activation of the optogenetic actuators *HcKCR1*, *HcKCR2* and *WiChR* in hiPSC-aCM monolayer can induce a K^+ current able to terminate AP formation and conduction. At the same time, we wanted to elucidate if the increased selectivity of *WiChR* to K^+ with consequent larger current amplitude induced a stronger AP inhibition effect compared to *HcKCR1* and *HcKCR2*.**

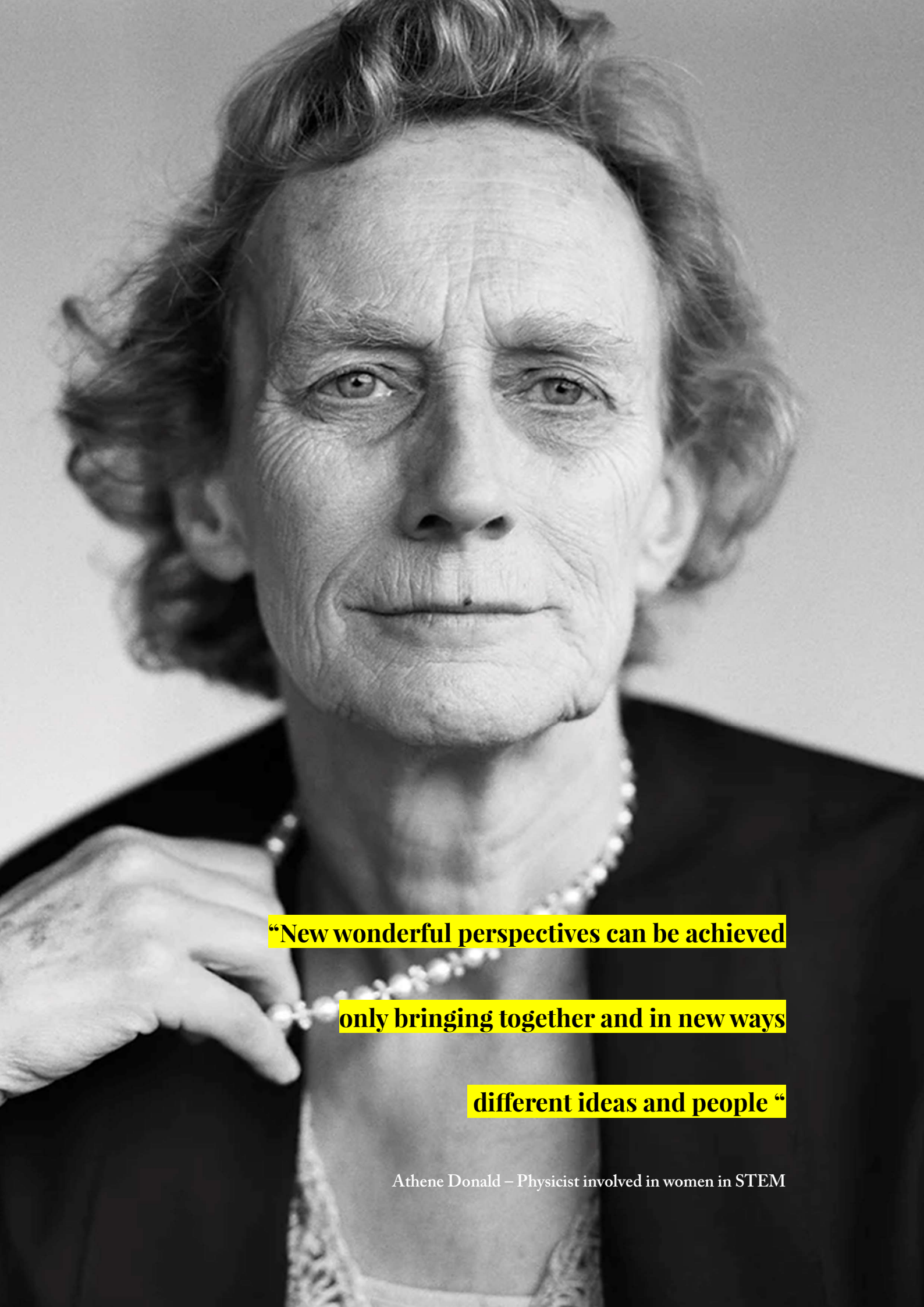
Aims

In order to study the ability of hiPSC-aCM sheets upon fibrillatory activity to undergo molecular remodeling mechanisms similar to those encountered in AF patients, we planned the following objectives:

1. **Development of a Differentiation Protocol.** Our first objective is to develop a reliable and repeatable protocol for differentiating hiPSC into atrial-like cardiomyocytes. This protocol will be applied to two distinct hiPSC lines. The differentiated cells will be comprehensively characterized in terms of their molecular, electrophysiological, and mechanical properties to ensure their resemblance to native atrial cardiomyocytes.
2. **Analysis of AF Re-entry Mechanisms.** The second objective involves determining the minimal surface area necessary for hiPSC-aCM sheets to spontaneously develop re-entry mechanisms, akin to those seen in AF. This phenomenon will be evaluated using optical mapping techniques, providing insights into the spatial dynamics of arrhythmic activity.
3. **Gene Expression and Pathway Analysis:** Our third objective is to analyze the changes in gene expression and cellular pathways in hiPSC-aCM sheets under conditions of fibrillatory activity. This analysis will be compared to hiPSC-aCM with linear signal propagation, aiming to isolate the molecular signatures specific to AF-like conditions.

On the other hand, to assess the effect of the optogenetic actuators *HcKCR1*, *HcKCR2* and *WiChR* in hiPSC-aCM, we planned the following objectives:

1. **Transfection Efficiency with Optogenetic Actuators:** Our initial goal here is to achieve efficient transfection of hiPSC-aCM with optogenetic actuators - *HcKCR1*, *HcKCR2*, and *WiChR* - using lipofectamine. The success of this transfection will be pivotal for subsequent experiments.
2. **Assessment of Action Potential Modulation:** The final objective is to investigate the extent to which prolonged exposure to light impacts the action potentials in hiPSC-aCM transfected with these optogenetic actuators. We aim to determine the differences in action potential inhibition among *HcKCR1*, *HcKCR2*, and *WiChR*, focusing particularly on the enhanced selectivity and amplitude of the K⁺ currents mediated by *WiChR*.



**“New wonderful perspectives can be achieved
only bringing together and in new ways
different ideas and people “**

Athene Donald – Physicist involved in women in STEM

Material & Methods

3.1 Cell culture

For this thesis two different hiPSC lines were used and differentiated into both ventricular and atrial cardiomyocytes. Each cell culture method from hiPSC reprogramming to cardiomyocytes maturation will be described in detail in the following paragraphs.

3.1.1 Selection of hiPSC lines

Foreskin dermal fibroblasts were obtained from pediatric patients of 9 and 2.5 years with no known pathologies. One hiPSC line was generated at the Centro de Medicina Regenerativa in Barcelona using sendai viral infection (CytoTune –iPS 2.0 Sendai reprogramming kit, A16517 life technologies) with ectopic expression of 4 transcription factors (Oct4, Sox2, Klf4 y c-Myc). The second hiPSC line used was obtained from a neonate healthy individual patient through ATCC. Fibroblasts were reprogramed following the method reported by Yu in 2007 (207), a lentiviral vector expressing Oct4, Nanog, Lin 28 and Sox2 genes was used. In this case, the cell line was generated at the Centro Nacional de Investigaciones Cardiovasculares.

3.1.2 hiPSC maintaining

Two hiPSC lines from healthy donors were maintained under feeder-free conditions with mTeSRTM1 medium (Stem Cell Technologies) with changes every second day and kept at 37°C and 5% CO₂. When the cells reached 80-95% confluency, passage was performed. Ideally, the confluency was reached after 4-5 days, however, the doubling population of hiPSC growth might vary from cell line to cell line. In this section, the description of material and methods will describe the protocol for 6-well plates format. However, in Table 2.1 the respective volume for other plates format and flasks is reported. For passaging, plates were coated with 1 mL of cold Matrigel Matrix (Corning) and kept in the incubator for at least 1 hour (alternatively, plates were prepared the day before and kept in a cold room overnight).

PLATE SIZE	MATRIGEL VOLUME	MEDIUM VOLUME
12-WELL PLATE	0,5 mL/well	1 mL/well
6-WELL PLATE	1 mL/well	2 mL/well
T25 FLASK	3 mL/flask	6 mL/well

Table 3.1 Appropriate matrigel coating and medium volume that have been used for culturing hiPSC depending on the different well sizes.

Once the coat was ready, mTeSRTM1 Culture Medium and Disgregation Buffer (EDTA-based, ThermoFisher) were prewarmed to 20-25°C. The Matrigel was aspirated from the precoated culture plates, and a 1 mL volume of mTeSRTM1 Culture Medium was added to avoid the coating dries out. Meanwhile, a 15mL falcon with 2 mL of mTeSRTM1 medium was prepared for each well that needed to be dissociated. This medium would be used later for detaching the cells after enzyme addition. The disgregation started by aspirating the medium of hiPSC, carefully washing with 1 mL Disgregation Buffer and finally adding 1 mL of Disgregation Buffer for an incubation of 3-5 minutes with minimal movement. The optimal incubation time was determined for each cell line; however, it was observed that the longer the incubation was, the smaller the cell clumps were.

Once the clumps of hiPSC started to desegregate and the borders of single cells were visible, the Disgregation Buffer was aspirated, and cells were rapidly washed off with the 2 mL previously prepared medium. For this step, a p1000 pipette was used and settled at 250 µL. Excessive pipetting was avoided in order to keep small clumps intact. At this point, the desired amount of hiPSC was plated into the prepared matrigel-coated plates performing a split ratio of 1:3. This ratio could be adjusted depending on the time the cell line requires to reach the confluency and it could depend on the hiPSC line itself. However, a ratio under 1:3 and over 1:10 was not indicated to keep the pluripotency. After plating the desired amount, cells were carefully shaken for an homogenous distribution and then incubated at 37°C and 5% CO₂. The medium was changed every two days with 2 mL of fresh and pre-

warmed mTeSR™1 Medium and cells were checked everyday to ensure both morphology and confluency.

3.1.3 hiPSC subtype differentiation

The matrigel coating was prepared as previously described. mTeSR™1 medium as well as Accutase Disgregation Reagent (Thermo Fisher) were prewarmed. Also in this case, a 15 mL falcon with 2 mL of mTeSR™1 medium was prepared for each well that needed to be dissociated. For hiPSC differentiation plating, Accutase was preferred respect to EDTA-based Disgregation Buffer. Indeed, to prepare the differentiation plate it is ideal to obtain a homogeneous population of single cells instead of clumps. To start the splitting the medium was aspirated, cells were carefully washed with 1 mL EDTA and finally incubated with 500 μ L Accutase for 3-5 min. However, the optimal incubation time was determined for each cell line. During this time of enzyme disgregation, minimal movement of the plate was indicated.

When the hiPSC colonies were dissociated up to single cells, the 2 mL medium previously prepared in the 15mL falcon were added using a p1000 pipette. The same tip was used to desegregate the cells, but without excessive pipetting. Afterwards, cells were placed into a 15mL falcon and centrifuged at 200 g for 5 min. Once the centrifuge was done, the supernatant was aspirated, and 1 mL of pre-warmed medium was added. At this point, a p1000 pipette was used in order to

obtain an homogeneous population of single cells. Cells were diluted up to 5 mL with a serological pipette and then counted.

At this point, the desired number of cells was plated following Table 2.2 in order to have the respective number of cardiomyocytes at the end of the differentiation. Considering that the optimal seeding density for plating is cell line-dependent; the cell number might vary in the range between 15,000-26,000 cells/cm².

PLATE SIZE	N OF HIPSC PLATED	N OF CMS OBTAINED
12-WELL PLATE	60,000 – 100,000	1 million
6-WELL PLATE	150,000 – 260,000	2-4 million
T-25 FLASK	1 million	20-25 million

Table 3.2 Appropriate number (N) of hiPSC to plate to start a differentiation and the respective number of cardiomyocytes (CMs) that can be obtained from it.

The mTeSRTM1 medium was changed every two days and, when cells reached 80-95% of confluency, differentiation was started. The optimal cell confluency was crucial for a successful differentiation and was determined empirically for each cell line. The following timeline, as well as Figure 3.1 explain in detail each step performed for both ventricular (hiPSC-vCM) and atrial differentiation (hiPSC-aCM).

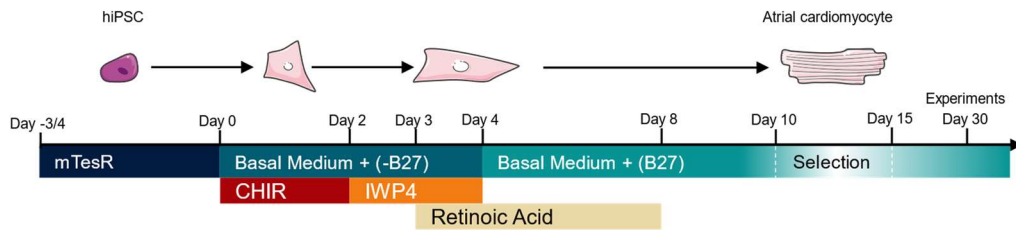


Figure 3.1 HiPSC cardiac differentiation. Timeline of hiPSC differentiation and experiments.

When mentioned “basal medium”, we referred to the medium composed by Roswell Park Memorial Institute (RPMI) 1640 with Glutamax and HEPES (Thermo Fisher Scientific) and 0.2 mg/mL L-ascorbic acid 2-phosphate (Sigma-Aldrich). For all the steps 2 mL medium were used in one well of a 6-well plate. The following part describes each step for both atrial and ventricular differentiation:

Day 0-2

The mesoderm induction was started by adding the basal medium supplemented with B-27 Supplement Minus Insulin (Thermo Fisher Scientific) and 6 μ M of CHIR99021 (StemCell Technologies) and keep it for two days.

Day 2-4

After the two days of mesoderm induction, the medium was aspirated, cells were washed with pre-warmed phosphate buffered saline (PBS) and a new freshly prepared basal medium with B-27 Supplement Minus Insulin and 5 μ M of IWP4 (StemCell Technologies) was added and kept for other two days. For atrial differentiation, 1 μ M of retinoic acid was added directly to the medium on day 3.

Day 4-6

Subsequently, the medium was aspirated, and the cells were treated differently following ventricular or atrial differentiation. Indeed, for ventricular differentiation cells were washed with pre-warmed PBS and was added a freshly prepared basal medium with B-27 Supplement Minus Insulin. For atrial differentiation the same steps were taken, but with the addition of 1 μ M retinoic acid in the medium.

Day 6-8

Afterwards, for ventricular differentiation the medium was carefully aspirated and a basal medium supplemented with B-27 Supplement Minus Insulin was added. While for atrial differentiation the same step was taken, but with the addition of 1 μ L/mL retinoic acid in the medium.

Day 8-10

On day 8, for both ventricular and atrial differentiation cells were washed with pre-warmed PBS and the medium was changed with basal medium supplemented with B-27 Supplement and cells were kept with this medium for two days.

Day 10-15

At this point, on day 10 the cardiomyocyte selection was performed using a medium made of RPMI w/o glucose (Thermo Fisher Scientific) supplemented with 4 mM lactate (Sigma-Aldrich) and changed every second day for a total of 5 days.

Day 15

After medium selection, medium was changed to the basal medium supplemented with B-27 Supplement and changed every two days until the disgregation for replating cells at specific confluency depending on the experiment.

Following this protocol, a first spontaneous contractions of cultures could be observed after 8-10 days of differentiation and robust spontaneous contractions after 10-12 days. When, after 15 days of differentiation, no beating cells were observed, the differentiation was determined as failed.

3.1.4 hiPSC-CM disgregation

Digestion of hiPSC-derived atrial and ventricular cardiomyocytes was performed on day 20 with the aim of plating cells into desired well sizes and at specific cell densities depending on the experiment. For this step, PBS, Accutase and basal medium supplemented with B-27 Supplement, and 20% fetal bovine serum (FBS) were pre-warmed. The plates were pre-coated with Corning Matrigel. As first step, the medium was aspirated, and the cells were washed with PBS. Then 1 mL of Accutase per well was added and incubated at room temperature (RT) up to 30 min until cells started to visibly detach. Depending on cell density, culture conditions, and time point of differentiation, cells might detach after 15 min, but may take up to 30/45 min. To help the detachment process, a soft shake was performed, and cells

were checked every 5 minutes. In case after 30 min there were still big clumps of cells, gentle pipetting was performed using a p1000 in order to obtain single cells. Otherwise, an optional step was to add EDTA for another 5 minutes. To stop the digestion the double of the amount of the supplemented basal medium was added to the Accutase/EDTA mix. Afterwards, gentle pipetting was performed with a p1000, and cells were transferred to a fresh collection tube. The well was then washed another time with the same amount of supplemented medium to collect the remaining cells and add them to the collection tube. Finally, cells were centrifuged at 200 g for 7 minutes. The supernatant was carefully aspirated, and the tube flicked to dislodge the pellet. In case there were still big clumps of cells, the total suspension was strained through a 70 mm or 100 mm mesh cell strainer. Afterwards, cell counting was performed, the matrigel was aspirated from the pre-coated wells and cells were plated according to table 2.3.

PLATE SIZE	N OF CMS TO PLATE
48 WELL PLATE	90,000 – 150,000 cells/well
24 WELL PLATE	250,000 – 400,000 cells/well
12 WELL PLATE	500,000 – 700,000 cells/well
6 WELL PLATE	1-2 million cells/well
10 MM COVERSLIPS	100,000 cells/ well

Table 3.3 hiPSC-CM (CMs) density recommended for specific cell sizes and experiments. In the case of carrying out an immunostaining assay, the cell density was much lower because of the need to obtain single and isolated cells.

3.2 Analysis of cardiac markers

In order to investigate the distinctive features between atrial and ventricular cardiomyocytes, it was necessary to perform a molecular characterization. On the 30th day of the differentiation process, experiments were performed using a variety of highly specialized techniques elucidated in detail below.

3.2.1 RNA extraction and retro transcription

For RNA extraction, a 6-well plate was used and on day 30 of differentiation the cells were kept cold by placing the plates in a tray on ice. A PBS wash was performed, and RLT cell lysis buffer was added. Using a pipette, the lysate was collected in Eppendorf tubes. At this point, the cell lysate could be frozen at -80°C or used to proceed with RNA purification. The commercial column-based RNeasy Plus Mini Kit (Qiagen) was used to purify the RNA according to the manufacturer's instructions. The concentration of the extracted RNA was determined with a NanoDrop ND-1000 spectrophotometer (Thermo Fisher Scientific). The quality of the extracted RNA was determined by the absorbance ratios 260/280, indicating protein contamination, and 260/230, indicating contamination by organic components.

After RNA was isolated and quantified, it was used as a template to obtain complementary DNA (cDNA) by retro transcription. In order to do so, the

PrimeScript RT Reagent Kit (Takara, Kusatsu) was used according to the manufacturer's instructions. The reaction was carried out in an Eppendorf thermal cycler using 1 µg of RNA (whenever possible) in all samples. The time and temperature conditions for the retro transcription were the following: one cycle of 15 min at 37°C, one cycle of 5 sec at 85° and at the end maintained at 4°C. The cDNA was stored at -20°C until real-time quantitative polymerase chain reaction (RT-qPCR) was performed.

3.2.2 Real-time quantitative polymerase chain reaction

The RT-qPCR allows the determination of the relative amount of mRNA between different samples. The previously obtained cDNA was diluted 1:10 with nuclease-free water to prevent reverse transcription reagents from affecting RT-qPCR. The sense and antisense primers used were designed using the Primer-Blast tool (<https://www.ncbi.nlm.nih.gov/tools/primer-blast/>) and purchased from Condalab (Madrid, Spain). The TB Green® Premix Ex Taq™ (Takara) was used to perform RT-qPCR. Each RT-qPCR reaction consisted of 2 µl of diluted cDNA, 0.34 µl of each primer, 2.32 µl of nuclease-free water and 5 µl of Master Mix. Technical triplicates were performed for each sample and gene, as this is a very sensitive reaction and small variations in reagent concentrations can cause significant variations in the results obtained. The reactions were carried out using 384-well plates (Thermo Fisher Scientific) on a Viiia 7 Real-Time PCR System

thermal cycler (Applied Biosystems) using a denaturalization step of 20 minutes at 95°C, a second step of denaturalization and hybridization/extension of 15 s at 95°C and 1 minute at 60°C for 40 cycles and, finally maintained at 4°C. While the primers used in this work are detailed in table 2.5.

GENE	FORWARD PRIMER	REVERSE PRIMER
<i>OCT4</i>	ATGCACAACGAGAGGATTTT	CAGAGTGGTGACGGAGACAG
<i>TNNT2</i>	TCTGAGGGAGAGCAGAGACC	CACCAAGTTGGGCATGAACG
<i>CACNA1</i>	GACCAACTTCTCAGCCGAATA	GTGCAGAGGTGCTCATAGTT
<i>NR2F2</i>	GGAGCGAGCTGTTTGTGTTG	TGGTCCATAAAGGCGACCAC
<i>NPPA</i>	GACAGACTGCAAGAGGCTCC	GCTGCAGCTTAGATGGGATGA
<i>GJA1</i>	GGGTTAAGGGAAAGAGCGAC	CCCCATTCGATTTTGTCTGC
<i>MYL2</i>	AGGCGGAGAGGTTTTCCAAG	GGACCACTCTGCAAAGACGA
<i>IRX4</i>	AAGGGCGAGAAGATCATGCT	CTGCGTTCTTGGAGCTCTTGA
<i>HEY2</i>	CTCGGCGTCCGAGCTTC	GATCCCGACGCCTTTTCTCT
<i>IL16</i>	GCTGGCCTCCCAGGAAGGGA	TCGGGCATGGCCTCTGGAGT
<i>CXCL12</i>	GCCCTTCAGATTGTAGCCCG	GCCCCCTCCCCACGTCTTT
<i>IL18</i>	ATCGCTTCCTCTCGCAACAA	TTCCAGGTTTTTCATCATCTTCA
<i>CXCL8</i>	CACTGCGCCAACACAGAAAT	ATTCTCAGCCCTCTTCAAAAAC
<i>MMP1</i>	GTGTCTCACAGCTTCCCAGCG	GCACTCCACATCTGGGCTGCTT
<i>ICAM1</i>	CTGGTCCTGCTCGGGGCTCT	GGGCTGGTCACAGGAGGTGC
<i>LAMC2</i>	ATACCAGAGCCAAGAACGCT	CTACACTGAGAGGCTGGTCC
<i>VTN</i>	CCTTCTCATACTGGCCCTGC	CTCGTCACACTGGCACTTCT
<i>CDH1</i>	CCGAGAGCTACACGTTC	TCTTCAAAATTCACTCTGCC
<i>IL11</i>	TGACCCGCTCTCTCCTGGCG	GCACGTGCCGCAGGTAGGAC
<i>SDC4</i>	CGGAGTCGCCGAGTCGATCC	GGCTCCCAGACCCTGCCCTC

Table 3.4 List of primers used to analyze the mRNA expression of specific markers. All the primers had a size of around 20 nucleotides and a melting temperature of around 52-58°C.

3.2.3 Flow cytometry

To determine the percentage of hiPSC-aCM and hiPSC-vCM obtained during differentiation, atrial and ventricular markers expression were analysed by flow cytometry. On day 30 of differentiation, cells plated in 6-well plate were detached following the protocol described in 'hiPSC-CM disgregation' (section 2.1.3). After centrifugation, the supernatant was aspirated, and cells were resuspended and fixed with 4% paraformaldehyde (PFA) for 15 min at 4°C. The cells were then centrifuged again, the PFA was aspirated and three washes with PBS were performed. Cells were then blocked and permeabilised with blocking and permeabilization solution made of 0.5% FBS and 0,01% Triton-X100 (Sigma-Aldrich) in PBS for 30 min at RT. Cells were centrifuged, the supernatant removed and incubated with a dilution of 1:200 of the primary antibody against the ventricular isoform of myosin light chain 2 (MLC2v; Abcam), troponin I (cTnI, Abcam) and Chicken Ovalbumin Upstream Promoter Transcription Factor II (COUP-TFII; R&D). Cells were then washed twice with PBS and incubated with the corresponding secondary antibody at 1:200 dilution (anti-mouse Alexa Fluor 488 and anti-rabbit Alexa Fluor 647, Thermo Fisher Scientific) for 1h at RT. The percentage of each marker was determined with FlowJo X software (TreeStar Inc).

3.2.4 Immunostaining

In order to perform a qualitative and further quantitative analysis of atrial and ventricular markers, immunostaining was performed. On day 20 cells were detached following the protocol described in 'hiPSC-CM disaggregation' (section 2.1.3) and seeded into 6-well plate. After 5 days of recovery, cells were detached again and seeded into coverslips at low confluency (see table 2.3) and, on day 30, experiment was performed. For this experiment, cells could not be plated directly on coverslip after the first disaggregation because of the thickness of glass coverslips. In fact, since cardiomyocytes contracts, it is not recommended to keep the too long on coverslips since they would easily detach. The immunostaining protocol was the same that we used for the flow cytometry assays with the difference that a final incubation step to stain nuclei with DAPI (200 ng/mL) for 10 min at RT was added. Coverslips were mounted with FluorSave™ reagent (CalbioChem) and images were acquired with a Leica DM2500 fluorescence microscope (Leica Microsystems) and a confocal microscope (Leica TCS-SP5-AOBS).

3.2.5 Transfection of hiPSC-aCM

Cell transfection was performed in both hiPSC-aCM to express the optogenetic channels HcKCR1, HcKCR2 and WiChR. For transient expression of HcKCR1-mCerulean, HcKCR2-mScarlet and WichR-mScarlet cells were seeded on coverslips of 10 mm diameter at a density of 250,000 cells/cm² and were

transiently transfected with using Lipofectamine Stem Cell Reagent (Thermo Fisher Scientific). Specifically, 6 μL of Lipofectamine Stem Cell Reagent and 1.5 μg of DNA in 100 μL of optimum medium (Thermo Fisher Scientific). The mix was vortexed and left at RT for 10 min. Afterwards, 25 μL of the mix was added in one well of 24-well plate with hiPSC-aCM on coverslips. Cells were kept in the incubator protected from light for 48h. Then the medium was changed and experiments were performed.

3.3 Electrophysiological and mechanical analysis

In order to confirm the distinctive features between atrial and ventricular cardiomyocytes, in addition to the molecular phenotype, it was necessary to perform a functional characterization. Electrophysiological and mechanical analysis were performed in Freiburg (DE) during the secondment at the Department of Cardiovascular Medicine. The work was supervised and led by Professor Ursula Ravens and Doctor Remi Peyronnet.

3.3.2 Patch Clamp for action potential recordings

Cells seeded on coverslips of 10 mm diameter, at day 30 of maturation and a density of 100,000 cells/cm², were placed in a bath imaging chamber (RC-26G, Warner Instruments) at RT. Bath solution was a freshly prepared Tyrode's solution (NaCl 140 mM, KCl 5.5 mM, HEPES 10 mM, MgCl₂ 1 mM, Glucose 10 mM, CaCl₂ 1.8 mM). The solution kept in the fridge only up to one week and, before the experiment, the necessary amount needed for the experiment (around 50 mL) was incubated at 37°C. Single cells were recorded using the patch clamp technique in the whole-cell configuration. Experiments were performed at RT, using a patch-clamp amplifier (200B, Axon Instruments) and a Digidata 1440A interface (Axon Instruments). Recordings were digitized at 3 kHz and low pass filtered at 1 kHz. Cells were stimulated at 0.5 Hz and action potential was analysed with a self-made

MatLab script. Borosilicate made patch pipettes, with an average resistance of 2-3 M Ω , were filled with the internal solution (K-aspartate 130 mM, GTP-Na 2 0.1 mM, HEPES 10 mM, Na²-ATP 5 mM, EGTA 11 mM, CaCl₂ (2xH₂O) 5 mM, MgCl₂ (7xH₂O) 2 mM). The analysis focused on: resting membrane potential (RMP), maximum upstroke velocity and action potential duration at 20%, 50% and 90% of repolarization (APD20, APD50 and APD90).

3.3.3 Sharp electrode for optogenetics experiments

Two days post-transfection, cells were placed in a perfusion chamber (RC-26G, Warner Instruments) under constant flow controlled with a peristaltic pump (Easy-Load II Pump, Masterflex L/S) at 2 mL/min at 35 \pm 2 °C. Temperature was controlled via a flow-through channel (SH-27B, Warner Instruments) and a chamber heater (PH1, Warner Instruments) using a two-channel controller (TC-344B; Warner Instruments). Bath solution was an oxygenated normal Tyrode's solution (NaCl 140 mM, KCl 5.5 mM, HEPES 10 mM, MgCl₂ 1 mM, Glucose 10 mM, CaCl₂ 1.8 mM). Microelectrodes with a resistance of 15-20 M Ω were obtained by pulling glass capillaries (Clark borosilicate with filament, OD 1.00/ID 0.58, 100 mm, Warner Instruments) using a Sutter P-97 micropipette puller (Sutter Instrument) and used to impale cells forming large multi-layered clusters. The microelectrodes, filled with 3 M KCl, were linked to a bridge amplifier (BA-01X, NPI Electronic) via an Ag-Ag-Cl electrode. The reference electrode, situated in the

bath, comprised an Ag-AgCl pellet connected to a wire electrode (E205, \varnothing 1.0 mm, Harvard Apparatus). Micropositioning of the electrode was facilitated using a TSC Sensapex micromanipulator and regulated through an IX70 microscope (Olympus). Recordings, acquired at 50 kHz, underwent a 10 kHz filter using a LabView (National Instruments) custom-made script. Light, emitted by a 460 nm LED using a 460/20 nm bandpass excitation filter, produced a light intensity of up to 3 mW/mm² in the object plane. During spontaneous cell beating, light pulses were managed with a custom-built script (Essel Research and Development). Following functional experiments, hiPSC-aCM were fixed using 4% PFA in PBS for 15 minutes at room temperature (RT). Fixed samples underwent three PBS washes and were stored at 4°C before further processing. Incubation in PBS with 0.1% Tween-20 and 300 nM DAPI for 10 minutes at RT preceded washing three times in PBS for 10 minutes. The samples were then immediately utilized for confocal imaging. hiPSC-aCM expressing HcKCR1-mCerulean, HcKCR2-mScarlet, and WiChR-mScarlet were captured using an inverted confocal microscope (Leica SP8X).

3.3.4 Nanoindentation for mechanical studies

On day 20 cells were digested and plated on 6-well plates and, after 5 days of recovery cells were dissociated again and seeded on coverslips of 10 mm diameter at a density of 100,000 cells/cm². For the experiments, we used the Chiaro Nanoindenter system from Optics11, a technology that provides accurate and

precise measurements of the micro-mechanical properties of small samples and cells. The instrument makes use of a one-piece optical probe that consists of an optical fiber, a cantilever and a sphere. When the probe touches the sample, the cantilever bends, and this displacement is detected by the optical fiber (Figure 4.3). Using interferometry, the instrument can measure the phase of the light detecting the smallest displacement of the cantilever, which in our case was correlated to the spontaneous contraction of hiPSC-CM. Manufacturer's instructions were followed for optical and geometrical calibrations. Cells were kept at 37°C in the same chamber and bath solution used for patch clamp recording. Also for this experiment, the solution was freshly prepared and kept up to a maximum of one week in the fridge. Before the experiment, a small amount of solution (around 50 mL) was pre-warmed.

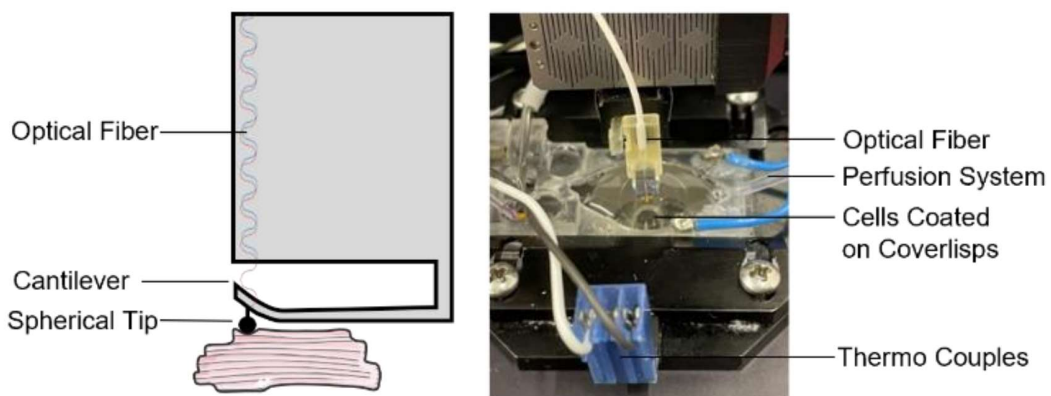


Figure 4.3 On the left a representation of the optical probe used to measure contraction measurements of hiPSC-vCM and hiPSC-aCM. On the right a picture of the set up used for mechanical experiments of hiPSC-CM.

For the recording, a spherical glass tips with 3.0–3.4 μm radius and 0.033 N/m stiffness were used to indent the surface of the cell. Indented cells were first identified by visualization at the microscope (isolated and spontaneously contracting cells) and then manually approached with the probe by 1 μm steps. After touching the cell, the tip was lifted by 7 μm and a displacement of 10 μm was initiated with a speed of 5 $\mu\text{m}/\text{s}$ and, after a 20 s long recording, retracted at the same speed.

3.3.5 Optical mapping experiments

For calcium transient (CaT) imaging, hiPSC-CM were kept from day 20 to day 30 in a cell density of 250,000 cells/ cm^2 in wells with different sizes: 9.6 cm^2 , a well size that we suspected did not allow rotor formation and 0.32 cm^2 , a smaller size that we hypothesized does not maintain re-entries.

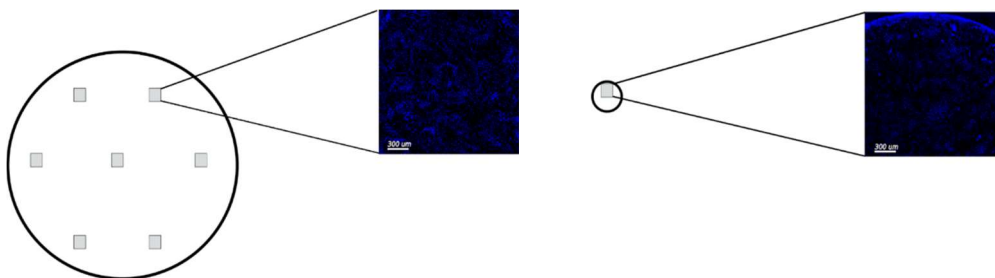


Figure 4.4 Cell nuclei counting of small and large surfaces. On the left large surfaces with grey square representing the portion of the surface where the images for nuclei counting were taken. On the right-side representation of small surface area with corresponding cell counting. DAPI = blue staining.

Cells were dyed by keeping them for 30 min at 37°C with 5% CO₂ in Tyrode solution with rhod 2-AM (Ca²⁺-sensitive probe; Abcam) dissolved in DMSO (1 mM stock solution; 3.3 µl/ml in culture medium) and probenecid (TEFLabs) at 420 µM. After dye incubation, the cells were washed, and the solution was changed to fresh Tyrode solution at 37°C that was also used for the previous electrophysiological experiments. To excite rhod 2-AM, hiPSC-aCM were illuminated with a filtered green light emitting diode (LED) light source: LED CBT-90-G (peak power output 58 W; peak wavelength 524 nm; Luminus Devices), with a plano-convex lens (LA1951; focal length = 25.4 mm; Thorlabs) and a green excitation filter (D540/25X; Chroma Technology). Two such light sources were used to achieve homogeneous illumination. Fluorescence was recorded with an electron multiplying charge-coupled device (Evolve-128: 128 X 128, 24 X 24 µm square pixels, 16 bit; Photometrics, Tucson, AZ), with a custom emission filter (ET585/50 – 800/200M; Chroma Technology) suitable for rhod 2 emission placed in front of a high-speed camera lens (DO-2595; Navitar). The complexity of the arrhythmias was assessed using optical mapping using a custom software written in MATLAB (MATLAB 9.11, MathWorks). Using this script, we assessed the dominant frequency computed as the maximum peak of the spectrum at each pixel, as well as the mean activation period calculated as the inverse of the dominant frequency obtained in each signal.

3.3.6 Optical contraction measurements

Two days post transfection, hiPSC-aCM were transferred to a stage-top incubator, creating a humidified environment at 5% CO₂ and 37 °C (STXF/STX-CO₂O₂) and were allowed to equilibrate for a minimum period of 20 minutes. The incubator was mounted onto an inverted microscope (DMi8, Leica) equipped with a mercury lamp (HXP 120V) coupled via a light guide to the epifluorescence port. The activation light, filtered through a 470/40 nm excitation filter and reflected by a 495 nm dichroic mirror, produced a light intensity of 0.2 mW/mm² in the object plane. A shutter, governed by an externally provided TTL pulse, was used to control the light exposure. Transmission light passed through a 640/20 nm filter, and an additional 630/75 nm emission filter was positioned in front of the camera (Zyla 5.5 ZsCMOS, Andor - Oxford Instruments) to prevent artefacts from the activation light. Using an HC FL PLAN 10×/0.25 objective (Leica), transmission images were captured at 20 Hz with a 50 ms exposure time and 2×2 binning at 500×500 pixels using the AndorSolis software.

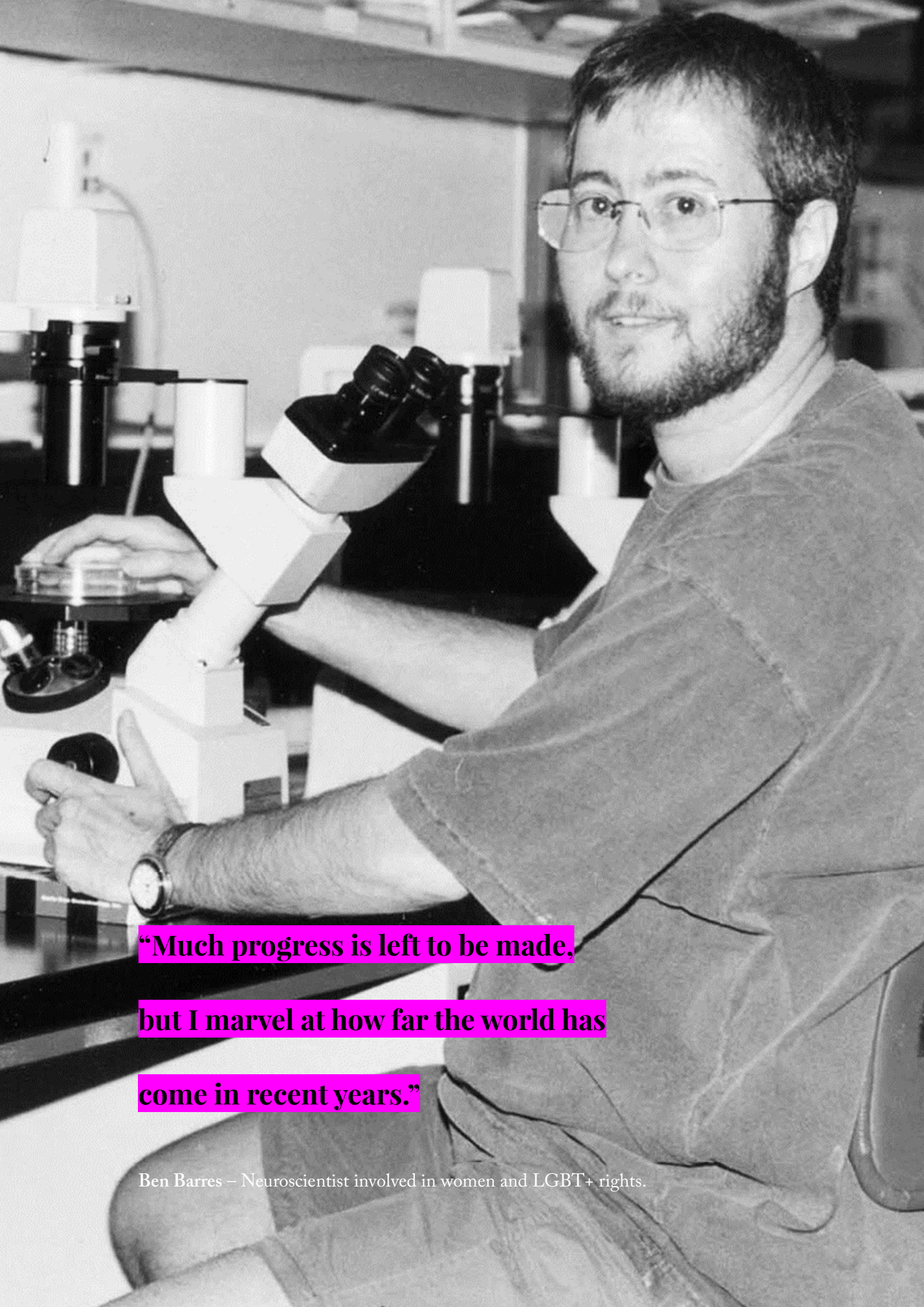
3.4 RNA-seq

For RNA isolation, the protocol described in the paragraph 2.2.1 “RNA extraction and retro transcription” was used. The process of the sample was performed in Leiden (NE) during the secondment in GenomeScan, a company specialized in transcriptomic analysis. The work was supervised by Doctor Sander Tuit.

Samples were processed using the kit NEBNext Ultra II Directional RNA Library Prep Kit for. Briefly, mRNA was isolated from total RNA using the oligo-dT magnetic beads and, after fragmentation of the mRNA, cDNA was synthesized and subsequently used for PCR amplification. For measuring the quality and yield after sample preparation the 5300 Fragment Analyzer (Agilent) was used. The size of the resulting products was consistent with the expected size distribution (a broad peak between 300-500 bp). Clustering and DNA sequencing was performed using the NovaSeq6000 according to manufacturer's protocols. A concentration of 1.1 nM of cDNA was used. Image analysis, base calling, and quality check was performed with the Illumina data analysis pipeline RTA3.4.4. FASTQ files were processed by GenomeScan using Cufflinks v2.2.1 to obtain the count table for each gene. Differential expression analysis of RNAseq expression profiles was performed with iDEP, g:Profiler and ShinyGO. Gene expression differences were considered statistically significant with an adjusted p-value < 0.05 and biologically relevant with an absolute log₂ fold change > 1.

3.5 Statistical analysis

For experiments whose analysis was not previously described, statistical studies were performed with GraphPad Prism 8[®] software (GraphPad Software Inc., La Jolla, CA, USA). We opted to conduct the Mann-Whitney U test, and represent the mean \pm SD, while the significance is represented with *P<0.05, **P<0.01, ***P<0.001, ****P<0.0001. Differences were considered statistically significant at $p<0.05$, with a 95% confidence interval.



“Much progress is left to be made,

but I marvel at how far the world has

come in recent years.”

Ben Barres – Neuroscientist involved in women and LGBT+ rights.

Results

4.1 Characterization of hiPSC differentiation

Although AF stands as one of the most prevalent cardiac arrhythmias, there exists a scarcity of human experimental models that can faithfully reproduce its intricate nature. For this reason, we have opted to explore the potential suitability of hiPSC as an ideal model for studying AF mechanisms. Our objective revolves around establishing a model that can faithfully replicate the general mechanisms underlying common AF, as opposed to those specific to AF caused by genetic mutations. To achieve this, for our investigation we have deliberately chosen two distinct hiPSC lines obtained from healthy donors. We deliberately choose to use two different cell lines in order to introduce a patient variability also in our *in-vitro* model. However, so far most of the protocols for hiPSC differentiation into cardiomyocytes are focused on obtaining a population enriched with ventricular-like cardiomyocytes. Indeed, only few studies investigated the possibility to obtain atrial-like cardiomyocytes from hiPSC. Since this study focuses on atrial arrhythmia mechanisms, the first step of this research was to characterize the pluripotency of our two hiPSC lines, Ctrl1 (hiPSC-CM1) (208) and FiPS Ctrl2-SV4F-1 (hiPSC-CM2) registered at the Spanish National Bank of Stem Cell lines and investigate whether the all-trans retinoic acid treatment (ATRA), essential for atrial subtype differentiation (209), could affect the differentiation success compared to our standard protocol for ventricular differentiations. To do so, we performed in parallel hiPSC differentiation into ventricular-like (ATRA-) and atrial-like cardiomyocytes

(ATRA+) and tracked in time (from day 0 to day 30 of the differentiation) the pluripotency markers. For ATRA- we followed the standard protocol used in our laboratory, which is based on the protocol described by Cyganek et al. (210). Since ATRA+ differentiation was undertaken for the first time in our lab, we adapted the established protocol by Cyganek et al. to our two cell lines (164). Indeed, it has been previously established that the differentiation potential of stem cell lines varies, necessitating the adaptation of protocols to accommodate these individual differences.

First, we fixed undifferentiated cells, and we analysed different pluripotency genes by immunostaining. Images acquired by confocal microscopy revealed that both hiPSC lines nicely expressed octamer-binding transcription factor 4 (*OCT4*) as well as Homeobox protein NANOG (*NANOG*) during their pluripotent stage (Figure 5.1 A). Tracking in time the expression of *OCT4* by qPCR, results showed that its expression was significantly decreased over time (Figure 5.2 B) in both ATRA- and ATRA+ differentiation in both hiPSC lines. Demonstrating that the addition of ATRA from day 3 to day 8 in both hiPSC cell lines differentiation successfully induced a loss of their pluripotency.

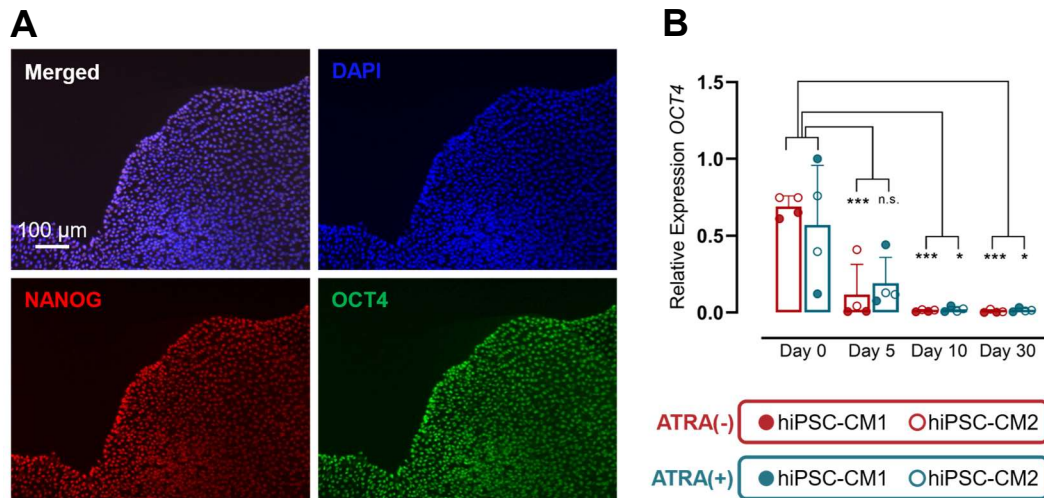


Figure 5.1 Analysis of pluripotent genes expression in hiPSC-CM1 and hiPSC-CM2. (A) representative images of of DAPI staining of nuclei (in blue), *NANOG* (red) and *OCT4* (green) of the undifferentiated cells. (B) Time course from day 0 to 30 of differentiation of *OCT4* expression in both ATRA⁻ (red, n=10) and ATRA⁺ (green, n=4) for both hiPSC lines (full dots correspond to hiPSC-CM1 and empty dots to hiPSC-CM2). Each dot represents an independent differentiation. GAPDH was used as control gene. Statistical analysis was performed using Mann Whitney u Test and represent the mean \pm SD, while the significance is represented with *P<0.05, **P<0.01, ***P<0.001, ****P<0.0001.

During ATRA⁻ and ATRA⁺ differentiation, we could appreciate changes in morphology as showed in Figure 5.2. Cells before starting the differentiation (day 0) were characterized by prominent nucleoli and were forming colonies with defined borders, a morphology characteristic of stem cells. After the mesoderm induction using CHIR99021, a transcription factor that activate the Wnt/ β -Catenin pathway, cell colonies could not be identified anymore. Instead, cells were spread in a monolayer and were characterized by a more yellow color. After addition of IWP4, a transcription factor that induce the cardiac progenitor differentiation by inhibiting

the Wnt/ β -Catenin pathway, cell monolayers had a more intense yellow/brown color. Around day 10 of differentiation 3D agglomerates of cells could be identified, a morphology characteristic of cardiomyocytes. Around this point of the differentiation, cells started showing the first spontaneous beatings. After disaggregation and replating, on day 30 of the differentiation cardiomyocytes morphology was characterized by elongated cells with a large, centered nucleus.

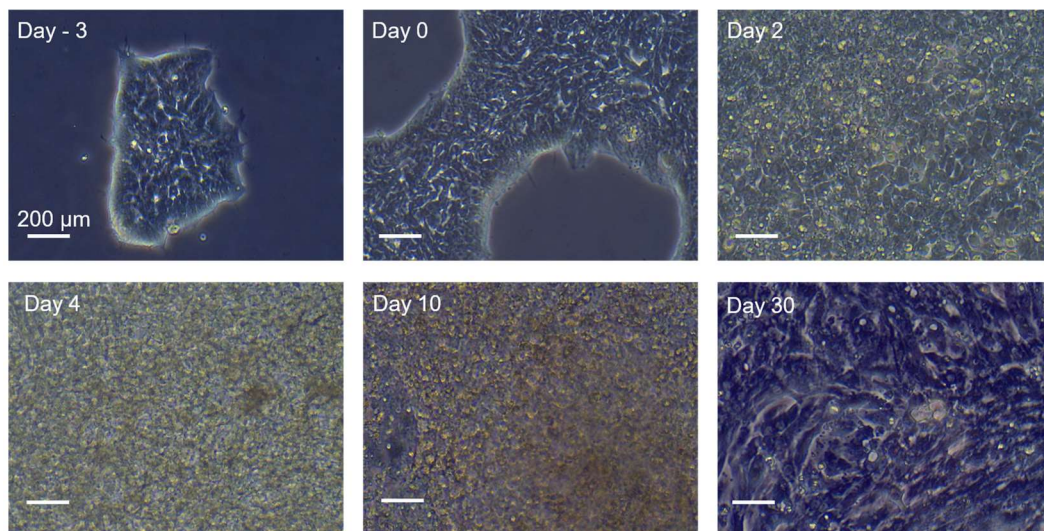


Figure 5.2 Representative pictures at different time point of the differentiation into cardiomyocytes of line hiPSC-CM1. Day -3 represent a colony of hiPSC after 24h of plating, day 0 shows the cell confluency at which the differentiation was started, day 2 represent cells after mesoderm induction, day 4 the cardiac progenitors after inhibition of the WNT pathway and day 10 the beating cardiomyocytes. Day 30 represents the cardiomyocytes after disaggregation and replating.

The mentioned morphology changes were followed by changes in cardiac markers. Indeed, cell types were then analysed by flow cytometry to calculate the percentage of cells positive to Troponin 2 (TNNT2). In this case, experiments were performed both before and after cardiomyocytes selection in order to investigate the

success of the selection process. Results showed that before selection both ATRA- and ATRA+ differentiations had 90% of TNNT2+ cells. While, after selection both populations expressed a percentage of TNNT2+ cells higher than 95%, indicating that the metabolic selection led to an increased percentage of cardiomyocytes in the total population (Figure 5.3 A, B).

A time course by qPCR of *TNNT2* expression at different time points underlined the progressive increased expression of troponin in both cell populations starting from day 5 of differentiations onwards (Figure 5.3 C), the time point in which hiPSC are differentiated into cardiac progenitors. The expression of this important cardiac biomarker was also confirmed by qualitative confocal images performed on day 30 of differentiation (Figure 5.3 D). Indeed, in both cell populations a nice sarcomere structure could be identified. Overall, those results confirmed that hiPSC could be successfully differentiated into cardiomyocytes independently to the introduction of ATRA in the differentiation protocol from day 3 to day 8.

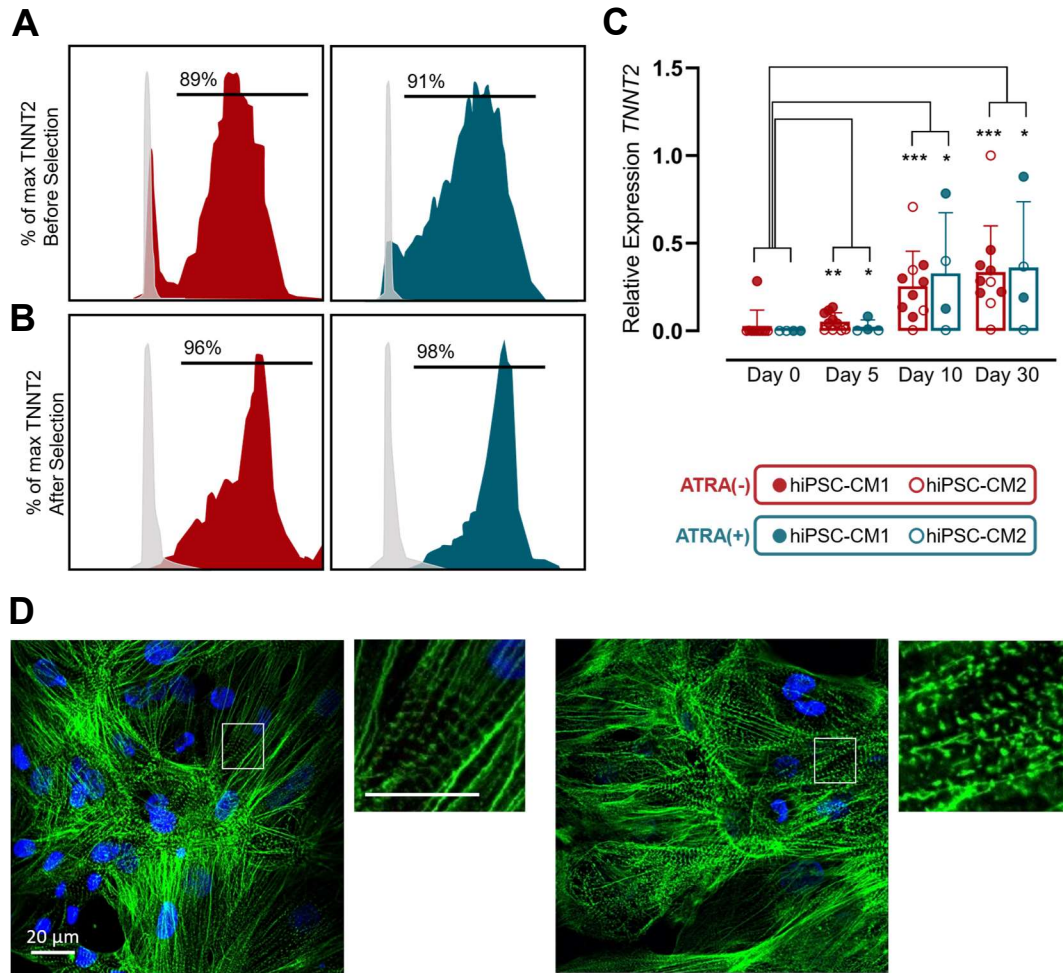


Figure 5.3 Analysis of TNNT2 expression in both ATRA- and ANTRA+ populations. (A) Percentage of TNNT2+ cells in both ATRA- (red) and ATRA+ (green) differentiations, before cardiac and (B) after cardiac selection. (C) Time course of TNNT2 expression in ATRA- (n=10) and ATRA+ (n=4) populations at different time points (Day 0, 5, 10 and 30), *GAPDH* was used as control gene lines. full dots correspond to hiPSC-CM1 and empty dots to hiPSC-CM2. Statistical analysis was performed using Mann Whitney u Test and represent the mean \pm SD, while the significance is represented with * $P < 0.05$, ** $P < 0.01$, *** $P < 0.001$, **** $P < 0.0001$. (D) Images of ventricular (left) and atrial (right) differentiations stained with DAPI staining of nuclei (in blue). and TNNT2 (green).

4.2 Characterization of hiPSC-vCM and hiPSC-aCM

In human myocardium, ventricular and atrial cells exhibit different molecular electrophysiological and mechanical characteristics. Therefore, we investigated whether the ATRA treatment could help us to obtain hiPSC-derived cardiomyocytes with atrial-like features, similar to those observed in the human myocardium.

4.2.1 Molecular characterization of hiPSC-vCM and hiPSC-aCM

To explore the molecular signatures of the differentiated cardiomyocyte subtypes, we selected four ventricular and four atrial markers for investigation using qPCR. Experiments were performed at 30 days of differentiation to assess the molecular phenotype pattern in both cell populations. Results showed that upon ATRA treatment, atrial differentiation exhibited higher expression of the atrial markers *CACNA1D* that encodes the alpha-1D subunit of the voltage-dependent calcium channel (Cav1.3), the Nuclear Receptor Subfamily 2 Group F Member 2 *NR2F2*, the Potassium Inwardly Rectifying Channel Subfamily J Member 3 (*KCNJ3*) and atrial natriuretic peptide (*NPPA*) compared to the ventricular differentiation (Figure 5.4 A). Conversely, cells treated with ATRA showed lower expression of the ventricular markers *GJA1* gene encoding connexin 43 (*Cx43*), myosin light chain 2 (*MYL2*), Iroquois homeobox protein 4 (*IRX4*) and

hairy/enhancer-of-split related with YRPW motif protein 2 (*HEY2*) in comparison to the not treated cells (Figure 5.4 B).

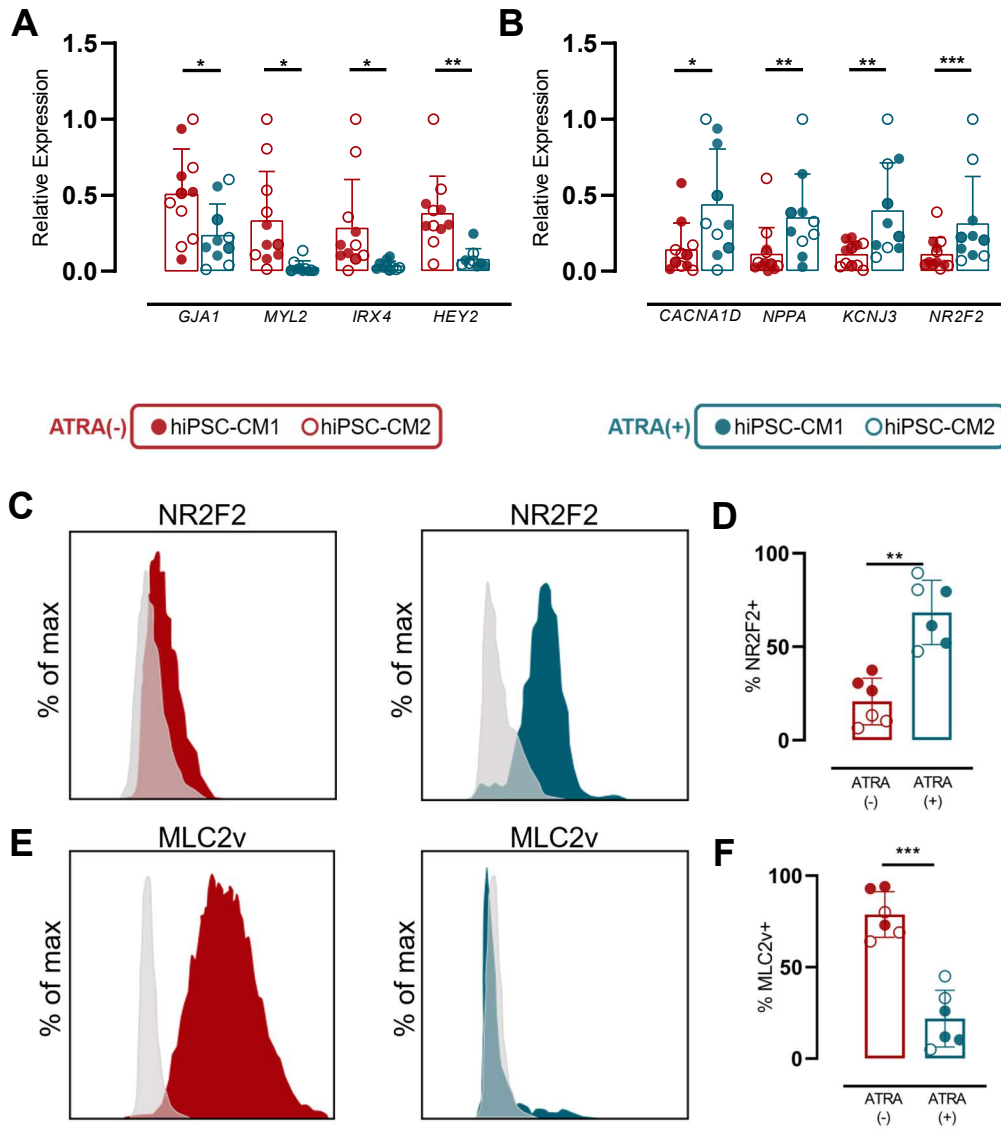


Figure 5.4 Expression analysis of ventricular and atrial markers in both ATRA⁻ and ATRA⁺ populations. (A) RT-qPCR of 8 selected genes at day 30 of differentiation of the ventricular markers *GJA1*, *MYL2*, *IRX4* and *HEY2* and (B) of the atrial markers *CACNA1D*, *NR2F2*, *KCNJ3* and *NPPA*. (C) Representative flow cytometry analysis of the ATRA⁻ and ATRA⁺ populations at day 30 of differentiation for the marker *NR2F2* and (D) percentage of *NR2F2*⁺ cells, as well as (E) for the marker *MLC2v* and (D) percentage of *MLC2v*⁺ cells. Statistical analysis was performed using Mann Whitney u Test and represent the mean ± SD, while the significance is represented with *P<0.05, **P<0.01, ***P<0.001, ****P<0.0001.

To further characterize the percentage of cells positive to ventricular and atrial markers in both differentiation types, flow cytometry experiments were performed. Since it is known from literature that NR2F2 is also expressed in non-myocytes such as venous endothelial cells or smooth muscle cells, for this experiment we investigated its expression in parallel with TNNT2. While, as ventricular-specific marker, we selected MLC2v. Flow cytometry experiments demonstrated that $64.2 \pm 13.1\%$ ATRA-treated cells were NR2F2+ compared to the only $33.8 \pm 11.1\%$ of the no treated cells (Figure 5.4 C, D). Furthermore, $86.3 \pm 11.8\%$ of the ventricular differentiation were MLC2v+, whereas only $16.1 \pm 8.6\%$ of the atrial differentiation were (Figure 5.4 E, F). As last step of the characterization, we performed immunostaining analysis using specific antibodies against TNNT2, MLC2v and NR2F2 in both ATRA- and ATRA+. Images showed higher MLC2v expression in ATRA- cells compared to the ATRA+, and lower NR2F2 expression (Figure 5.5 A, B), confirming previous results obtained by qPCR and flow cytometry. Altogether, those results suggest that the addition of $1 \mu\text{M}$ of ATRA from day 3 to day 8 of the differentiation in our hiPSC-CM1 and hiPSC-CM2 lines led to an increased expression of atrial markers and a decreased expression of ventricular markers.

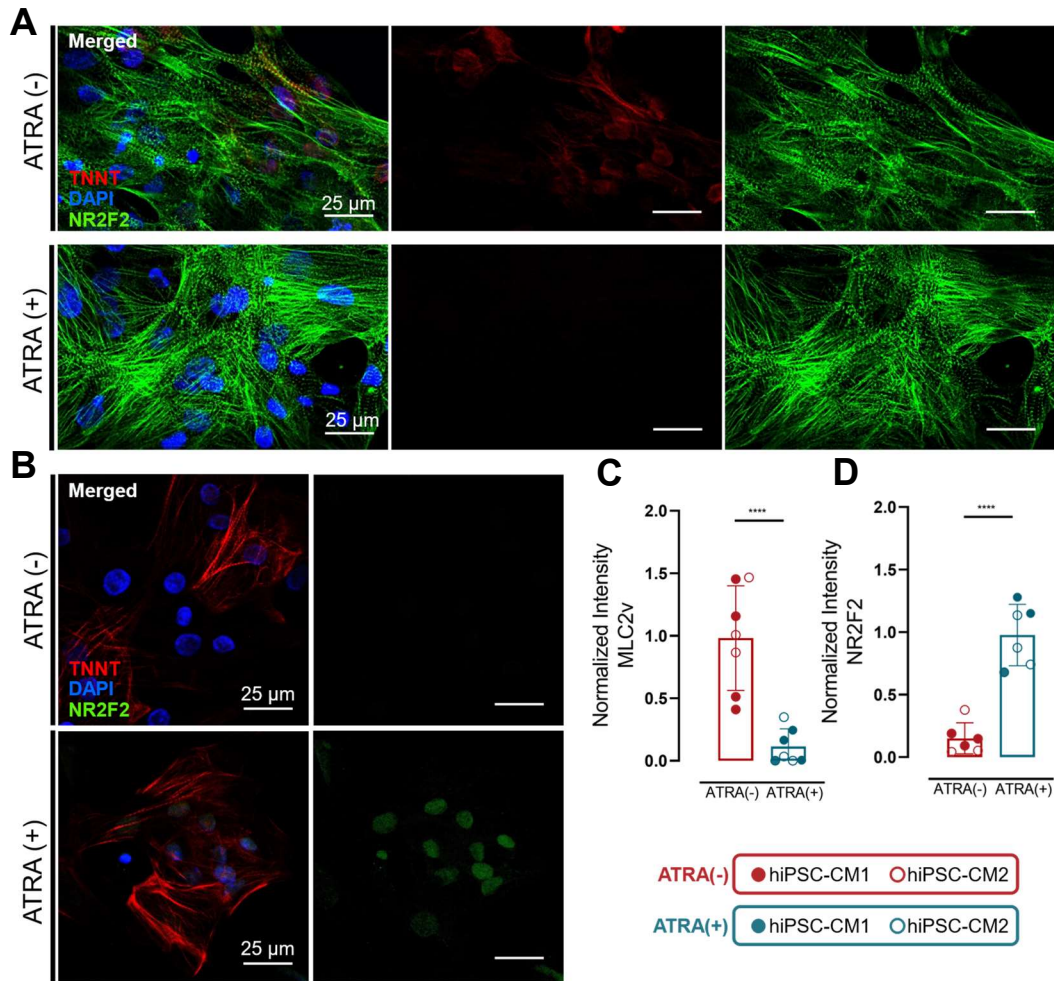


Figure 5.5 Images of MLC2v and NR2F2 expression in ATRA- and ATRA+. (A) Immunostaining images of MLC2v (red), TNNT2 (green) and DAPI (blue) at day 30 of differentiation of ATRA(-) and ATRA (+) cells. (B) Immunostaining images of NR2F2 (green), TNNT2 (red), DAPI (blue) at day 30 of differentiation of ATRA(-) and ATRA (+) cells. (C) Quantification with ImageJ of MLC2v intensity in both cell population normalized by number of nuclei. (D) Quantification with ImageJ of NR2F2 intensity in both cell population normalized by number of nuclei. Statistical analysis was performed using Mann Whitney u Test and represent the mean \pm SD, while the significance is represented with * $P < 0.05$, ** $P < 0.01$, *** $P < 0.001$, **** $P < 0.0001$.

4.2.2 Functional characterization of hiPSC-vCM and hiPSC-aCM

Cardiomyocytes are electrically active cells in the heart characterized by a specific action potential whose shape can differ depending on specific ionic currents. It is well known that ventricular and atrial cardiomyocytes are represented by distinctive electrophysiological properties. For instance, action potential duration (APD) is shorter in human atrial cardiomyocytes than in ventricular cardiomyocytes, as is conduction velocity, resulting from variations in gap junction distribution and expression. Additionally, atrial cardiomyocytes demonstrate different calcium handling capacity (159), and are characterized by faster calcium release and uptake than ventricular cardiomyocytes.

For this reason, in our study we investigated whether the differences in channel expression between ATRA- and ATRA+ differentiations corresponded to the particular functional phenotype of ventricular and atrial cardiomyocytes. To do so, patch clamp experiments were performed for both stem cell lines and a total of 19 ATRA- and 18 ATRA+ cells were recorded. The results revealed significant differences in action potential shape, as showed in the representative traces of Figure 5.6 A. Interestingly, focusing on the relation between APD and repolarization fraction, we could appreciate a clear distinction between the cell populations. From previous studies on isolated cardiomyocytes, it is known that in the human heart atrial cardiomyocytes have slightly more depolarized resting membrane potential (RMP) compared to the ventricular. In our model, we could appreciate a less negative RMP cells treated with ATRA, however no significant differences in RMP

could be appreciated between ATRA- -59.9 ± 8.4 mV and ATRA+ -64.1 ± 16.8 mV (Figure 5.6 C). Interestingly, for both ATRA- and ATRA+ the RMP was more depolarized compared to adult cardiomyocytes, underlying the immaturity of our cells. Moreover, ATRA- displayed a slower maximum rate of depolarization (9.2 ± 11.6 mV/ms) compared to ATRA+ (25.7 ± 13.1 mV/ms) (Figure 5.6 C), revealing a much faster phase 0 of the action potential. Results also demonstrated that not treated cells had a higher area under the curve (AUC) compared to the ATR treated ones, 21.6 ± 8.8 V·s vs. 3.6 ± 1.9 V·s respectively (Figure 5.6 D). Finally, concerning action potential duration, ATRA- showed to have a longer APD20 (180.1 ± 57.0 ms vs. 12.4 ± 7.8 ms), APD50 (290.8 ± 62.9 ms vs. 30.5 ± 12.9 ms) and APD90 (371.5 ± 67.0 ms vs. 182.4 ± 54.2 ms) compared to ATRA+ (Figure 5.6 F). Taking together this data showed that despite the immaturity of the cardiomyocytes derived hiPSC, discernible electrophysiological distinctions manifest in both ATRA- and ATRA+ populations. This outcome underscores that the application of ATRA, precisely administered in terms of both temporal slot and concentration as outlined in our protocol, led the hiPSC differentiation into cardiomyocytes characterized by atrial-like electrophysiological attributes.

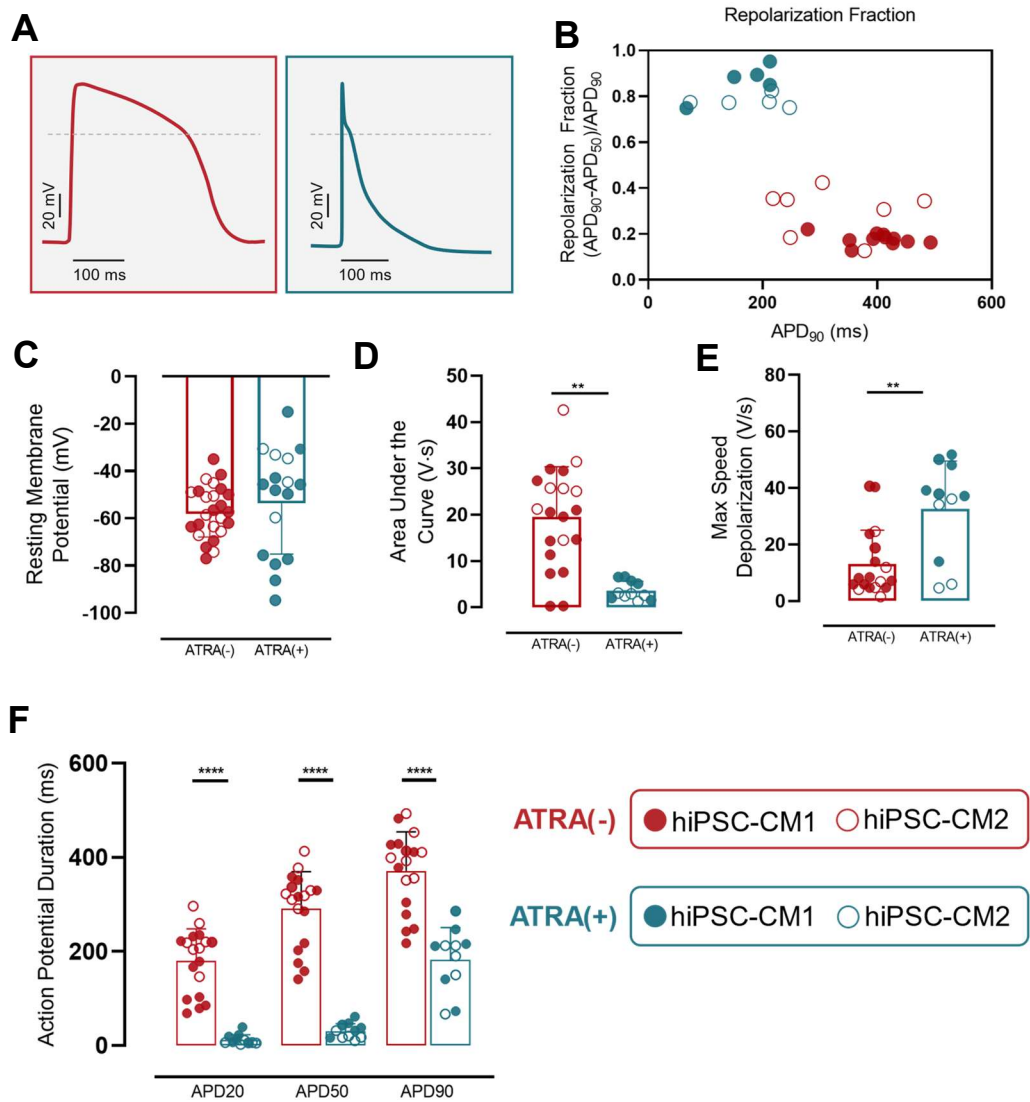


Figure 5.6 Electrophysiological characterization of ATRA⁻ and ATRA⁺ populations. (A) Representative traces of action potential measured with patch clamp in ATRA⁻ and ATRA⁺ at day 30 of differentiation. (B) Scatterplot for APD₉₀ versus repolarization fraction of AP recordings of ATRA⁻ and ATRA⁺ performed on patch clamp at room 4 temperature. (C) Patch clamp recordings of resting membrane potential (RMP) (D) area under the curve (AUC) and (E) maximum speed of depolarization. (F) Analysis of action potential duration at 20, 50 and 90 percent of repolarization for both cell populations. Statistical analysis was performed using Mann Whitney u Test and represent the mean ± SD, while the significance is represented with *P<0.05, **P<0.01, ***P<0.001, ****P<0.0001.

4.2.3 Mechanical characterization of hiPSC-vCM and hiPSC-aCM

Electrophysiological features of cardiomyocytes are a fundamental aspect that determines the mechanical characteristics of those cells. Indeed, the electrical depolarization of the membrane potential leads to the opening of the voltage-gated L-type calcium channels with consequent increase of the intracellular concentration of calcium (211). A key regulator that activates contraction of myofibrils in the cardiomyocytes (212). The previously described patch clamp experiments demonstrated strong electrophysiological differences of the action potential shapes between ATRA- and ATRA+. More specifically, APD at different percentages of depolarizations demonstrated the strong significant differences concerning the plateau phase of the AP. A phase which mainly depends on Ca^{++} intracellular concentration. Because of these strong electrophysiological differences of the action potential shape between ATRA- and ATRA+, we suspected that those two populations might be characterized by different mechanical properties too. For this reason, we wanted to address the mechanical features of ATRA+ and ATRA- populations. To characterize cell properties from a mechanical perspective, we opted for the nanoindentation technique. The contraction traces (Figure 5.7 A) were recorded measuring the radial displacement due to the contraction of single cells. Thanks to the homemade script by Dr. Ramona Emig, we were able to analyze different kinetics parameters represented in Figure 5.7 B such as the time-to-peak (TTP), the full width at half maximum (FWHM) and finally the time to 20%, 50% and 90% of relaxation (TTR20, TTR50 and TTR90 respectively).

Results showed that the treatment with ATRA from day 3 to day 8 of differentiation led to a clear difference in contraction of the cardiomyocytes (Figure 5.7 A). In fact, the detected time-to-peak (TTP) was 76.5 ± 17.6 ms and 45.2 ± 7.5 ms in ATRA- and ATRA+, respectively (Figure 5.7 C). Furthermore, contraction of not treated cells demonstrated significantly larger full width at half maximum (FWHM) values (Figure 5.7 D), 0.2 ± 0.05 s and 0.1 ± 0.02 s respectively, indicating longer contractions. In line with those results, also the relaxation kinetics represented by TTR20, TTR50 and TTR90 showed a significantly faster relaxation in cells treated with ATRA compared to the not treated ones (Figure 5.7 F). Finally, since cells were not electrically stimulated, we were able to measure contraction frequency. Results showed that vCM had a lower spontaneous contraction frequency compared to aCM: 1.0 ± 0.3 Hz vs. 2.0 ± 0.6 Hz, respectively (Figure 5.7 E). These findings confirm that the electrophysiological changes in ATRA-treated cells were followed by distinctive atrial-specific mechanical characteristics similar to those of human atrial myocardium. Henceforth, we refer to these cells as hiPSC-aCM.

4.3 hiPSC-aCM as *in-vitro* model of AF

In the previous chapter results demonstrated that hiPSC can be differentiated into atrial-like cardiomyocytes with molecular, electrophysiological and mechanical features similar to those of the human heart. hiPSC-CM characterization was performed in single cells to gain insight of their cellular properties. This present segment of the results, however, shifts its focus toward cell monolayers, with the primary objective of evaluating their potential to initiate atrial fibrillation. The shift to cell monolayer is essential to allow a more comprehensive understanding of cellular behaviour in a context that better mimics the physiological environment. In fact, as arrhythmia mechanisms is characterized by asynchronous and uncoordinated activity of multiple cells, examination of cell monolayers behaviour is essential. After analyzing hiPSC-aCM monolayer behaviour and their ability to maintain arrhythmia, the final part of this section will investigate the transcriptomic changes led by the arrhythmic state. This part of the study has indeed the aim to create an in-vitro model of atrial fibrillation that can recapitulate arrhythmia mechanisms observed in AF patients.

4.3.1 Spontaneous in-vitro atrial fibrillation in hiPSC-aCM

In a typical cardiac cycle, the impulse emanates from the sinoatrial node and propagates through the myocardium. Thanks to the tissue properties of the heart, successive calcium-mediated events are instigated, ultimately culminating in the

synchronous activation and contraction of the cardiac tissue. In the case of cardiac arrhythmias, this complex and cyclical mechanism breaks causing a rapid, irregular atrial activity with re-entrant patterns. In this section, we wanted to verify whether monolayers of hiPSC-aCM can replicate this complex phenomenon forming re-entry patterns in a dish. To do so, we opted for optical mapping measurements using the calcium dye Rhod-2AM. A technique that can record calcium impulse propagation detecting the emission of the calcium dye. On day 20 of differentiation, cells were uniformly plated in dishes of different size at density of 250,000 cells/cm² (Figure 5.8) and after 10 days in those conditions, experiments were performed. As previously stated, hiPSC-aCM were seeded into dishes of two different sizes: a small one of 0.32 cm², which we hypothesize being insufficient for sustaining re-entry mechanisms; and a large size of 9.6 cm², which we theorize being conducive to the formation of spontaneous re-entries and rapid, irregular activations.

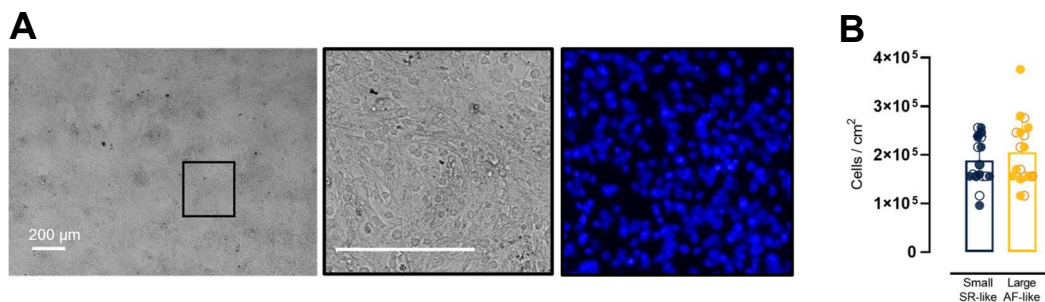


Figure 5.8 Cell density in small and large surfaces. (A) Representative images of cell density in bright-field at different magnifications and the respective nuclei staining with DAPI. (B) Cell density of hiPSC-aCM in small and large dishes analyzed as DAPI-stained nuclei per area. For large dishes each dot represents the average obtained by each position of acquisition represented in the material and methods section. Statistical analysis was performed using Mann Whitney u Test and represent the mean \pm SD, while the significance is represented with * $P < 0.05$, ** $P < 0.01$, *** $P < 0.001$, **** $P < 0.0001$.

A total of 18 large dishes and 20 small dishes were analyzed by optical mapping. Results showed that, depending on the size of the culture area, the impulse propagation exhibited different patterns (Figure 5.9 A, B). Dishes with smaller surface area exhibited a linear propagation of the signal, while dishes with larger surface area were characterized by rotor formation. When representing the activation rate at each node as dominant frequency (Figure 5.9 C, D), the two cell culture conditions were characterized by distinct activation patterns. Small surfaces had a uniform dominant frequency among the whole monolayer. While large surfaces were characterized by areas with different dominant frequency leading to inhomogeneity in the whole monolayer. This difference is even more evident when focusing on the calcium transient (CaT) traces at 5th and 95th activation percentiles (Figure 5.9 E, F). The greater variability in activation timing in large dishes was confirmed also by the median activation period. In fact, the median activation period was significantly shorter in the large dishes exhibiting fibrillation (0.8 ± 0.2 s) compared to the small dishes maintaining linear propagation (1.2 ± 0.3 s) (Figure 5.9 G). Further analysis of the standard deviation of activation periods within each well revealed less variability in cells under sinus rhythm-like (SR-like) behaviour (0.04 ± 0.08 s) than in those under in AF-like state (0.50 ± 0.22 s) (Figure 5.9 H).

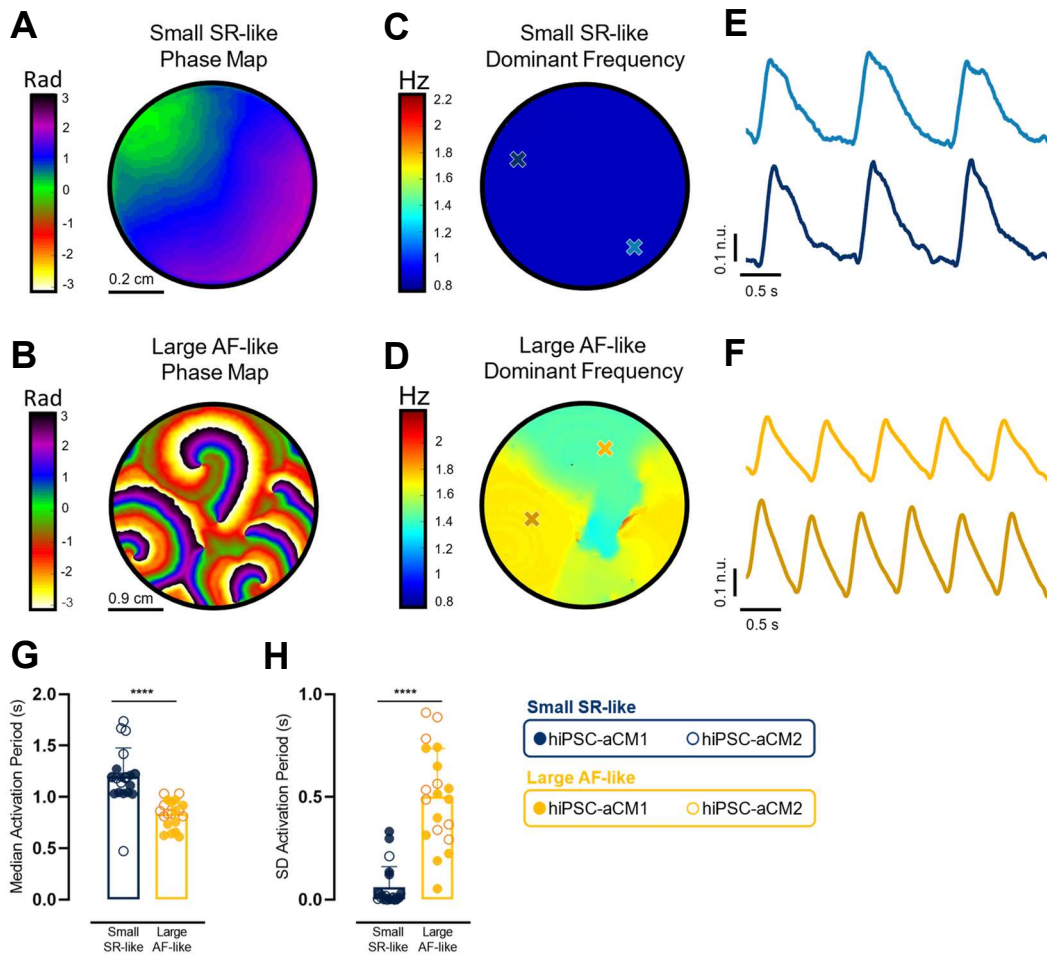


Figure 5.9 Ability of hiPSC-aCM to spontaneously initiate atrial fibrillation. (A) Representative phase maps of small dishes in regular activation and (B) on large dishes in fibrillatory activity. (C) Representation of dominant frequency in cells in small dishes with regular activation condition and (D) cells in large dishes with fibrillatory activity. (E) Representative traces of calcium transients at 5 (light) and 95 (dark) activation percentile in cells in small dishes. (F) Representative traces of calcium transients at 5 (light) and 95 (dark) activation percentile in cells in large dishes. (G) Median activation period in large wells in large dishes with fibrillatory activity compared to small ones in regular activation. (H) Standard deviation in large wells with AF compared to those in regular activation. Statistical analysis was performed using Mann Whitney u Test and represent the mean \pm SD, while the significance is represented with * $P < 0.05$, ** $P < 0.01$, *** $P < 0.001$, **** $P < 0.0001$.

Overall, our findings demonstrate that hiPSC-aCM in large surfaces effectively replicate the electrophysiological features of fibrillation with an AF-like activity, while all small dishes displayed linear propagation, akin to SR-like behaviour.

4.3.2 hiPSC-aCM in fibrillation undergo gene expression changes

Our current understanding of AF has been significantly enriched through meticulous investigations conducted on isolated tissue samples of AF patients (213)(214). These studies have unveiled that AF is characterized by substantial and intricate alterations in gene expression profiles. However, many molecular mechanisms that connect those transcriptomic alterations with the electrophysiological remodeling still need to be understood. We have previously showed that culturing hiPSC-aCM in wells with larger area leads to sustained fibrillatory activity in confluent monolayers, our subsequent objective was to explore whether such sustained fibrillatory activity would cause AF-like remodeling of gene expression *in-vitro*.

We therefore conducted RNAseq analysis of both cell lines in the two culture conditions, the large surface showing fibrillatory activity and the small surface displaying linear signal propagation similar to atria in SR (both assessed via optical mapping). The first condition will be called AF-like, while the second SR-like. Despite the acknowledged variability among stem cell lines (215), the principal

component analysis effectively distinguished the AF- and SR-like models in both cell lines (Figure 5.10 A) with a principal component 1 of 10% and a principal component 2 of 82%. Performing a differentially expressed gene (DEG) analysis, we found that a total of 473 genes were downregulated in the AF-like model, while other 1332 were upregulated (Figure 5.10 B). Among those genes, we could identify four different main groups of upregulated biological processes: inflammation (*CXCL2, IL32, CXCL8, IL18, IL11, TNFRSF*), ion transport (*ATP1A2, CACNA1H, KCND3, KCNJ5*) and extracellular matrix (ECM) modulation (*MMP1, COL9A2, COL2A1, CLDN, LAMA3, CHD1, LAMC, VTN*). While a last group of genes involved in DNA replication (*POLA2, POLQ, CDC6, CCNA2*) was downregulated as represented in the heatmap of Figure 5.10 D ($P_{\text{adjusted}} < 0.05$).

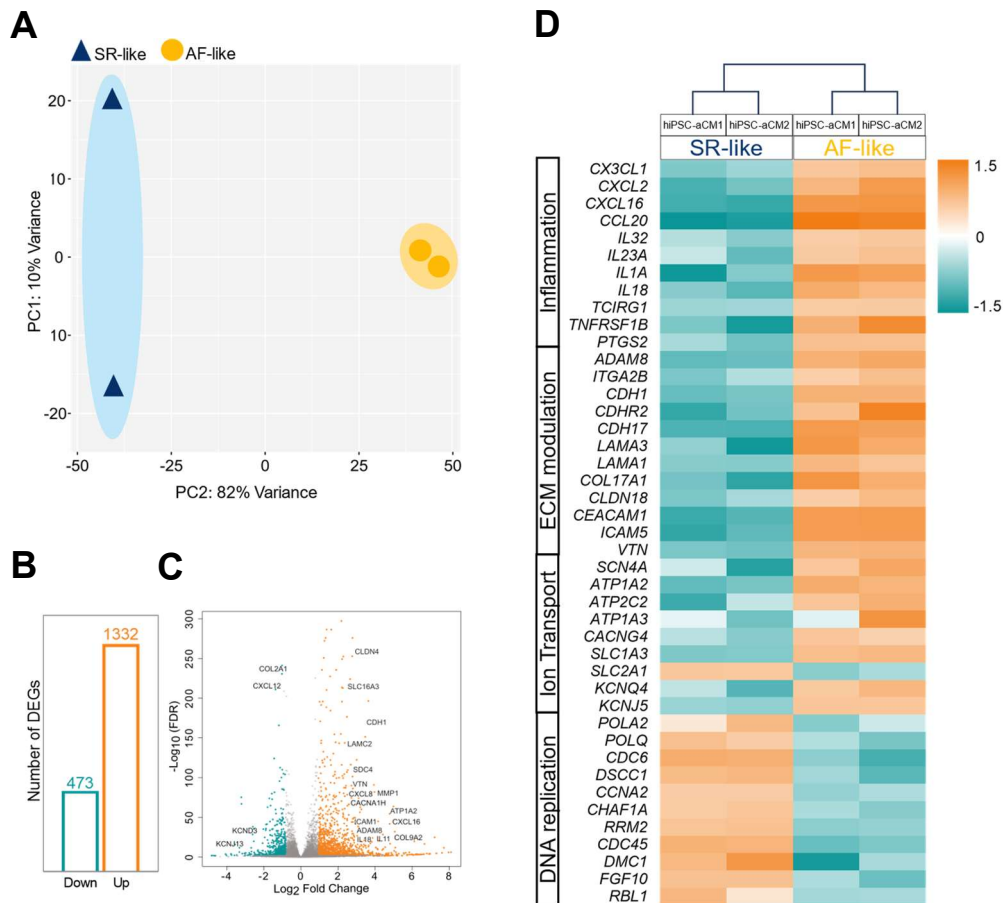


Figure 5.10 Different gene expression in SR-like and AF-like monolayers. (A) Principal component analysis of the different cell lines in AF-like and SR-like condition. (B) Differentially expressed genes analysis identified 473 downregulated genes (green) and 1332 upregulated in the AF model (orange). (C) Volcano plot of the differentially expressed genes. (D) Heatmap showing differentially expressed genes separated by biological function.

Next, a pathway analysis was performed using fold-change values of all genes, independently of the selected DEGs. Genes with noisy fold-changes (False Discovery Rate (FDR) cutoff > 1) were excluded and a pathway significance cutoff of 0.05 was applied. Bioinformatics analysis were performed to analyze GSEA (Gene Set Enrichment Analysis) using Gene Ontology (BP = GO biological process and MF = GO molecular function) and Kyoto Encyclopedia of Genes and

Genomes (KEGG) gene sets. The analysis confirmed the prominence of four major pathway groups: “immune system” (Figure 5.11), “ECM activity”, “ion transport” and “DNA activity” (Figure 5.12), which reinforces the significance of these pathways in AF initiation. Concerning the “immune system” group, biological processes such as “myeloid leukocyte mediated immunity”, “myeloid leukocyte activation” and “leukocyte activation involved in immune response” had an adjusted P value of $1.23e^{-2}$ and a number of 426, 495 and 525 genes involved respectively. Interestingly, also using the molecular function and KEGG gene sets, we could identify “cytokine activity” and “viral protein interaction with cytokine and cytokine receptor” with an adjusted P value of $1.62e^{-2}$ and $1.60e^{-2}$ respectively. For the “ECM activity” group, using the biological process, molecular function and KEGG dataset, we could identify the significant pathways “regulation of cell-matrix adhesion”, “microtubule cytoskeleton organization”, “tight junction” and “N-glycan biosynthesis” with a respectively adjusted P value of $1.23e^{-2}$, $1.23e^{-2}$, $1.54e^{-2}$ and $1.32e^{-2}$. While for the “ion transport” group, pathway such as “cardiac conduction system”, “phosphate ion transmembrane transporter activity” and “arrhythmogenic right ventricular cardiomyopathy” were found significantly activated in the AF-like monolayers with an adjusted P value of $1.23e^{-2}$, $1.62e^{-2}$ and $1.54e^{-2}$ respectively.

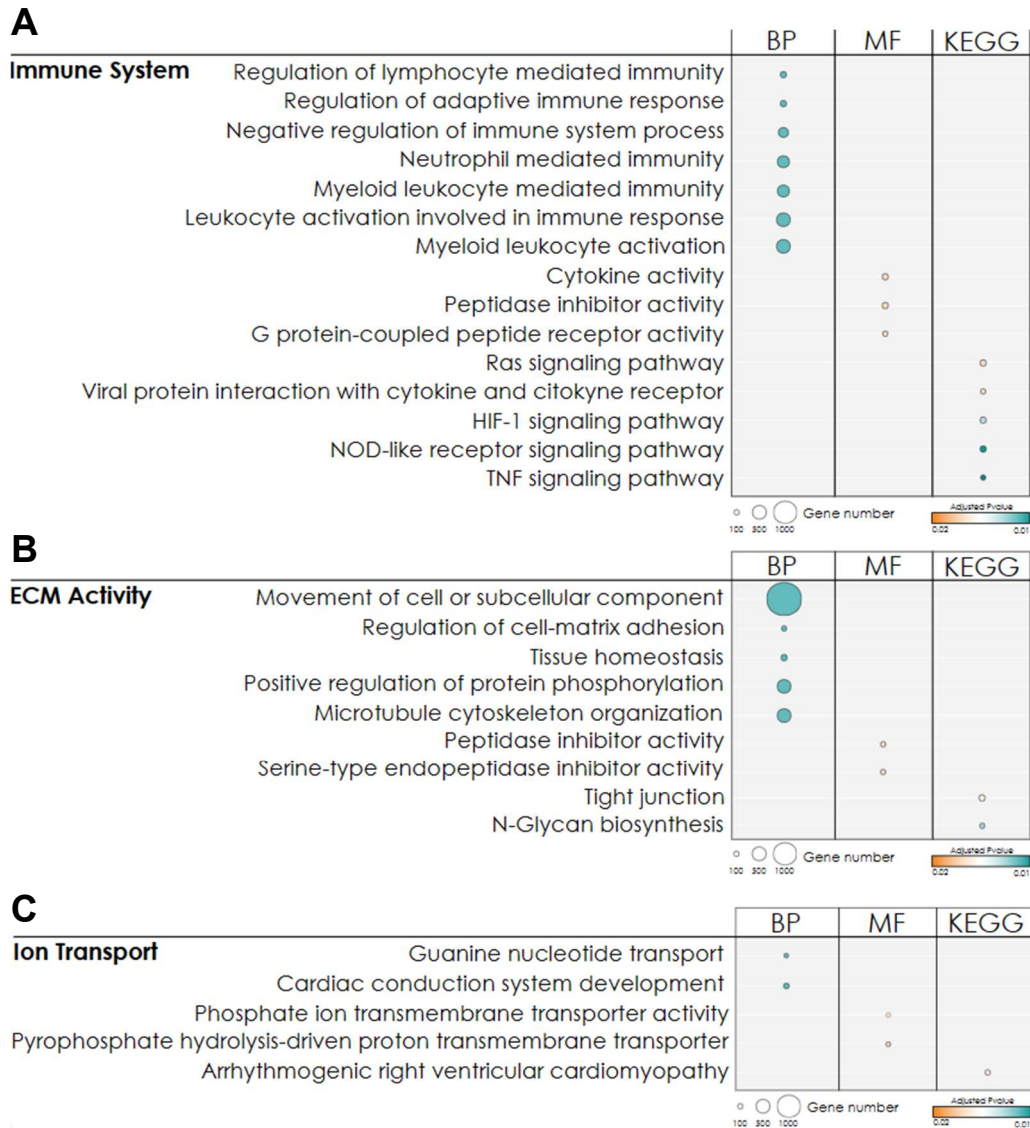


Figure 5.11 Significant pathways revealed by using three different gene sets. Pathway analysis performed using Gene Ontology and KEGG gene sets revealed significant pathway groups involved in (A) immune response, (B) ECM activity and (C) ion transport. BP = GO biological process, MF = GO molecular function, KEGG = Kyoto Encyclopedia of Genes and Genomes. The size of the dots are represented by the number of genes and the colour depends on the pathway significance.

Interestingly, a last group of less significant pathways was detected, the “DNA activity”. In this group different pathways such as “DNA repair”, “double-strand break repair”, “chromatin binding” and “nuclease activity” were found with an adjusted P value of $1.23e^{-2}$, $1.23e^{-2}$, $1.62e^{-2}$ and $1.17e^{-2}$. Biological process and molecular function gene sets were used. While, when KEGG gene set was used, pathways as “DNA replication” and “cell cycle” were found significant with an adjusted P value of $0.92e^{-2}$ and $0.94e^{-2}$, and a gene number of 32 and 116 respectively.

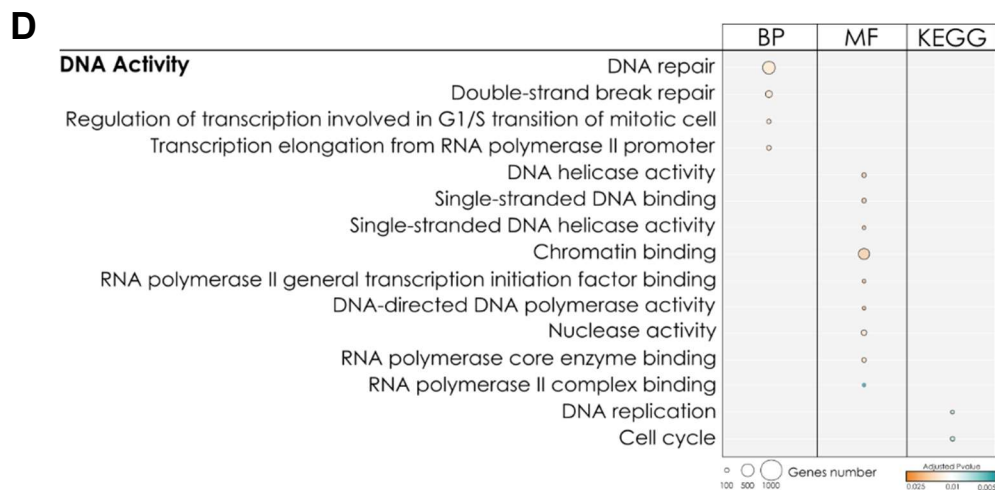


Figure 5.12 Pathway analysis revealed DNA activity as significant. Pathway analysis performed using Gene Ontology and KEGG gene sets revealed a last group of significant pathways, DNA activity. BP = GO biological process, MF = GO molecular function, KEGG = Kyoto Encyclopedia of Genes and Genomes. The size of the dots are represented by the number of genes and the colour depends on the significance.

Interestingly, when plotting the network of pathway analysis using the GO biological process dataset, we could identify significant interactions among leukocyte migration and cytokine activity pathways, together with cell adhesion and ECM receptor interaction (Figure 5.13). Altogether, those results empathizes the concept that fibrosis and inflammation are two major and parallel aspects of AF (216) (217).

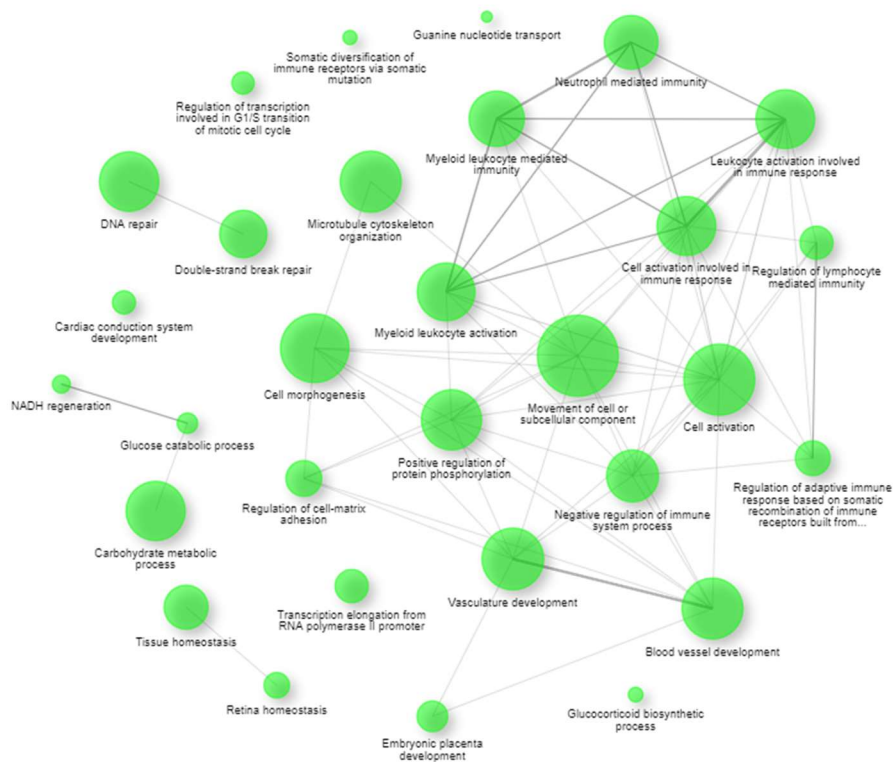


Figure 5.13 Network of pathway analysis using GO biological process as dataset. Analysis was performed using fold-change values of all genes and hence is independent of the selected DEGs. Bigger circles correspond to more significant pathways, while thicker lines correspond to more significant connections between two different pathways. Analysis shows a strong significant connection among pathways related to immune response and ECM modulation. GO = Gene Ontology, DEGs = Differentially Expressed Genes.

Finally, RNAseq results were validated with qPCR technique. To do so, we selected genes that showed more significance when performing DEG and were involved in numerous significant pathways. A number of 12 genes was selected and analyzed (Figure 5.14 A and 5.14 B). Results showed that 8 genes out of 12 were significantly higher expressed in the AF-like model compared to the SR-like. Four of them were part of the group “ECM modulation” (CDH1, MMP1, ICAM1, VTN), while other four were part of the “inflammatory response” group (IL16, CXCL12, CXCL8). Altogether, RNAseq and qPCR data are consistent with previous studies on tissues samples from AF patients. Specifically, inflammation and its associated immune response, along with fibrosis and calcium handling play a central role influencing the initiation and perpetuation of AF in humans.

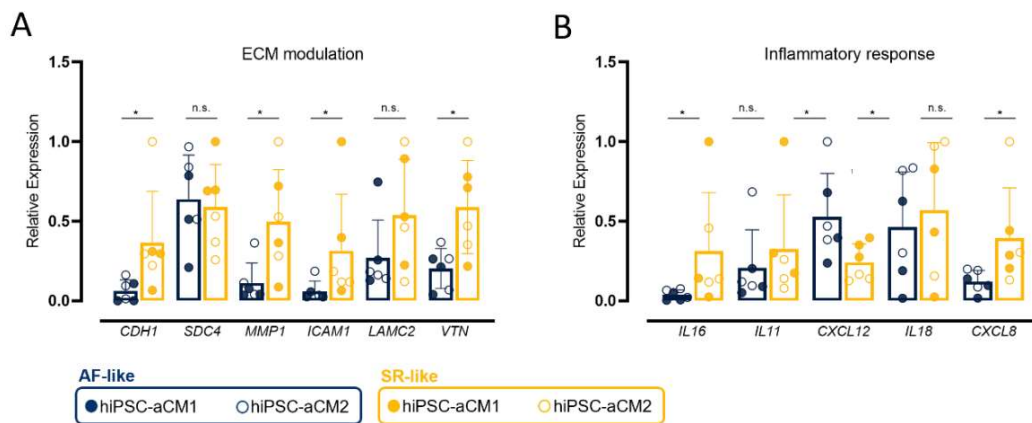


Figure 5.14 Gene expression of genes related to ECM modulation and inflammatory response. (A) qPCR experiments of genes belonging to ECM modulation and inflammatory response group. Data confirmed the alteration of *IL16*, *IL11*, *CXCL12*, *IL18* and *CXCL8*, (B) as well as of *CDH1*, *SDC4*, *MMP1*, *ICAM1*, *LAMC2* and *VTN* in hiPSC-aCM upon fibrillatory activity. Statistical analysis was performed using Mann Whitney u Test and represent the mean \pm SD, while the significance is represented with *P<0.05, **P<0.01, ***P<0.001, ****P<0.0001.

4.4 Perturbation of AP with optogenetics

In the previous section of results it has been demonstrated how monolayers of hiPSC-aCM can recapitulate cardiac arrhythmia mechanisms characterized by rapid, irregular heartbeats in the atria. Re-entrant phenomena, characterized by an asynchrony in time-space events, are one of the mechanisms that can lead to the initiation and maintenance of AF. Therefore, future therapies require the ability to perturb and control such altered cardiac activity in a spatiotemporally defined manner. Optogenetics, different from other techniques such as electrical, mechanical and chemical approaches, enables one to control cell-type specific activity with micrometer- and millisecond-precision. For this study, we focused on the use of three different optogenetic tools, namely the light-gated K⁺ channels HcKCR1, HcKCR2 and WiChR, and tested their ability to optically induce transmembrane currents for modulating action potentials in hiPSC-aCM.

4.4.1 HcKCR1 and HcKCR2 alter AP properties of hiPSC-aCM

Previous results on neuronal cells demonstrated how HcKCR1 and HcKCR2 enables optogenetic control of K⁺ gradients(195). Despite their characteristic of being the firstly identified light-gated K⁺ selective channels, so far, no studies have been conducted to test their effect on cardiomyocytes. In this study,

we aimed to test their effect on hiPSC-aCM and their potential implication in cardiac arrhythmias as tool to manipulate and alter spontaneous AP.

To do so, on day 28 of differentiation hiPSC-aCM were transfected with HcKCR1-mCerulean and HcKCR2-mScarlet. Transfection success was assessed by confocal microscopy (Figure 3.15 A, B). Images showed a robust channel expression in the sarcolemma for both HcKCR1 and HcKCR2. However, in both cases transfection was sparse.

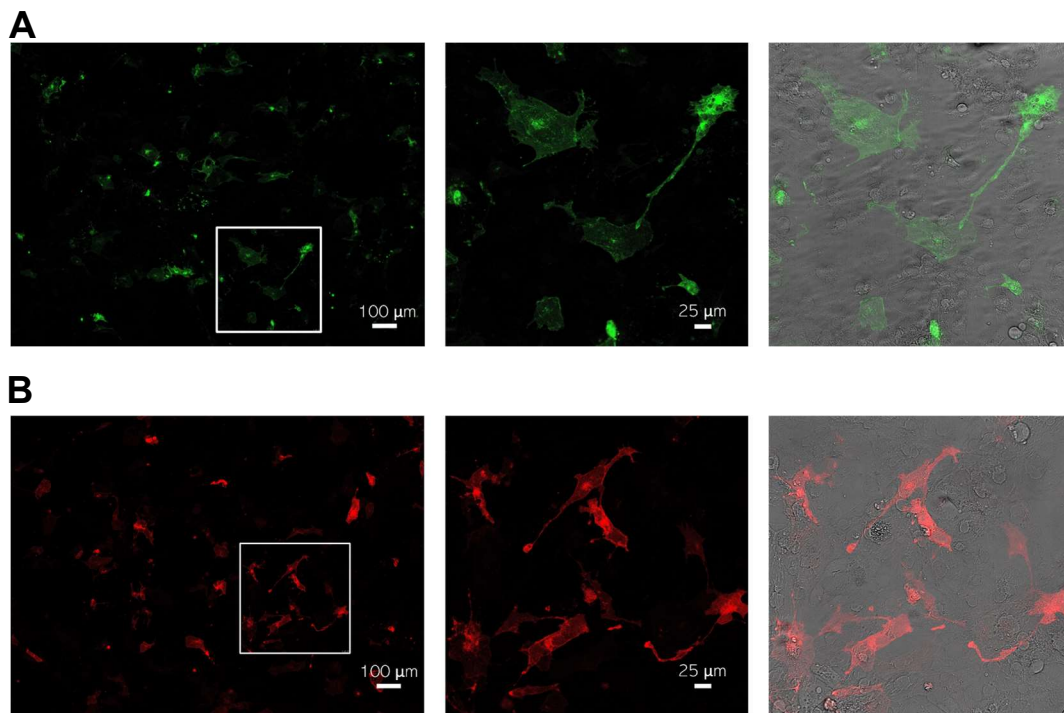


Figure 5.15 Images of hiPSC-aCM transfected with HcKCR1-mCerulean and HcKCR2-mScarlet Confocal images showing HcKCR1-mCerulean (in green) and HcKCR2-mScarlet expression (in red) in hiPSC-aCM. Images on the right side represent the merge including the transmission images of the areas. Images taken by Dr. Franziska Schneider-Warme,

48-96h after transfection, sharp electrode experiments were performed in order to measure electrical activity of individual cells in a monolayer of hiPSC-aCM. More specifically, recordings were performed before illumination (phase I), during a prolonged illumination of 15 s (phase II) and after illumination (phase III). Recordings showed that both HcKCR1-transfected cells as well as HcKCR2-transfected hiPSC-aCM maintained spontaneous action potentials activity upon prolonged illumination (Figure 3.16 A, B).

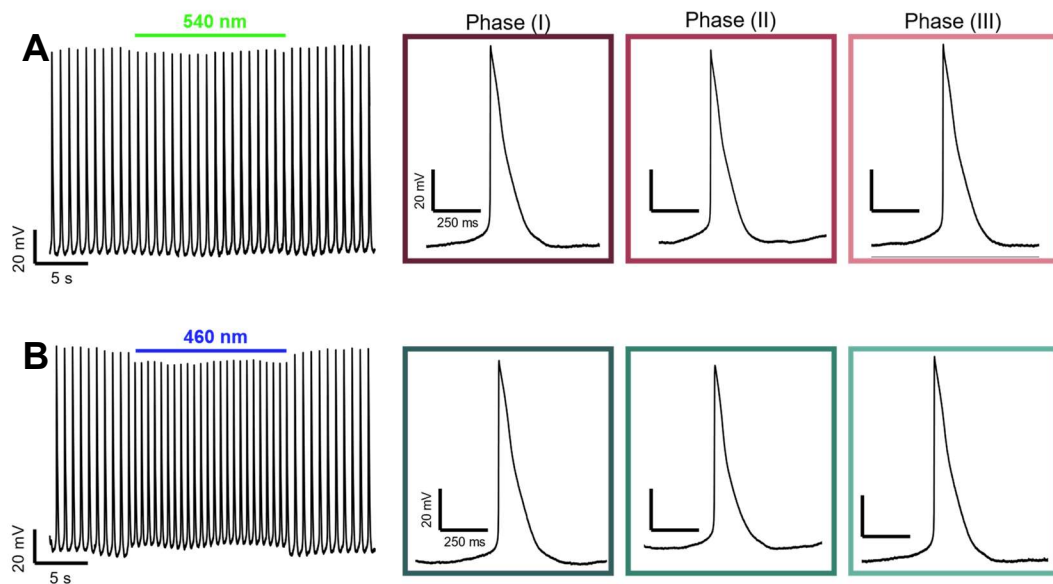


Figure 5.16 Representative traces of hiPSC-aCM transfected with HcKCR1-mCerulean and HcKCR2-mScarlet. (A) Representative AP traces showing HcKCR1-mediated alteration of AP shape with the respective AP before light activation (phase I), during light activation (phase II) and after light activation (phase III) (B) Representative AP showing HcKCR2-mediated alteration of AP shape and the respective AP during phase I, phase II and phase III.

Compared to non-transfected cells (WT), APD_{90} in transfected cells did not undergo changes in the absence of light (Figure 3.17 A). However, hiPSC-aCM

transfected with HcKCR1 and HcKCR2, showed significantly shorter APD₉₀ during light activation compared to APD₉₀ in phase (I) and phase (II) (Figure 3.17 A, B). Concerning resting membrane potential (RMP) and beating frequency, cells transfected with HcKCR1 and HcKCR2 showed different behavior. No differences in RMP and beating frequency compared to WT cells were observed in the absence of light (Figure 3.17 D). Upon light activation HcKCR1-transfected hiPSC-aCM did not show significant differences of RMP or beating frequency compared to the phases (I) and (III) before and after light (Figure 3.17 E). In contrast, HcKCR2-transfected hiPSC-aCM showed significant changes in RMP, which was -64.3 ± 10.1 mV during illumination compared to -66.2 ± 9.7 mV in phase (I) and -66.2 ± 9.8 mV in phase (III) (Figure 3.17 F). In HcKCR2, there were changes in beating frequency, analyzed to be 1.5 ± 0.5 Hz during illumination compared to phase (I) and phase (III), with beating frequencies of 1.1 ± 0.3 Hz and 1.1 ± 0.3 Hz, respectively, P value <0.0001 (Figure 3.17 I). Please note that comparisons are made within one recording (paired data analysis, One Way ANOVA Test). A similar behavior was observed also concerning AP amplitude. Both HcKCR1- and HcKCR2-transfected cells did not exhibit differences compared to WT when light was not applied (Figure 3.17 J). However, differently from HcKCR1-transfected cells, aCM transfected with HcKCR2 faced reduced AP amplitudes during light (92 ± 11 mV) compared to phase (I) (97 ± 11 mV) and phase (III) (97 ± 10 mV), for both comparison P value <0.0001 and paired data analysis One Way ANOVA Test were performed.

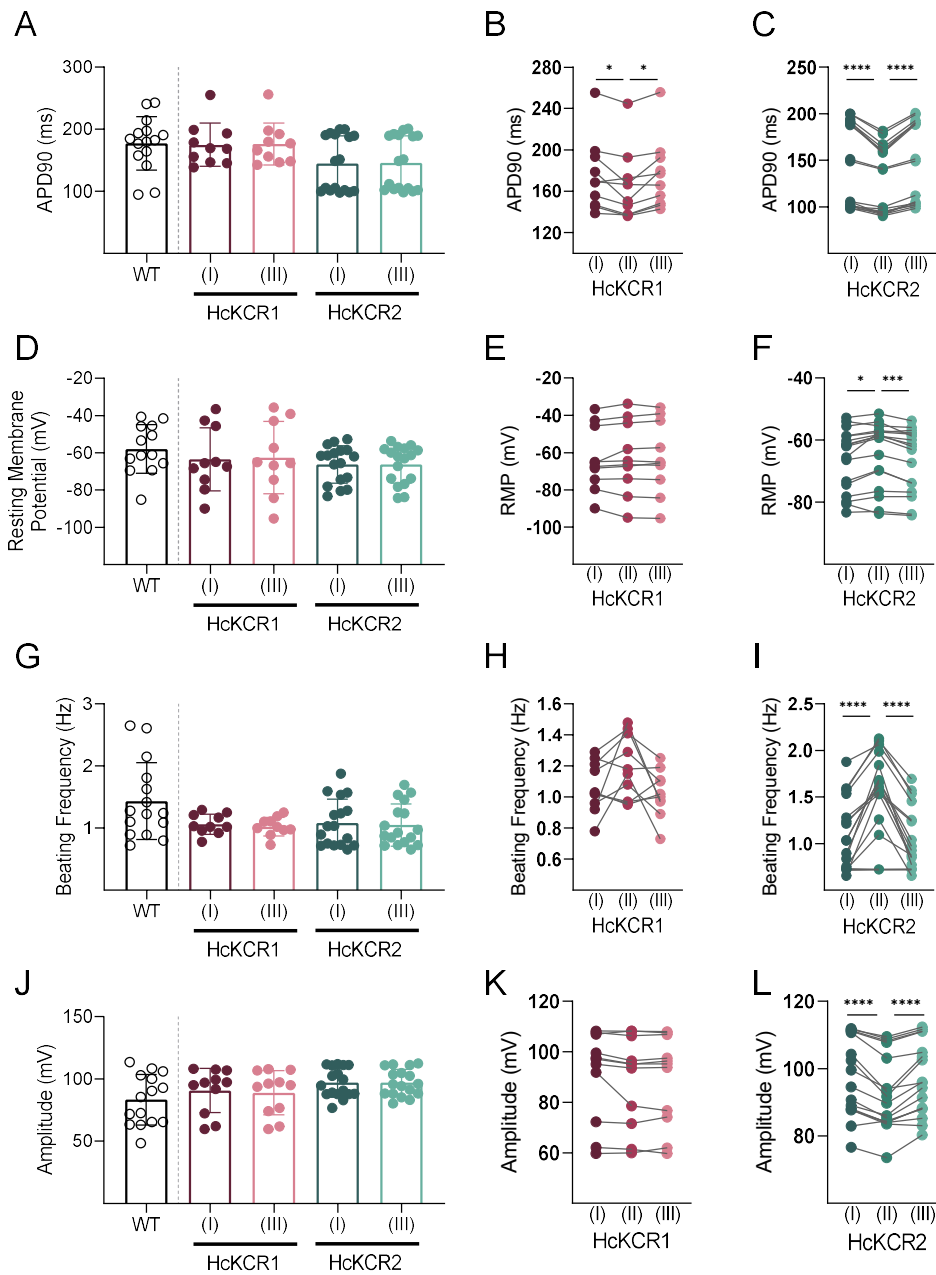


Figure 5.17 Comparison of AP properties of HcKCR1 and HcKCR2 expressing cells compared to WT cells, and comparisons before, during and after light. A-C) APD90, D-E) RMP, F-H) Beating frequency, J-L) Amplitude. For bar graphs Mann Whitney u Test was performed, while for the line graphs it was performed a Repeated Measures one-way ANOVA test. The significance is represented with *P<0.05, **P<0.01, ***P<0.001, ****P<0.0001.

We next compared the sizes of effects between the two channels. Indeed, APD was not significant, in HcKCR2-transfected cells -15.46 ± 10.18 ms compared to HcKCR1-transfected cells -9.85 ± 9.68 ms (Figure 3.18 A, B, C). Concerning RMP, only activation HcKCR2 demonstrated to have a significant depolarization. However, no significant differences have been encountered concerning the RMP when comparing the effect of the two channels (Figure 3.18 D). However, upon light activation cells transfected with HcKCR2 demonstrated to have a significantly larger increase of the beating frequency (0.44 ± 0.28 Hz) than cells transfected with HcKCR1 (0.13 ± 0.20 Hz). Finally, comparing the effects of the two channels to the AP amplitude, we could appreciate a significant difference. Upon light activation, HcKCR2-transfected cells undergo a decrease of AP amplitude of -4.5 ± 3.0 mV. While HcKCR1-transfected cells in phase (II) had a decrease of -2.5 ± 3.7 mV.

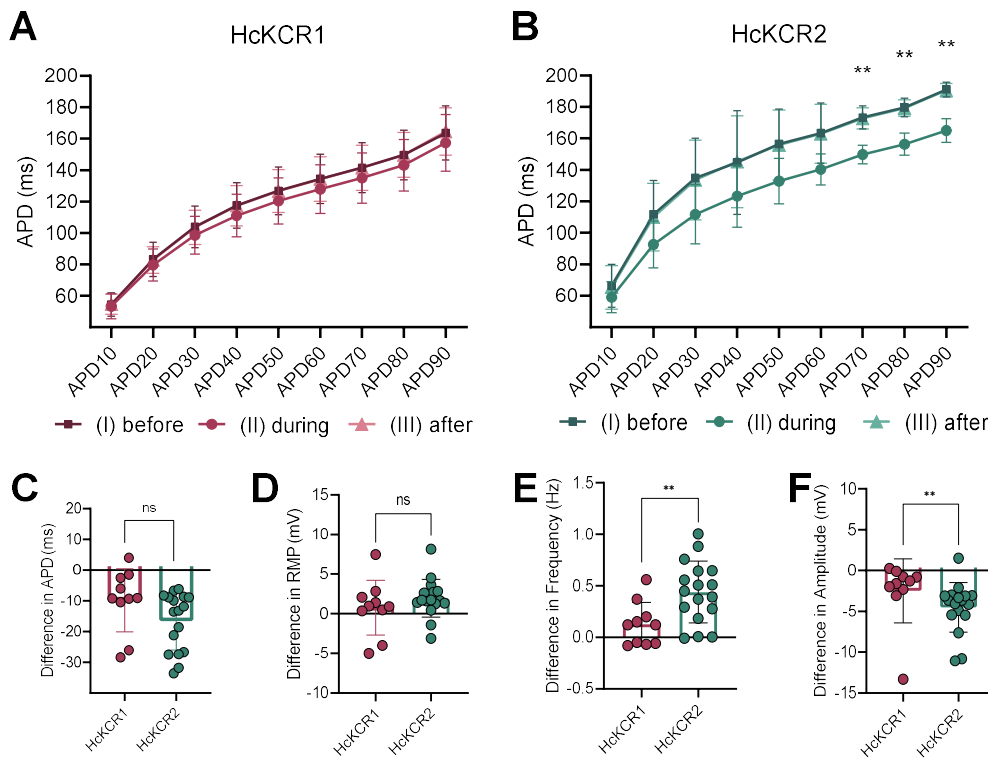


Figure 5.18 Comparison of HcKCR1 and HcKCR2 effects. (A) AP mean curve at different percentage of repolarization of hiPSC-aCM transfected with HcKCR1 and (B) with HcKCR2. Differences in (C) APD, (D) RMP, (E) AP frequency and (F) amplitude. The significance is represented with * $P < 0.05$, ** $P < 0.01$, *** $P < 0.001$, **** $P < 0.0001$.

4.4.2 WiChR efficiently inhibits the activity of hiPSC-aCM

With the discovery of WiChR from *Wobbia lunata*, scientists introduced a novel KCR with improved K^+ selectivity and improved light sensitivity compared to HcKCR1 and HcKCR2. Due to its peculiarity, we tested the ability of WiChR to inhibit spontaneous AP of hiPSC-aCM and compared WiChR effects to those obtained with the previously mentioned KCRs. To this end, hiPSC-aCM were transiently transfected with plasmids encoding WichR-mScarlet, leading to sparse,

but robust, channel expression in the sarcolemma as visualized by mScarlet fluorescence (Figure 3.19).

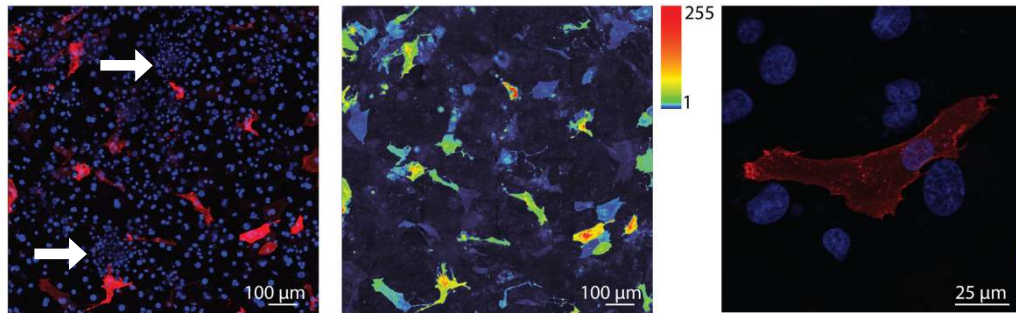


Figure 3.19 Images of hiPSC-aCM transfected with WiChR-mScarlet. Confocal image showing WiChR-mScarlet expression (in red) and DAPI staining of nuclei (in blue). White arrows indicate cell clusters from which cells were chosen for sharp electrode recordings (in a blinded way in respect to mScarlet fluorescence). Images taken by Dr. Franziska Schneider-Warme,

In WiChR-transfected cultures, AP were reversibly inhibited during blue light application (n=10/11 recordings, N=2 cultures, Figure **A). Only one recording did not show a complete inhibition of the spontaneous AP. In this particular case, during illumination AP had a smaller amplitude, shorted APD and an irregular frequency as shown in the representative trace.

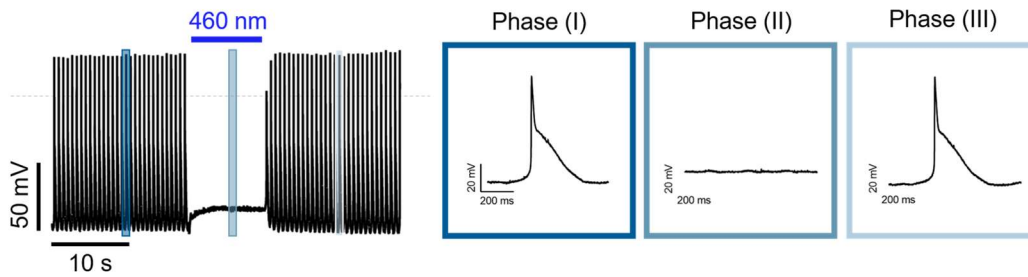


Figure 5.20 Representative trace of AP of hiPSC-aCM transfected with WiChR-mScarlet. Sharp electrode recording showing reversible inhibition of AP during blue light application. Representation on the right-side show AP shape before light (phase I), the absence of AP during illumination (phase II), and AP after light (phase III).

In all the 11 recordings, APD_{90} , RMP and beating frequency of WiChR-transfected cells in the absence of light were not significantly different compared to those of WT (Figure 3.21 A, B, C). and AP parameters recovered to baseline values after illumination. Indeed, baseline AP parameters such as APD, RMP and frequency were restored within 10 AP post-illumination (Figure 3.21 A, B, C). Furthermore, before illumination maximum diastolic potentials (MDP) and take-off potentials (TOP)(Figure 3.21 D) were not significantly altered compared to the WT (Figure 3.21 E, F). Importantly, RMP during light application was only slightly depolarized compared to MDP before and after light application ($p=0.013$) but was not different to TOP of control cells and cells before and after light application (Figure 3.21 E, F). Finally, in line with inhibition of AP, spontaneous contractions recorded by optical measurements were reversibly blocked by illumination of

WiChR-expressing cultures, with illumination for 10 seconds causing relaxation beyond those obtained in diastolic intervals between AP (Figure 3.21 G).

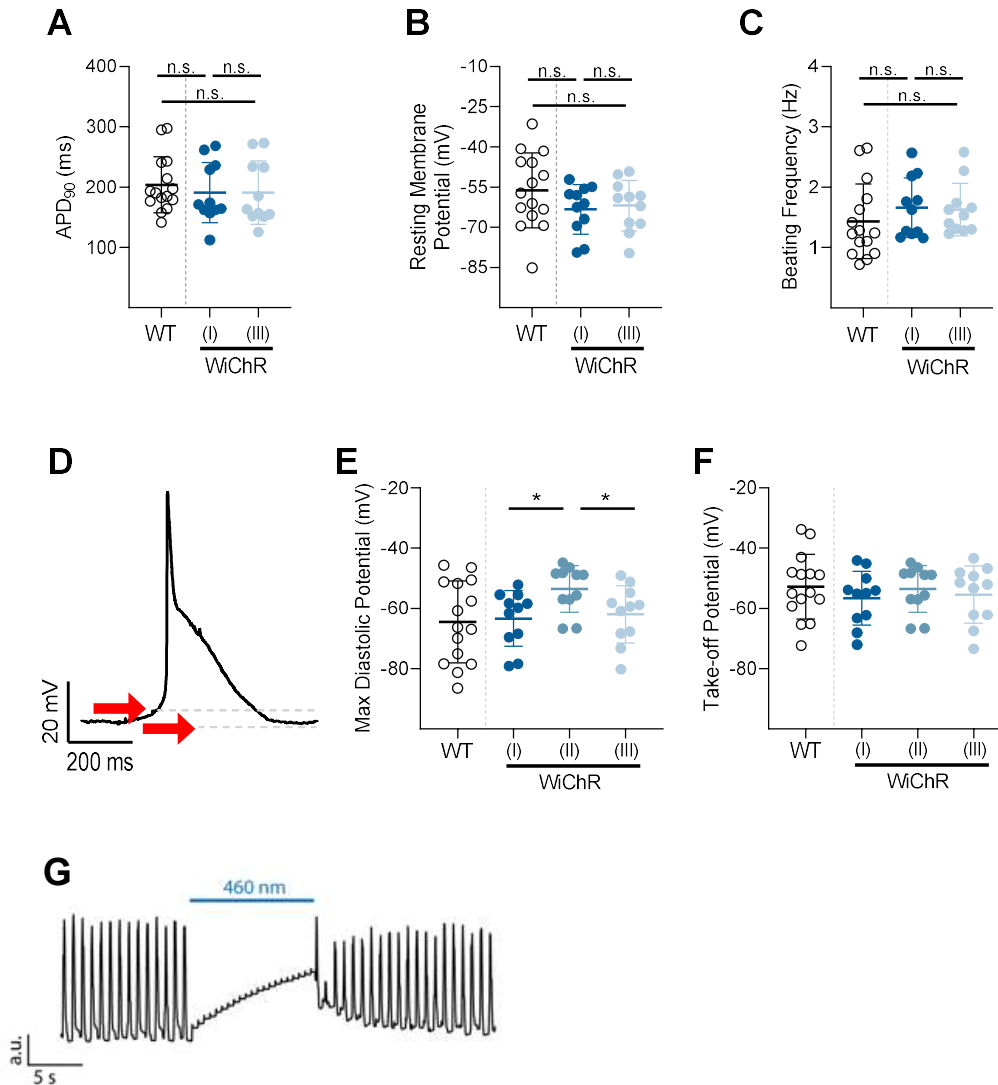


Figure 3.21 Comparison of AP properties of WiChR expressing cells compared to WT cells, and comparisons before, during and after light. (A) Quantification of action potential duration at 90% of repolarization (APD₉₀), (B) resting membrane potential (RMP) and (C) beating frequency before and after light application comparing non-transfected control cultures (WT) to cultures expressing WiChR. (D) AP representation with red arrows indicating the two parameters: max diastolic depolarization (MDP) and take-off potential (TOP). (E) and (F) Comparison of maximum diastolic potential and take-off potential in control cultures to WiChR-expressing cultures in phases I (average of 10 AP before light application) and III (average of 11th to 20th AP after light), respectively. For phase II (during light application), the average membrane potential between 4.5 and 5.5 s of illumination is plotted. Mann-Whitney test was used for group-wise statistical analyses. (G) Analysis of representative video showing WiChR-mediated inhibition of contractio



**“We need to challenge the way
things have been done and create safe
spaces to build trust in our institutions.”**

Clara Barker – Material scientist and activist for inclusion in STEM.

Discussion

5.1 hiPSC as a valuable model for atrial cells

5.1.1 Comparison of hiPSC-aCM differentiatiton protocols

For studying atrial arrhythmias under a molecular aspect, it is fundamental to have a human model of atrial cardiomyocytes. Despite the first protocol to differentiate hiPSC into cardiomyocytes monolayers dates back to 2011(132), so far have been published only seven different protocols to differentiate into the atrial cardiomyocytes subtype (160,163,165,166,169,218). In order to assess the correct phenotype of the differentiated hiPSC, in each on these studies hiPSC-aCM have been extensive characterized under a molecular and functional aspect. Indeed, previous studies using isolated cells from the human heart have revealed that human atrial and ventricular cardiomyocytes possess distinct molecular properties. And the distinct transcriptional signature between these two cell types is the main cause of differences in their electrophysiological and contractile behaviors.

Compared to the first atrial differentiation protocol by Zhang et al (160), many improvements have been done to obtain a more pure population of atrial-like cardiomyocytes (Table 6.1). The first published protocols had an efficiency of 50% of TNNT2+ atrial-like cardiomyocytes, while current protocols yield 70/90% of TNNT2+ / MLC2v- hiPSC-CM. In our case, adapting the protocol by Cyganek et al. to our cell lines by extending the addition time of ATRA, we were able to obtain a population of 90% of TNNT2+/NR2F2+. A percentage that ranks with the highest of the protocols published so far. However, a percentage of 20% are still

MLC2v+, meaning that the final cell product is not atrial-like pure and that current protocols still need to be improved to reach that goal. Other than optimizing the timing and concentration of ATRA application, it is important to better characterize the mesodermal population obtained. Indeed, all the protocols introduced a concentration of 1 μ M ATRA during the late mesoderm stage to lead the differentiation into atrial fate. However, it has been shown that RALDH2+ mesodermal population has a higher potential to differentiate into atrial-like subtypes, compared to its counterpart of CYP26A1+ mesodermal cells (163).

Concerning the electrophysiological feature of those cells, most of the characterization focused on action potential and calcium transient properties. While few of them explored the role of potassium currents I_{Kur} or $I_{K,Ach}$ kinetics (162,163). Action potential properties were recorded in different temperature, solutions, and instrumental conditions among the studies. The recorded properties in hiPSC-aCM revealed a RMP between -50 mV and -70 mV, similar to the respective hiPSC-vCM. As well as an APD90 between 150 ms and 250 ms, a much shorter duration compared to the hiPSC-vCM. Also in our study, results showed that differentiated hiPSC-aCM have a RMP of -64.1 ± 16.8 mV and an APD90 of 182.4 ± 54.2 ms. Measurements that are in accordance with previous studies (162,218).

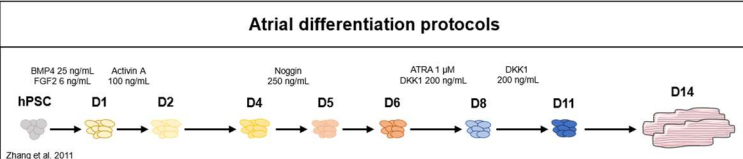
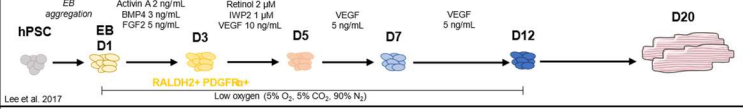
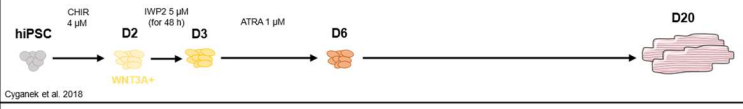
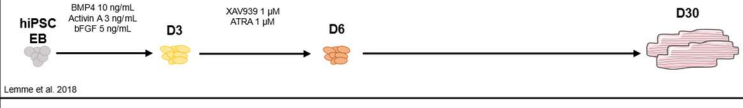
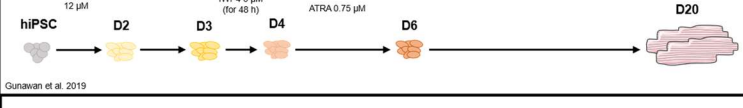
Atrial differentiation protocols		Efficiency	Readouts
 <p>Zhang et al. 2011</p>	<p>D14 50.7% TNNT2+</p>	<p>- Atrial-like AP - CaT properties</p>	
 <p>Devatta et al. 2015</p>	<p>D15 50% NKX2-5+</p>	<p>- Atrial-like AP - Currents I_{Kur} and I_{KAch}</p>	
 <p>Lee et al. 2017</p>	<p>D20 85% TNNT2+/MLC2V-</p>	<p>- Atrial-like AP - Currents I_{KAch}</p>	
 <p>Cyganek et al. 2018</p>	<p>D20 87% TNNT2+</p>	<p>- Atrial-like AP - CaT properties</p>	
 <p>Lemme et al. 2018</p>	<p>D20 75-95% TNNT2+</p>	<p>- Atrial-like AP - Contraction kinetics (optical recordings)</p>	
 <p>Gunawan et al. 2019</p>	<p>D20 74% TNNT2+/MLC2-</p>	<p>- Atrial-like AP - CaT properties</p>	
 <p>Casini et al. 2023</p>	<p>D20 85-95% TNNT2+</p>	<p>- Atrial-like AP - Contraction kinetics</p>	

Figure 6.1 Schematic representation of differentiation protocols for the generation of atrial cardiomyocytes from hiPSC. Cells colored in grey represent the undifferentiated stem cells, in yellow the mesoderm cells, in orange the cardiac progenitors. For those studies that analyzed atrial marker expression at different time points atrial-cardiac subtypes progenitors were colored in blue. BMP4 = Bone Morphogenetic Protein 4, FGF2 = Fibroblast Growth Factor 2, DKK1 = Dickkopf-1, SCF = Stem Cell Factor, VEGF = Vascular Endothelial Growth Factor, IWP4 = Inhibitor of Wnt Production-2, bFGF = basic Fibroblast Growth Factor. (Modified table from Wiesinger et al. 2021)

Despite AP properties having been extensively explored in each study of atrial differentiation, very little is known about the contraction kinetics of these cells. The only work that presented data about contraction properties has been from Lemme et al. (165) using the optic measurement CelloPTIQ. So far, various approaches have been used so far to study mechanical features, including carbon fiber force-length, MEMS force transducer, atomic force microscopy, micropillar

arrays, InGaN/GaN nanopillar arrays, traction force microscopy and video-based analysis (200,219). In our study we chose to explore the potential of the nanoindentation technique. An instrumentation that enabled us to measure direct force of contraction as well as kinetics properties of hiPSC-vCM and hiPSC-aCM. Data showed significant differences between the two cell populations concerning full width at half maximum, maximum and time to peak, giving insight to the contraction properties of hiPSC-aCM and underlying their contraction feature differences with hiPSC-vCM.

Altogether, those results demonstrated how the ATRA application after the mesoderm induction of hiPSC lead to different molecular, electrophysiological, and mechanical properties of the cardiomyocytes.

5.1.2 Comparison of hiPSC-aCM with adult atrial cardiomyocytes

For a translational application of those cells, a comparison with atrial cardiomyocytes isolated from human heart samples is required. For instance, adult ventricular cardiomyocytes are known to be enriched of the myosin isoform *MYH7* and *MYL2* (133,134), and of the transcription factors *IRX4* and *HEY2* (153,220). While atrial cardiomyocytes express mainly the myosin isoform *MYL7* and *MYL4* (156), as well as the transcription factor *NPPA* (157). Since the expression of *MYL7* is also a sign of immaturity (221,222), it was not an ideal marker for our atrial and ventricular differentiations. However, we could appreciate differences concerning

the expression of the transcription factors *IRX4* and *HEY2*, *NPPA* and *NR2F2*. A pattern that resembles the genetic signature of atrial-like and ventricular-like adult cardiomyocytes (152,153,223,224).

The advent of single cell transcriptomic has empowered the scientific community to delve deeper into the molecular profiles of distinct cell types within the cardiac tissue. A work from Litvinuková, et al. (225), elucidated that atrial cardiomyocytes can be categorized in five different subtypes groups. And that their percentage distribution differs between the right and left chamber. Each subtype is distinguished by a unique molecular signature. However, the temporal dynamics of subgroup formation remain unclear. Specifically, in the context of hiPSC-aCM, the differentiation trajectory towards specific atrial subgroups induced by ATRA is yet to be elucidated. A comprehensive molecular phenotype characterization holds promise in unraveling the timing of subgroup formation and identifying the transcription factors orchestrating the differentiation process into specific atrial subtypes.

Concerning the electrophysiological features, RMP of human atrial cells is less negative compared to the ventricular (226). However, in our study as well as in none of the protocols, we could not appreciate any significant difference between hiPSC-vCM and hiPSC-aCM. Comparing the RMP values of hiPSC-aCM with those of mature cardiomyocytes, we can also appreciate a more depolarized membrane potential. Such a difference could be explained by insufficient expression of the inwardly rectifying potassium channels $K_{ir2.1}$ and $K_{ir2.2}$ (227,228). Channels

that are fundamental to establish and maintain the RMP. The immaturity of hiPSC-aCM compared to atrial adult cardiomyocytes is also the slower maximum speed of depolarization. While in our study we could appreciate an upstroke velocity of 25.7 ± 13.1 V/s, in mature atrial cardiomyocytes the values reach velocities of 300-400 V/s (158). A difference that could be explained by a lower activity or expression of the sodium channels encoded by SCN5A. Finally, despite the APD90 of hiPSC-aCM and hiPSC-vCM were significantly different, its duration was shorter compared to adult cardiomyocytes whose APD90 at 1 Hz ranges between 150 and 500 ms,

As previously described, for contraction studies we chose the nanoindentation technique, which has been previously used for cardiotoxicity studies in adult cardiomyocytes (229). However, a direct comparison between our differentiated cardiomyocytes with adult cardiomyocytes is difficult to interpret. Indeed, compared to adult cardiomyocytes, hiPSC-CM have different myofibril structure and organization (230,231) Indeed, comparing the amplitude of our hiPSC-vCM (10.24 ± 1.31 nN) and hiPSC-aCM (9.89 ± 1.03 nN) with radial force measurements in adult cardiomyocytes, we can appreciate that the force of contraction perpendicular to the long axis of the adult cardiomyocytes is twice the amplitude we measured in hiPSC-CM (219). Since the measured force is perpendicular to the main orientation of the cardiomyocyte's filaments, nanoindentation technique might not be ideal for this type of assessment. However, its use can give great insight into kinetics contraction properties. Nonetheless,

similar differences in contraction kinetics between hiPSC-vCM and hiPSC-aCM have been observed as well in adult ventricular and atrial cardiomyocytes (232).

This study delineated the impact of treating hiPSC with ATRA from day 3 to day 8 during their differentiation process. This treatment protocol resulted in a notable upregulation of transcription factors pivotal for the development of atrial-subtype cardiomyocytes. Notably, the resultant molecular profile of the hiPSC-derived atrial cardiomyocytes closely resembled that of adult atrial cardiomyocytes. The observed transcriptomic distinctions between hiPSC-derived ventricular cardiomyocytes (hiPSC-vCM) were accompanied by electrophysiological and mechanical characteristics akin to those exhibited by adult cardiomyocytes. Despite these promising findings, it's important to note that defining distinct subtypes within the population of atrial cardiomyocytes remains a challenge, and the electrophysiological features indicated that cardiomyocytes derived from hiPSCs are still in an immature developmental stage.

To address these limitations, various strategies have been employed, as detailed in the work by (233) encompassing diverse techniques such as 3D cultures, co-culture systems, and micropatterned surfaces. These methodologies aim to further refine the differentiation process and enhance the maturation of hiPSC-derived cardiomyocytes. However, it is evident that considerable efforts are still required to comprehensively advance our understanding and capabilities in this intricate scientific domain.

5.2 hiPSC-aCM recapitulate basic AF mechanisms

After characterizing the hiPSC-aCM differentiation, our investigation's next stage involved determining if a monolayer of hiPSC-aCM is able to mimic functional re-entries and high-frequency focal activity. As well as if such model could give insight into the pathophysiological processes involved in AF development, such as structural, electrical or metabolic remodeling. Indeed, the primary pathophysiological mechanisms underlying AF development are triggered by mechanical and oxidative stress, inflammation (4,36,217). These processes lead to remodeling involving tissue fibrosis (structural remodeling), alterations in the distribution, expression, and activity of ion channels, exchangers, pumps, and connexins (electrical remodeling) (29). Consequently, a substrate is formed, providing a possible conducive environment for the initiation of re-entrant electrical activity by focal ectopic activity (trigger) (10). This, in turn, results in the generation of rapid, irregular atrial activity with re-entrant patterns whose circuits may vary depending on the severity of the tissue remodeling (19,25,64). However, the precise mechanisms of initiation, maintenance and perturbation of this mechanisms is still unclear and complicated to investigate (234).

A way to increase our knowledge of basic AF mechanisms is to create experimental models that better resemble this clinical condition. So far, several experimental models have been used to elucidate those mechanisms: *in vivo*, *ex vivo*, *in silico* and *in vitro* models. Specifically, *ex vivo* acute models involving pressure

increases or pharmacological interventions like carbachol in isolated heart Langendorff systems have been employed (235). In other cases, weeks or months of atrial stimulation have been used to induce fibrillation *in vivo* models (236). While these approaches have significantly advanced our understanding of AF, they come with notable limitations, including species differences in cardiac ion channels and ethical concerns. On the other hand, *in silico* models have the ability to test drugs in a cheap and reproducible way but are still far from reproducing the complicated architecture of a biological atrium (97,237). When it comes to *in vitro* models, much of our current understanding is based on the analysis of ventricular cells (238) or interspecies models like HL-1 cells (30). These approaches often present translational challenges due to species-specific differences. In this context, the emergence of hiPSC and their ability to differentiate into hiPSC-aCM represents a significant advancement, offering a more clinically relevant platform for *in vitro* studies of AF (239). So far, only few studies explored hiPSC-aCM as AF *in vitro* model (174,240). Thorpe et al. showed that hiPSC-aCM can form 'rotor style arrhythmia', while Seibert et al. explored the electrical remodeling that cells undergo under rapid pacing. Demonstrating a connection between alteration of L-type Ca^{2+} ($I_{\text{Ca,L}}$), acetylcholine-activated inward-rectifier K^{+} ($I_{\text{K,Ach}}$) and inward rectifier K^{+} current (I_{K1}).

On our side, we established a SR-like model using surfaces whose area was too restricted to sustain the nature of the re-entrant activity. On the other hand, large surfaces allowed spiral re-entries providing increased space for spiral wave

rotation without interference or disruption due to boundaries. In this second AF-like model, hiPSC-aCM sheets displayed not only a faster mean activation period compared to cells in SR-like conditions, but also irregularities in the time between activations. These characteristics confirm a higher activation frequency typical for AF, providing a platform to investigate the mechanisms underlying AF initiation and maintenance. Finally, we wanted to analyze whether hiPSC-aCM cultured in AF-mimicking conditions with sustained fibrillatory activity undergo alterations of gene expression. In fact, from literature it is known that AF causes irregular and rapid contractions of hiPSC-aCM leading to a progression of electrical and structural changes in the heart (29). These changes occur rapidly (electrical remodeling) and over a longer period (structural remodeling), with the latter involving alterations in the extracellular matrix and the development of atrial fibrosis. While altered gene expression plays a vital role in adapting to these changes, its specific impact on AF remains understudied, particularly in human atria and *in vitro* models.

Initial studies of gene remodeling in AF using qPCR and Western blot techniques revealed differences in potassium and calcium channels such as *CACNA1C*, *KCNA5*, *KCNQ1*, *KCNH2* and *KCNJ2/12/4*. However, conflicting results have been reported among different labs (31). Thanks to the advent of RNA sequencing technology researchers could perform more comprehensive investigations of the genes, pathways and their interplay during AF progression (241). Nonetheless, in recent years it has been discovered that the basic genetic

mechanisms involved in AF initiation and progression are not only connected to channel expression, but also to inflammation response (242), ECM formation (243) and endothelial dysfunction (214), three phenomena orchestrated by the interplay of different cell types such as cardiomyocytes, fibroblasts and macrophages. Despite the release of cytokines and extracellular matrix modulator it is associated mainly to fibroblasts and macrophages, there are evidence that another actor takes part of this scenario, cardiomyocytes. Emerging studies demonstrated that cardiomyocytes could act as initiation of processes involved in inflammation coordinating leukocyte recruitment (244).

On our side, in a model built only on hiPSC-aCM we observed upregulated expression of genes associated with ECM formation, including metalloproteinase family member *MMP1* and ECM glycoproteins *ICAM1*, *LAMC2*, and *VTN* in when cultured in AF-like conditions. A gene signature that likely contributes to fibrosis (245–247) and subsequent structural remodeling, culminating in the development of AF. Indeed, previous studied demonstrated how *MMP1* is involved in the degradation of different collagen types (32) and laminin (248). As well as *ICAM1* is a recruiter of different proinflammatory cytokines taking part of the cardiac remodeling (249).

Furthermore, as illustrated in Figure 6.2, we detected that in hiPSC-aCM under fibrillatory activity expression levels of interleukins IL11 and IL16, as well as the chemokine CXCL8 were higher. Remarkably, prior research has underscored the significance of IL11 and IL16 in driving the synthesis of pro-fibrotic proteins

(250) and initiating cytokine cascades, which are strongly implicated in pathological cardiac remodeling. More specifically, chronic treatment of rats with IL11 revealed shortening of atrial refractoriness period as well as of cardiomyocytes volume and stretching. This effect was justified by an hypertrophy-dependent increment of stretch-dependent ionic currents with consequent membrane hyperpolarization (251). However, IL11 effects are not limited to cardiomyocytes. This cytokine is indeed able to recruit T cells and activate fibrogenic protein synthesis in fibroblast through its receptor IL11RA (250). On another side, IL16 demonstrated be involved the fibrotic process through activation of macrophages infiltration and consequent release of TGFβ1 as well as mediator of other cytokine production (252,253).

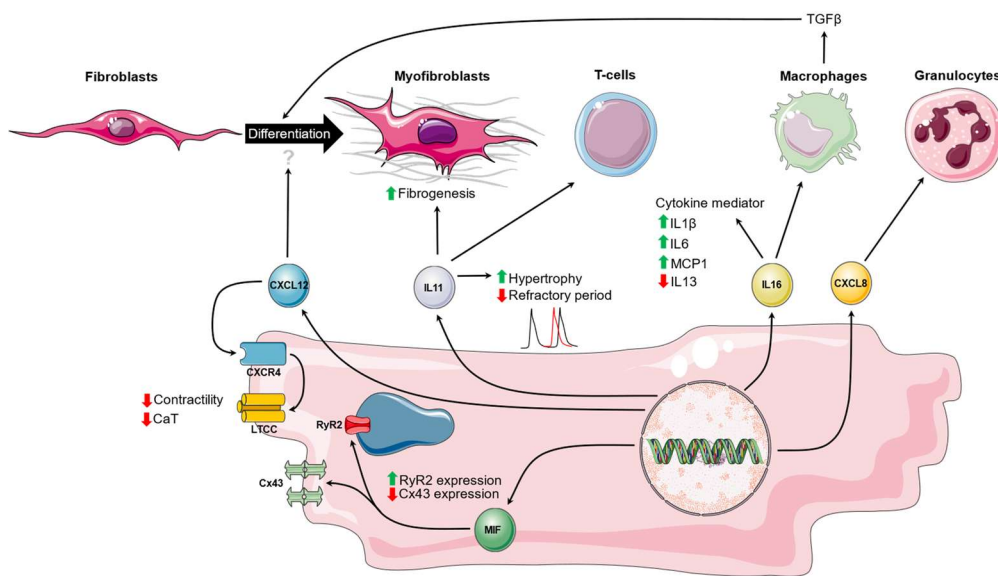


Figure 6.2 Schematic representation of the effects correlated to the altered cytokines expression in hiPSC-aCM under fibrillatory activity. The cytokines CXCL8, IL16, IL11, CXCL12 and MR have direct and indirect effects on cardiac remodeling. CaT = calcium transient, LTCC = L-type calcium transient, Cx43 = connexin 43, RyR2 = Ryanodine Receptor 2, MCP1 = Monocyte chemoattractant protein 1, TGFβ = transforming growth factor beta.

Strikingly, we observed a reduction of CXCL12 expression. While its ionotropic effect on cardiomyocytes has been clarified (254), there are still controversies about the effect on fibrosis and cardio protection (35). The loss of CXCL12 signaling may alter the migration and homing of specific cell types within the atrial tissue, thereby affecting the tissue microenvironment and promoting AF progression. However, the opposite pattern of an upregulated expression of CXCL12 and its receptor CXCR4 has been related to atrial remodeling (255). Thus, these discrepancies should be further investigated. Finally, in hiPSC-aCM upon fibrillatory activity we could detect an increased expression of the Macrophage Migration Inhibitory Factor (MIF). In mice experiments its expression was shown to be induced by external stimuli such as myocardial infarction induction (256). Interestingly, previous studies tested its effect on HL-1 atrial myocytes and detected downregulation of Cx43 (78) and higher expression of the Ryanodine Receptor 2, with consequent increase of CaTs (257). However, while we could appreciate differences in MIF expressions as well as in CaT frequencies, RNAseq experiments did not detect any alteration of RyR or Cx43 expression. Ultimately, the observed transcriptomic changes concerning DNA replication and activity remain unexplained at present. These findings warrant further investigation for future studies to elucidate the underlying mechanisms and significance of these alterations.

Taking together, these results confirm that the transcriptional remodeling of hiPSC-aCM *in vitro* can recapitulate changes involved in inflammation and fibrosis during AF initiation and remodeling. Two biological processes that so far were

mainly correlated to fibroblasts and macrophages. Thus, the model we introduce has a potential for investigating the contribution of cardiomyocytes to inflammation and fibrosis in heterocellular preparations. As well as to study the dependent mechanisms among structural, electrical and immune remodeling and their mutual promotion during AF progression. Finally, given the patient-specific origins of hiPSC, this model could be used for high throughput screening of potential new therapeutic strategies involved in fibrosis and inflammation mechanisms.

5.3 Comparison with other AF models

In this chapter will be discussed advantages and disadvantages of our model in comparison to other cellular models of different origin. *In vitro* models for AF studies, indeed, comprehend human tissue-derived atrial cardiomyocytes, primary animal-derived atrial cardiomyocytes, immortalized rodent atrial cardiomyocytes and, finally, hiPSC-aCM.

Patients-derived atrial cardiomyocytes have been broadly used to study AF-related cellular electrophysiological and molecular abnormalities (31). Indeed, the features of isolated cardiomyocytes better resemble physiological conditions compared to those of hiPSC-aCM (see chapter “5.1.2 Comparison of hiPSC-aCM with adult atrial cardiomyocytes”). Nevertheless, the constraint of this model is reflected in the diverse nature of tissue procurement from patients, encompassing individuals of varying ages, with distinct cardiac pathogenesis, and subjected to diverse drug treatments (93). Finally, isolated cardiomyocytes limit the investigation of AF mechanisms to single cells. Because of its inability to form multicellular sheets, this model cannot be used to phenomena such as re-entry circuits and arrhythmia complexity, parameters on which we focused for our study.

On the other hand, primary animal-derived cardiomyocytes offer a great platform to study mechanisms and processes involved in AF initiation, propagation and termination in a multicellular format. Previous studies on neonatal rat atrial cardiomyocytes succeeded in inducing AF-like functional re-entry with a rotor

frequency of 14.1 ± 7.4 Hz (258–260). However, such high frequency is a consequence of the known differences in cardiac electrophysiology compared to human cardiomyocytes (261). The difference in composition, properties and activity of cardiac ion channels limits the translational value of these models. Finally, an additional drawback of this model is the ethical consequences of using animal models as source for research investigation (262). Nevertheless, one of the advantages of this model, especially compared to our hiPSC-aCM model, is its affordability and broadly established isolation protocol.

A way to overcome the sustained use of animals is the generation of permanent immortalized cardiomyocytes from transgenic mice, such as the HL-1 cell line. A cell line that can proliferate while retaining an immature atrial cardiomyocyte phenotype. Numerous studies used a model of rapidly stimulated HL-1 cells to identify proteins and pathway involved in AF-related remodeling (30,263,264). Interestingly, the pathways identified in in HL-1 cells do not belong to ECM formation or immune responses as in our hiPSC-aCM model. The different results might be explained by the large structural and electrophysiological heterogeneity among HL-1 cells, that reside in different phases of cell cycle. For the same reason, it might be also explained the slow CV recorded in those cells (CV: 0.5–4 cm/s, Activation frequency: $2.83 \pm 1.43 - 3.02 \pm 0.56$ Hz) (265). Numbers that resemble those obtained on hiPSC-aCM. However, while for HL-1 the drawback of different cell cycles cannot be overcome, for hiPSC-aCM there are

different studies focused on enhancing the cardiomyocytes maturity in order to reach higher CV and a more physiological condition (222,233).

No functional cardiac myocytes meeting the criteria for subsequent utilization as an atrial arrhythmia model were obtained from the conditionally immortalized cell lines. These unsatisfactory outcomes led Liu et al. to explore an alternative approach for producing conditionally immortalized cardiac myocyte lines, leading to the development of the iAM-1 cell line (266) for AF studies. Immortalized iAM-1 cells demonstrated to surpass the structural and electrophysiological maturation of HL-1 and hiPSC-aCM, exhibition consistent behaviours across multiple cell passages. Indeed, in cell sheets of iAM-1 with CV of 21 ± 1 cm/s and activation frequency of 18.9 ± 1.3 Hz. However, one of the major drawback of this model is the concern for in vivo applications because of the presence of a viral oncogene in their genome (267,268). Finally, for patient-specific studies iAM-1 should undergo a complex genome editing procedure that could be avoided with the use of patient-specific hiPSC lines.

Overall, hiPSC-aCM could potentially represent a more relevant AF model than those obtained with animal cells, especially considering their patient-specific properties. However, more research needs to be done to improve their immaturity, cell heterogeneity and cost effectiveness for a broader application.

5.4 Optogenetic to study arrhythmia mechanisms

In the previous chapter we discussed the ability of hiPSC-aCM monolayers to recapitulate re-entrant phenomena leading to the abnormal electrical activity that sustains the chaotic and rapid rhythm of AF. On a cellular level, re-entries can be initiated and sustained by different factors such as calcium handling abnormalities (EADs and DADs) and shortened refractory period. Altogether, these factors create a complex interplay each influencing and potentially amplifying the effects of the others, contributing to a further electrophysiological and structural remodeling. Therefore, to avoid the arrhythmia-driven remodeling, future therapies require the ability to perturb and control the altered cardiac activity on a spatiotemporally defined manner. Optogenetics, differently from other techniques such as electrical, mechanical and chemical approaches, enables one to control cell-type specific activity with micrometer- and millisecond-precision.

In this study, we focused on the use of three different optogenetic tools: HcKCR1, HcKCR2 and WiChR. The aim was to test their ability to optically induce transmembrane currents under prolonged illumination and to assess their effects on AP kinetics in hiPSC-aCM. Firstly identified channelrhodopsins from green algae (such as ChR1 and ChR2 from *Chlamydomonas reinhardtii*) are light-gated cation-nonspecific channels, and were shown to mediate passive ion flux of protons, sodium, potassium, calcium and magnesium (186). As result, activation of cation channelrhodopsins leads to a depolarization of the membrane potential in

cardiomyocytes (269). In contrast, the light-gated channels tested in this study (HcKCR1, HcKCR2 and WiChR) were previously reported to predominantly conduct K^+ . In our hiPSC-aCM model, we observed depolarizing currents upon HcKCR2 activation, depolarising the cell to about -64.3 ± 10.1 mV. The different effects between the tested KCR could be explained by their different selectivity ratio for K^+ to other cations (195). Accordingly, a lower selectivity for K^+ in HcKCR2 would directly lead to a less negative reversal potential due to the contribution of Na^+ and Ca^{2+} to photocurrents. In hiPSC-aCM, depolarization will shift the membrane potential closer to the take-off potential of an action potential, thereby enhancing the spontaneous AP frequency with consequent reduction of the APD. Such restitution change might be achieved by a contribution of both light-gated channel and intrinsic channels such as K^+ channel activation. In HcKCR1-expressing cells, we did not observe a change in membrane potential, but AP shortening only. This observation would be in line with an increased K^+ selectivity of HcKCR1, as previously proposed. In this case, due to a more negative reversal potential, average of diastolic membrane potential was not altered, but outward K^+ currents lead to AP shortening at more depolarised potentials during the AP.

When activating the WiChR channel in aCM, in all recordings we observed a fast and small hyperpolarization of 4 ± 1.2 mV within a few ms of light activation, with aCM reaching voltage levels comparable to the maximum diastolic potentials. During prolonged illumination, the membrane voltage depolarized to levels comparable to the take-off potential. We hypothesize that WiChR activation leads

to the opening of hyperpolarization-activated cyclic nucleotide-gated channels (HCN), and potentially also T-type Ca^{2+} channels, which together with directly WiChR mediated K^+ currents establish a new equilibrium potential. Differently from HcKCR1- and HcKCR2-transfected cells, WiChR-transfected hiPSC-aCM AP were silenced because of the higher ion selectivity, slower kinetics, and higher light sensitivity of the WiChR channel that altogether provoked the 'shunting phenomenon' clamping the close to the reversal potential of WiChR. A similar silencing effect has been observed before with the two-component optical silencer system PAC/K composed of a photoactivated cyclase and the small cyclic nucleotide-gated K^+ channel SthK (194). Using this system, AP was inhibited with no changes in RMP. However, because of its mechanisms of action, PAC/K kinetics are at least one order of magnitude slower than WiChR closing kinetics, which may hamper PAC/K application for studying arrhythmia mechanisms. Other optogenetic inhibitory constructs include light-driven proton pumps (270), light-activated sodium pump (271), light-gated chloride channels (272,273). Nevertheless, their activation requires a large intense light for maximization of ion transport across the membrane. Indeed, for the transport of one ion the absorption of one photon is required. Furthermore, it has been demonstrated that their prolonged activation in cardiomyocytes led to changes in resting membrane potential.

Overall, the results demonstrated that the three tested channels, HcKCR1, HcKCR2 and WiChR, can be used to perturb and/or control electrical activity of

hiPSC-aCM. Tools like HcKCR1 and HcKCR2 might be especially useful for mimicking AP shortening as observed during early stages of AF. The ability to induce AP shortening in a spatiotemporally defined manner could help one to dissect cellular and molecular mechanisms underlying arrhythmogenesis, but also serve as model for testing the effects of antiarrhythmic drugs. Even more interesting for application might be the use of WiChR. Its ability of silencing spontaneous AP keeping the membrane potential close to the take-off potential opens a new chapter in the use of optogenetic approaches for terminating atrial arrhythmia. Indeed, previously used light-gated K^+ channels had insufficiently fast kinetics for a proper application in arrhythmia studies (194). Previous studies using light-gated cation channels, including ChR2- and ReachR, showed their ability to terminate atrial arrhythmia. However, their opening is associated with an influx of ions such as H^+ , Na^+ and Ca^{2+} . For this reason, their prolonged activation could induced a overload of intracellular ions thus promoting arrhythmogenic effects (274), limiting their application in the context of arrhythmia termination. On the other hand, thanks to its fast kinetics and strong K^+ selectivity, WiChR might be an interesting tool to rapidly induce AP inhibition with consequent arrhythmia termination without arrhythmogenic side-effects. However, before clinical applications, the optogenetic approaches needs to be tested in larger animals that better resemble physiological conditions of the human heart. At the same time, development of improved and selective gene-transfer methods needs to be done.

Conclusions & Limitations

Conclusions

Thanks to the study conduct in this thesis, the overall conclusions of this work are:

1. Treatment with ATRA after mesoderm induction (day 3 of differentiation) until cardiomyocytes progenitor state (day 8 of differentiation) lead the differentiation into hiPSC-aCM with molecular, electrophysiological, and mechanical features comparable to atrial cardiomyocytes of the heart.
2. Re-entries, a basic mechanism of AF initiation and maintenance, can be spontaneously induced in hiPSC-aCM sheets by modulating surface area.
3. Sheets of hiPSC-aCM under fibrillatory activity undergo molecular, structural, and immune remodeling comparable to those encountered in literature about tissues from AF patients.
4. hiPSC-aCM AF-like might be use for future studies to understand the role of cardiomyocytes into AF initiation, as well as for in deep molecular mechanisms and drug screening studies.
5. Optogenetics actuators *HcKCR1* and *HcKCR2* are not able to inhibit spontaneous AP of hiPSC-aCM upon prolonged light activation. Their activation, however, induce changes in AP shape and RMP.
6. The optogenetic actuator *WiChR* upon prolonged light activation is able to inhibit spontaneous AP in hiPSC-aCM.
7. *WiChR* might be a useful tool for studying arrhythmia termination and cardioversion mechanisms.

Despite exhibiting characteristics of immature myocardium, such as slow conduction velocity and depolarized resting membrane potentials, hiPSC-aCM demonstrated the formation and maintenance of electrical activity that closely resemble the self-sustaining drivers observed in AF. However, further attempts to increase the hiPSC-CM maturity such as micropatterned surfaces, 3-D engineered tissues or co-culture should be made. Indeed, to better resemble heart tissue *in vivo*, our model should include more complexity with other cell types such as fibroblasts, endothelial cells and immune cells, which would more closely mimic the heterocellular microenvironment of the atrial tissue. On the other hand, the use of 3D cultures, tissue-engineered constructs or organoids could provide a more physiologically-relevant platform for studying AF mechanisms and might bolster cardiomyocyte maturation. Future investigations could explore the fibrillatory activity and gene expression alterations and related proteins at various time points, which might provide valuable information to better understand AF progression and its remodeling. Another important aspect would be to investigate the relative contribution of hiPSC-CM to inflammation and fibrosis in heterocellular preparations, where highly specialized cells such as immune cells or fibroblasts are present. Nonetheless, this cellular model of AF is a cost-effective and time-efficient approach providing high experimental flexibility. In the context of automated drug screening, this model offers a valuable resource for the identification and personalization of potential therapeutic candidates for the treatment of AF.

Contributions & Trainings

Contributions

Published papers:

- **WiChR, a highly potassium-selective channelrhodopsin for low-light one- and two-photon inhibition of excitable cells** - J. Vierock, E. Peter, C. Grimm, A. Rozenberg, I. Chen, L. Tillert, A. G. Castro Scalise, M. Casini, S. Augustin, D. Tanese, B. C. Forget, R. Peyronnet, F. Schneider-Warme, V. Emiliani, O. Béjà, P. Hegemann - *Science Advances*, 2022 - DOI: 10.1126/sciadv.add7729
- **Impact of mechanically-induced fibrosis on atrial electromechanical function** - T. Schiatti, M. Casini, T. Hutschalik, M. Koch, R. Emig, R. Peyronnet, U. Ravens - *Conference Paper Computing in Cardiology*, 2023 - DOI: 10.22489/CinC.2022.426
- **Modeling cardiotoxicity in pediatric oncology patients using patient-specific iPSC-derived cardiomyocytes reveals downregulation of cardioprotective microRNAs** - I. Reinal, I. Ontoria-Oviedo, M. Selva, M. Casini, E. Peiró-Molina, C. Fambuena Santos, A. M. Climent, J. Balaguer, A. Cañete, J. Mora, Á. Raya, P. Sepulveda - *Antioxidants*, 2023 – DOI: 10.3390/antiox12071378.

Papers under revision:

- **Uncovering the Pathophysiology of Atrial Fibrillation through Human Pluripotent Stem Cell-Derived Atrial Cardiomyocytes** - M. Casini, C. Fambuena, N. Reinal, I. O. Oviedo, R. Peyronnet, U. Ravens, A. Climent, P. Sepulveda – *Stem Cells Translational Medicine* – Under Revision
- **M1 Macrophages cause cardiac arrhythmia in an in vitro hiPSC coculture model of inflammation-induced atrial fibrillation** - T. Hutschalik, O. Özgül, M. Casini, B. Szabo, R. Peyronnet, M. Argenziano, U. Schotten, E. Matsa PhD - *Cardiovascular Research* – Under Revision

Congresses:

- **Subtype-specific Differentiation of Atrial and Ventricular Cardiomyocytes from Human iPSCs** - M. Casini, I. Reinal, I. O. Oviedo, A. M. Climent, P. Sepulveda - *European Society for Gene and Cell Therapy, 2021* - Poster presentation
- **Deep molecular characterization of hiPSC-derived atrial cardiomyocytes** - M. Casini, R. Peyronnet, U. Ravens, I. Reinal, I. O. Oviedo, A. M. Climent, P. Sepulveda - *Frontiers in Cardiovascular Biomedicine, 2022* - Poster presentation
- **Molecular, functional and mechanical characterization of hiPSC-derived atrial and ventricular cardiomyocytes** - M. Casini, M. Koch, R. Emig, R. Peyronnet, U. Ravens, P. Kohl, I. Reinal, I. O. Oviedo, A. M. Climent, P. Sepulveda - *ESC Working Group on Cardiac Cellular Electrophysiology, 2022* - Poster presentation
- **The role of rotors in atrial arrhythmogenic remodelling: an in-vitro study on hiPSC-derived atrial cardiomyocytes** - M. Casini, C. Fambuena, N. Reinal, I. O. Oviedo, R. Peyronnet, U. Ravens, A. Climent, P. Sepulveda - *ISSCR Congress, 2023* - Poster presentation
- **Invitro model of atrial fibrillation: investigating the initiation and maintenance of atrial remodeling using hiPSC-aCM** - M. Casini, C. Fambuena, N. Reinal, I. O. Oviedo, R. Peyronnet, U. Ravens, A. Climent, P. Sepulveda - *ESC Congress, 2023* - Oral presentation

Trainings

- **Data mining and statistics summer school** at Polytechnic University of Valencia, October – November 2020. Topics: electrophysiology and atrial fibrillation, medical registration and standards, basic signal and image processing, data Mining and Big Data, outcome prediction models and statistics, information search, team building workshop, digital tools and Open Science.
- **Advanced signal and image processing workshop** at Maastricht University, January 2021. Topics: systems biology and atrial fibrillation, advanced biomedical signal processing, advanced image processing, diversity in research, best teaching practices, time management.
- **Experimental electrophysiology and heart computer models summer school** at University of Bordeaux, July 2021. Topics: Heart modelling and numerical simulation, forward and inverse calculations, cardiac mapping laboratory, scientific writing, intellectual property protection
- **Clinical management of AF and bioengineering workshop** at Research Institute Hospital La Fe, January 2022. Topics: cell culturing and stem cells differentiation, transcriptomic and proteomic analysis, next Generation Sequencing Technologies, clinical management of atrial fibrillation, ethics in research, public engagement
- **Communication skills summer school** at Simula Research Laboratory, July 2022. Topics: fluid mechanics modelling and turbulence, communication and dissemination skills
- **Regulatory workshop** at University of Bologna, January 2023. Topics: gender issues in research, people management and leadership, female leadership, medical instrumentation regulation, medicament products regulation
- **Industry and career workshop** at Karlsruhe Institute of Technology, June 2023. Topics: funding sources and grant writing, innovation, start-up constitution, technology transfer process, market access and market research, career opportunities in industry, careers opportunities in academia, career opportunities workshop.

Secondments

- **University of Freiburg**, March 2022 – July 2022

Supervised by Professor Ursula Ravens and Doctor Remi Peyronnet

The Institute for Experimental Cardiovascular Medicine is a highly specialized Institute in cardiac electrophysiology and mechanics of the of the University of Freiburg. Thanks to this secondment as part of the Cell Biophysics Group, the PhD candidate had the possibility to perform the functional and mechanical characterization of the hiPSC-aCM, as well as the optogenetic experiments on hiPSC-aCM transfected with *HcKCR1*, *HcKCR2* and *WiChR*.

- **GenomeScan Company**, January 2023 – March 2023

Supervised by Doctor Sander Tuit

GenomeScan is a highly specialized company in omics studies. The program of this secondment aimed to acquire RNAseq data from hiPSC-aCM to detect arrhythmia biomarkers, providing an introduction into sequencing and processing data.

- **University of Oxford**, September 2023 – October 2023

Supervised by Professor Blanca Rodriguez

The program of the secondment at the Department of Computer Science of the University of Oxford aimed to learn the use of computer models for simulations of the established experimental model of hiPSC-aCM under fibrillatory activity. During the stay many collaborations started with expert in cardiac simulations.

Bibliography

1. Jiao M., Liu C., Liu Y., Wang Y., Gao Q., Ma A. Estimates of the global, regional, and national burden of atrial fibrillation in older adults from 1990 to 2019: insights from the Global Burden of Disease study 2019. *Front Public Heal* 2023;11. Doi: 10.3389/fpubh.2023.1137230.
2. Hindricks G., Potpara T., Dagres N., et al. 2020 ESC Guidelines for the diagnosis and management of atrial fibrillation developed in collaboration with the European Association for Cardio-Thoracic Surgery (EACTS). *Eur Heart J* 2021;42(5):373–498. Doi: 10.1093/eurheartj/ehaa612.
3. Schnabel RB., Yin X., Gona P., et al. 50 year trends in atrial fibrillation prevalence, incidence, risk factors, and mortality in the Framingham Heart Study: A cohort study. *Lancet* 2015;386(9989). Doi: 10.1016/S0140-6736(14)61774-8.
4. Falk RH. Etiology and Complications of Atrial Fibrillation: Insights from Pathology Studies. *Am J Cardiol* 1998;82(7 A). Doi: 10.1016/S0002-9149(98)00735-8.
5. Schotten U., Verheule S., Kirchhof P., Goette A. Pathophysiological mechanisms of atrial fibrillation: A translational appraisal. *Physiol Rev* 2011;91(1):265–325. Doi: 10.1152/physrev.00031.2009.
6. Chen YC., Voskoboinik A., Gerche A La., Marwick TH., McMullen JR. Prevention of Pathological Atrial Remodeling and Atrial Fibrillation: JACC State-of-the-Art Review. *J Am Coll Cardiol* 2021;77(22):2846–64. Doi: 10.1016/j.jacc.2021.04.012.
7. Al-Makhamreh H., Alrabadi N., Haikal L., et al. Paroxysmal and Non-Paroxysmal Atrial Fibrillation in Middle Eastern Patients: Clinical Features and the Use of Medications. Analysis of the Jordan Atrial Fibrillation (JoFib) Study. *Int J Environ Res Public Health* 2022;19(10). Doi: 10.3390/ijerph19106173.
8. Lévy S. Classification system of atrial fibrillation. *Curr Opin Cardiol* 2000.

Doi: 10.1097/00001573-200001000-00007.

9. Ogawa H., An Y., Ikeda S., et al. Progression from paroxysmal to sustained atrial fibrillation is associated with increased adverse events. *Stroke* 2018;49(10). Doi: 10.1161/STROKEAHA.118.021396.
10. Heijman J., Voigt N., Nattel S., Dobrev D. Cellular and molecular electrophysiology of atrial fibrillation initiation, maintenance, and progression. *Circ Res* 2014;114(9):1483–99. Doi: 10.1161/CIRCRESAHA.114.302226.
11. Roselli C., Chaffin MD., Weng LC., et al. Multi-ethnic genome-wide association study for atrial fibrillation. *Nat Genet* 2018;50(9):1225–33. Doi: 10.1038/s41588-018-0133-9.
12. Kalstø SM., Siland JE., Rienstra M., Christophersen IE. Atrial Fibrillation Genetics Update: Toward Clinical Implementation. *Front Cardiovasc Med* 2019;6(September):1–16. Doi: 10.3389/fcvm.2019.00127.
13. Elliott AD., Middeldorp ME., Van Gelder IC., Albert CM., Sanders P. Epidemiology and modifiable risk factors for atrial fibrillation. *Nat Rev Cardiol* 2023. Doi: 10.1038/s41569-022-00820-8.
14. Feinberg WM., Blackshear JL., Laupacis A., Kronmal R., Hart RG. Prevalence, Age Distribution, and Gender of Patients With Atrial Fibrillation: Analysis and Implications. *Arch Intern Med* 1995;155(5). Doi: 10.1001/archinte.1995.00430050045005.
15. Streur M. Atrial Fibrillation Symptom Perception. *J Nurse Pract* 2019;15(1). Doi: 10.1016/j.nurpra.2018.08.015.
16. Feghaly J., Zakka P., London B., Macrae CA., Refaat MM. Genetics of atrial fibrillation. *J Am Heart Assoc* 2018;7(20):1–15. Doi: 10.1161/JAHA.118.009884.
17. Nazarzadeh M., Pinho-Gomes AC., Bidel Z., et al. Genetic susceptibility,

- elevated blood pressure, and risk of atrial fibrillation: a Mendelian randomization study. *Genome Med* 2021;13(1). Doi: 10.1186/s13073-021-00849-3.
18. Wong GR., Nalliah CJ., Lee G., et al. Genetic Susceptibility to Atrial Fibrillation Is Associated With Atrial Electrical Remodeling and Adverse Post-Ablation Outcome. *JACC Clin Electrophysiol* 2020;6(12). Doi: 10.1016/j.jacep.2020.05.031.
 19. Jansen HJ., Bohne LJ., Gillis AM., Rose RA. Atrial remodeling and atrial fibrillation in acquired forms of cardiovascular disease. *Hear Rhythm O2* 2020;1(2). Doi: 10.1016/j.hroo.2020.05.002.
 20. Roney CH., Wit AL., Peters NS. Challenges associated with interpreting mechanisms of AF. *Arrhythmia Electrophysiol Rev* 2019. Doi: 10.15420/AER.2019.08.
 21. Schotten U., Lee S., Zeemering S., Waldo AL. Paradigm shifts in electrophysiological mechanisms of atrial fibrillation. *Europace* 2021;23. Doi: 10.1093/europace/euaa384.
 22. Wakili R., Voigt N., Käab S., Dobrev D., Nattel S. Recent advances in the molecular pathophysiology of atrial fibrillation. *J Clin Invest* 2011. Doi: 10.1172/JCI46315.
 23. Antzelevitch C., Burashnikov A. Overview of Basic Mechanisms of Cardiac Arrhythmia. *Card Electrophysiol Clin* 2011. Doi: 10.1016/j.ccep.2010.10.012.
 24. Cheniti G., Vlachos K., Pambrun T., et al. Atrial fibrillation mechanisms and implications for catheter ablation. *Front Physiol* 2018. Doi: 10.3389/fphys.2018.01458.
 25. Pandit S V., Jalife J. Rotors and the dynamics of cardiac fibrillation. *Circ Res* 2013;112(5):849–62. Doi: 10.1161/CIRCRESAHA.111.300158.

26. Jalife J. Déjà vu in the theories of atrial fibrillation dynamics. *Cardiovasc Res* 2011. Doi: 10.1093/cvr/cvq364.
27. Jalife J. Rotors and spiral waves in atrial fibrillation. *J Cardiovasc Electrophysiol* 2003. Doi: 10.1046/j.1540-8167.2003.03136.x.
28. Al-Kaisey AM., Parameswaran R., Kalman JM. Atrial fibrillation structural substrates: Aetiology, identification and implications. *Arrhythmia Electrophysiol Rev* 2020;9(3). Doi: 10.15420/AER.2020.19.
29. Allesie M., Ausma J., Schotten U. Electrical, contractile and structural remodeling during atrial fibrillation. *Cardiovasc Res* 2002. Doi: 10.1016/S0008-6363(02)00258-4.
30. Climent AM., Guillem MS., Fuentes L., et al. Role of atrial tissue remodeling on rotor dynamics: An in vitro study. *Am J Physiol - Hear Circ Physiol* 2015;309(11). Doi: 10.1152/ajpheart.00055.2015.
31. Dobrev D., Ravens U. Remodeling of cardiomyocyte ion channels in human atrial fibrillation. *Basic Res Cardiol* 2003. Doi: 10.1007/s00395-003-0409-8.
32. Fan D., Takawale A., Lee J., Kassiri Z. Cardiac fibroblasts, fibrosis and extracellular matrix remodeling in heart disease. *Fibrogenes Tissue Repair* 2012. Doi: 10.1186/1755-1536-5-15.
33. Sohns C., Marrouche NF. Atrial fibrillation and cardiac fibrosis. *Eur Heart J* 2020. Doi: 10.1093/eurheartj/ehz786.
34. Shen MJ., Choi EK., Tan AY., et al. Patterns of baseline autonomic nerve activity and the development of pacing-induced sustained atrial fibrillation. *Hear Rhythm* 2011;8(4). Doi: 10.1016/j.hrthm.2010.11.040.
35. Yao Y., Yang M., Liu D., Zhao Q. Immune remodeling and atrial fibrillation. *Front Physiol* 2022. Doi: 10.3389/fphys.2022.927221.
36. Al Ghamdi B., Hassan W. Atrial remodeling and atrial fibrillation:

- Mechanistic interactions and clinical implications. *J Atr Fibrillation* 2009. Doi: 10.4022/jafib.v1i7.537.
37. Yue L., Xie J., Nattel S. Molecular determinants of cardiac fibroblast electrical function and therapeutic implications for atrial fibrillation. *Cardiovasc Res* 2011;89(4):744–53. Doi: 10.1093/cvr/cvq329.
 38. Liao CH., Akazawa H., Tamagawa M., et al. Cardiac mast cells cause atrial fibrillation through PDGF-A - Mediated fibrosis in pressure-overloaded mouse hearts. *J Clin Invest* 2010;120(1). Doi: 10.1172/JCI39942.
 39. Sun Z., Zhou D., Xie X., et al. Cross-talk between macrophages and atrial myocytes in atrial fibrillation. *Basic Res Cardiol* 2016;111(6). Doi: 10.1007/s00395-016-0584-z.
 40. Yue L., Melnyk P., Gaspo R., Wang Z., Nattel S. Molecular mechanisms underlying ionic remodeling in a dog model of atrial fibrillation. *Circ Res* 1999;84(7). Doi: 10.1161/01.RES.84.7.776.
 41. Dobrev D., Voigt N., Wehrens XHT. The ryanodine receptor channel as a molecular motif in atrial fibrillation: Pathophysiological and therapeutic implications. *Cardiovasc Res* 2011. Doi: 10.1093/cvr/cvq324.
 42. Li N., Chiang DY., Wang S., et al. Ryanodine receptor-mediated calcium leak drives progressive development of an atrial fibrillation substrate in a transgenic mouse model. *Circulation* 2014;129(12). Doi: 10.1161/CIRCULATIONAHA.113.006611.
 43. Neef S., Dybkova N., Sossalla S., et al. CaMKII-Dependent diastolic SR Ca²⁺ leak and elevated diastolic Ca²⁺ levels in right atrial myocardium of patients with atrial fibrillation. *Circ Res* 2010;106(6). Doi: 10.1161/CIRCRESAHA.109.203836.
 44. El-Armouche A., Boknik P., Eschenhagen T., et al. Molecular determinants of altered Ca²⁺ handling in human chronic atrial fibrillation. *Circulation* 2006;114(7). Doi: 10.1161/CIRCULATIONAHA.106.636845.

45. Ehrlich JR. Inward rectifier potassium currents as a target for atrial fibrillation therapy. *J Cardiovasc Pharmacol* 2008. Doi: 10.1097/FJC.0b013e31816c4325.
46. Dobrev D., Friedrich A., Voigt N., et al. The G protein-gated potassium current $I_{K,ACh}$ is constitutively active in patients with chronic atrial fibrillation. *Circulation* 2005;112(24). Doi: 10.1161/CIRCULATIONAHA.105.575332.
47. Girmatsion Z., Biliczki P., Bonauer A., et al. Changes in microRNA-1 expression and IK1 up-regulation in human atrial fibrillation. *Hear Rhythm* 2009;6(12). Doi: 10.1016/j.hrthm.2009.08.035.
48. Makary S., Voigt N., Maguy A., et al. Differential protein kinase c isoform regulation and increased constitutive activity of acetylcholine-regulated potassium channels in atrial remodeling. *Circ Res* 2011;109(9). Doi: 10.1161/CIRCRESAHA.111.253120.
49. Beyer EC., Berthoud VM. Gap junction gene and protein families: Connexins, innexins, and pannexins. *Biochim Biophys Acta - Biomembr* 2018;1860(1). Doi: 10.1016/j.bbamem.2017.05.016.
50. Duffy HS., Wit AL. Is there a role for remodeled connexins in AF? No simple answers. *J Mol Cell Cardiol* 2008. Doi: 10.1016/j.yjmcc.2007.08.016.
51. Kostin S., Klein G., Szalay Z., Hein S., Bauer EP., Schaper J. Structural correlate of atrial fibrillation in human patients. *Cardiovasc Res* 2002;54(2). Doi: 10.1016/S0008-6363(02)00273-0.
52. Polontchouk L., Haefliger JA., Ebel B., et al. Effects of chronic atrial fibrillation on gap junction distribution in human and rat atria. *J Am Coll Cardiol* 2001;38(3). Doi: 10.1016/S0735-1097(01)01443-7.
53. Dhein S., Rothe S., Busch A., et al. Effects of metoprolol therapy on cardiac gap junction remodelling and conduction in human chronic atrial fibrillation. *Br J Pharmacol* 2011;164(2 B). Doi: 10.1111/j.1476-5381.2011.01460.x.

54. Dhein S., Salameh A. Remodeling of cardiac gap junctional cell–cell coupling. *Cells* 2021. Doi: 10.3390/cells10092422.
55. Matějková A., Šteiner I. Association of Atrial Fibrillation with Morphological and Electrophysiological Changes of the Atrial Myocardium. *Acta Medica (Hradec Kral 2016;59(2))*. Doi: 10.14712/18059694.2016.88.
56. Wight TN., Potter-Perigo S. The extracellular matrix: An active or passive player in fibrosis? *Am J Physiol - Gastrointest Liver Physiol* 2011;301(6). Doi: 10.1152/ajpgi.00132.2011.
57. Kendall RT., Feghali-Bostwick CA. Fibroblasts in fibrosis: Novel roles and mediators. *Front Pharmacol* 2014. Doi: 10.3389/fphar.2014.00123.
58. Tai Y., Woods EL., Dally J., et al. Myofibroblasts: Function, formation, and scope of molecular therapies for skin fibrosis. *Biomolecules* 2021. Doi: 10.3390/biom11081095.
59. Goudis CA., Kallergis EM., Vardas PE. Extracellular matrix alterations in the atria: Insights into the mechanisms and perpetuation of atrial fibrillation. *Europace* 2012. Doi: 10.1093/europace/eur398.
60. Soans KG., Norden C. Shining a light on extracellular matrix dynamics in vivo. *Semin Cell Dev Biol* 2021. Doi: 10.1016/j.semcdb.2021.05.008.
61. Doxakis A., Polyanthi K., Androniki T., Savvas P., Eleni Z. Targeting metalloproteinases in cardiac remodeling. *J Cardiovasc Med Cardiol* 2019;6(3). Doi: 10.17352/2455-2976.000092.
62. Leask A. Potential therapeutic targets for cardiac fibrosis: TGF β , angiotensin, endothelin, CCN2, and PDGF, partners in fibroblast activation. *Circ Res* 2010. Doi: 10.1161/CIRCRESAHA.110.217737.
63. LI CY., ZHANG JR., HU WN., LI SN. Atrial fibrosis underlying atrial fibrillation (Review). *Int J Mol Med* 2021. Doi: 10.3892/ijmm.2020.4842.
64. Verheule S., Schotten U. Electrophysiological consequences of cardiac

- fibrosis. *Cells* 2021. Doi: 10.3390/cells10113220.
65. Rücker-Martin C., Pecker F., Godreau D., Hatem SN. Dedifferentiation of atrial myocytes during atrial fibrillation: Role of fibroblast proliferation in vitro. *Cardiovasc Res* 2002;55(1). Doi: 10.1016/S0008-6363(02)00338-3.
66. Ausma J., Wijffels M., Van Eys G., et al. Dedifferentiation of atrial cardiomyocytes as a result of chronic atrial fibrillation. *Am J Pathol* 1997;151(4).
67. Marchianò S., Bertero A., Murry CE. Learn from Your Elders: Developmental Biology Lessons to Guide Maturation of Stem Cell-Derived Cardiomyocytes. *Pediatr Cardiol* 2019;40(7). Doi: 10.1007/s00246-019-02165-5.
68. Thijssen VLJL., Ausma J., Borgers M. Structural remodelling during chronic atrial fibrillation: Act of programmed cell survival. *Cardiovasc Res* 2001. Doi: 10.1016/S0008-6363(01)00367-4.
69. Flores-Vergara R., Olmedo I., Aránguiz P., Riquelme JA., Vivar R., Pedrozo Z. Communication Between Cardiomyocytes and Fibroblasts During Cardiac Ischemia/Reperfusion and Remodeling: Roles of TGF- β , CTGF, the Renin Angiotensin Axis, and Non-coding RNA Molecules. *Front Physiol* 2021. Doi: 10.3389/fphys.2021.716721.
70. Boldt A., Wetzel U., Weigl J., et al. Expression of Angiotensin II Receptors in Human Left and Right Atrial Tissue in Atrial Fibrillation with and Without Underlying Mitral Valve Disease. *J Am Coll Cardiol* 2003;42(10). Doi: 10.1016/j.jacc.2003.07.014.
71. Dartsch T., Fischer R., Gapelyuk A., et al. Aldosterone induces electrical remodeling independent of hypertension. *Int J Cardiol* 2013;164(2). Doi: 10.1016/j.ijcard.2011.06.100.
72. Spät A., Hunyady L. Control of Aldosterone Secretion: A Model for Convergence in Cellular Signaling Pathways. *Physiol Rev* 2004. Doi:

- 10.1152/physrev.00030.2003.
73. Schultz JEJ., Witt SA., Glascock BJ., et al. TGF- β 1 mediates the hypertrophic cardiomyocyte growth induced by angiotensin II. *J Clin Invest* 2002;109(6). Doi: 10.1172/jci200214190.
74. Heger J., Warga B., Meyering B., et al. TGF β receptor activation enhances cardiac apoptosis via SMAD activation and concomitant NO release. *J Cell Physiol* 2011;226(10). Doi: 10.1002/jcp.22619.
75. Li S., Jiang Z., Chao X., Jiang C., Zhong G. Identification of key immune-related genes and immune infiltration in atrial fibrillation with valvular heart disease based on bioinformatics analysis. *J Thorac Dis* 2021;13(3). Doi: 10.21037/jtd-21-168.
76. Tian Y., Liu S., Zhang Y., et al. Immune infiltration and immunophenotyping in atrial fibrillation. *Aging (Albany NY)* 2023;15(1). Doi: 10.18632/aging.204470.
77. Lazzarini PE., Abbate A., Boutjdir M., Capecchi PL. Fir(e)ing the Rhythm: Inflammatory Cytokines and Cardiac Arrhythmias. *JACC Basic to Transl Sci* 2023. Doi: 10.1016/j.jacbts.2022.12.004.
78. Li X., Rao F., Deng CY., et al. Involvement of ERK1/2 in Cx43 depression induced by macrophage migration inhibitory factor in atrial myocytes. *Clin Exp Pharmacol Physiol* 2017;44(7). Doi: 10.1111/1440-1681.12766.
79. Liew R., Khairunnisa K., Gu Y., et al. Role of tumor necrosis factor- α in the pathogenesis of atrial fibrosis and development of an arrhythmogenic substrate. *Circ J* 2013;77(5). Doi: 10.1253/circj.CJ-12-1155.
80. Jackson EK., Zhang Y., Gillespie DD., Zhu X., Cheng D., Jackson TC. SDF-1 α (stromal cell-derived factor 1 α) induces cardiac fibroblasts, renal microvascular smooth muscle cells, and glomerular mesangial cells to proliferate, cause hypertrophy, and produce collagen. *J Am Heart Assoc* 2017;6(11). Doi: 10.1161/JAHA.117.007253.

81. Bucci T., Proietti M., Shantsila A., et al. Integrated Care for Atrial Fibrillation Using the ABC Pathway in the Prospective APHRS-AF Registry. *JACC Asia* 2023;3(4). Doi: 10.1016/j.jacasi.2023.04.008.
82. Li J., Gao M., Zhang M., et al. Treatment of atrial fibrillation: A comprehensive review and practice guide. *Cardiovasc J Afr* 2020. Doi: 10.5830/CVJA-2019-064.
83. Yarlagadda B., Vuddanda V., Dar T., et al. Safety and efficacy of inpatient initiation of Dofetilide versus Sotalol for atrial fibrillation. *J Atr Fibrillation* 2017;10(4). Doi: 10.4022/jafib.1805.
84. Aguilar M., Xiong F., Qi XY., Comtois P., Nattel S. Potassium channel blockade enhances atrial fibrillation-selective antiarrhythmic effects of optimized state-dependent sodium channel blockade. *Circulation* 2015;132(23). Doi: 10.1161/CIRCULATIONAHA.115.018016.
85. Burashnikov A., Antzelevitch C. Atrial-selective sodium channel block for the treatment of atrial fibrillation. *Expert Opin Emerg Drugs* 2009. Doi: 10.1517/14728210902997939.
86. D.Sc. EMVWDM. Classification of antidysrhythmic drugs. *Pharmacol Ther Part B Gen Syst* 1975;1(1). Doi: 10.1016/0306-039X(75)90019-7.
87. Kühlkamp V., Bosch R., Mewis C., Seipel L. Use of β -blockers in atrial fibrillation. *Am J Cardiovasc Drugs* 2002. Doi: 10.2165/00129784-200202010-00005.
88. Hindricks G., Potpara T., Dagres N., et al. Corrigendum to: 2020 ESC Guidelines for the diagnosis and management of atrial fibrillation developed in collaboration with the European Association for Cardio-Thoracic Surgery (EACTS): The Task Force for the diagnosis and management of atrial fibrillation of the European Society of Cardiology (ESC) Developed with the special contribution of the European Heart Rhythm Association (EHRA) of the ESC (*Eur Heart J* (2021) 42 (373–498) DOI:

- 10.1093/eurheartj/ehaa612). Eur Heart J 2021. Doi: 10.1093/eurheartj/ehab648.
89. Do U. Adverse reactions to antiarrhythmic drugs. *Cardiovasc Prev Pharmacother* 2023;5(1). Doi: 10.36011/cpp.2023.5.e1.
90. Hussain S., Sohrabi C., Providencia R., Ahsan S., Papageorgiou N. Catheter Ablation for the Management of Atrial Fibrillation: An Update of the Literature. *Life* 2023. Doi: 10.3390/life13081784.
91. Anic A., Lever N., Martin A., et al. Acute safety, efficacy, and advantages of a novel cryoballoon ablation system for pulmonary vein isolation in patients with paroxysmal atrial fibrillation: Initial clinical experience. *Europace* 2021;23(8). Doi: 10.1093/europace/euab018.
92. Blomström-Lundqvist C., Gizurarson S., Schwieler J., et al. Effect of Catheter Ablation vs Antiarrhythmic Medication on Quality of Life in Patients with Atrial Fibrillation: The CAPTAF Randomized Clinical Trial. *JAMA - J Am Med Assoc* 2019;321(11). Doi: 10.1001/jama.2019.0335.
93. Nattel S., Sager PT., Hüser J., Heijman J., Dobrev D. Why translation from basic discoveries to clinical applications is so difficult for atrial fibrillation and possible approaches to improving it. *Cardiovasc Res* 2021;117(7). Doi: 10.1093/cvr/cvab093.
94. van Gorp PRR., Trines SA., Pijnappels DA., de Vries AAF. Multicellular In vitro Models of Cardiac Arrhythmias: Focus on Atrial Fibrillation. *Front Cardiovasc Med* 2020;7(March):1–17. Doi: 10.3389/fcvm.2020.00043.
95. Tran TT Van., Tayara H., Chong KT. Recent Studies of Artificial Intelligence on In Silico Drug Distribution Prediction. *Int J Mol Sci* 2023. Doi: 10.3390/ijms24031815.
96. Ekins S., Mestres J., Testa B. In silico pharmacology for drug discovery: Methods for virtual ligand screening and profiling. *Br J Pharmacol* 2007. Doi: 10.1038/sj.bjp.0707305.

97. Sacan A., Ekins S., Kortagere S. Applications and limitations of in silico models in drug discovery. *Methods Mol Biol* 2012. Doi: 10.1007/978-1-61779-965-5_6.
98. Kiani AK., Pheby D., Henehan G., et al. Ethical considerations regarding animal experimentation. *J Prev Med Hyg* 2022. Doi: 10.15167/2421-4248/jpmh2022.63.2S3.2768.
99. Edwards AG., Louch WE. Species-dependent mechanisms of cardiac arrhythmia: A cellular focus. *Clin Med Insights Cardiol* 2017. Doi: 10.1177/1179546816686061.
100. Wang Y., Wang M., Samuel CS., Widdop RE. Preclinical rodent models of cardiac fibrosis. *Br J Pharmacol* 2022. Doi: 10.1111/bph.15450.
101. Bacmeister L., Schwarzl M., Warnke S., et al. Inflammation and fibrosis in murine models of heart failure. *Basic Res Cardiol* 2019. Doi: 10.1007/s00395-019-0722-5.
102. Xia Y., Lee K., Li N., Corbett D., Mendoza L., Frangogiannis NG. Characterization of the inflammatory and fibrotic response in a mouse model of cardiac pressure overload. *Histochem Cell Biol* 2009;131(4). Doi: 10.1007/s00418-008-0541-5.
103. Joukar S. A comparative review on heart ion channels, action potentials and electrocardiogram in rodents and human: extrapolation of experimental insights to clinic. *Lab Anim Res* 2021. Doi: 10.1186/s42826-021-00102-3.
104. Piktel JS., Wilson LD. Translational Models of Arrhythmia Mechanisms and Susceptibility: Success and Challenges of Modeling Human Disease. *Front Cardiovasc Med* 2019. Doi: 10.3389/fcvm.2019.00135.
105. Davidson MM., Nesti C., Palenzuela L., et al. Novel cell lines derived from adult human ventricular cardiomyocytes. *J Mol Cell Cardiol* 2005;39(1). Doi: 10.1016/j.yjmcc.2005.03.003.

106. Liu D., Yang M., Yao Y., et al. Cardiac Fibroblasts Promote Ferroptosis in Atrial Fibrillation by Secreting Exo-miR-23a-3p Targeting SLC7A11. *Oxid Med Cell Longev* 2022;2022. Doi: 10.1155/2022/3961495.
107. Wei L., Li W., Entcheva E., Li Z. Microfluidics-enabled 96-well perfusion system for high-throughput tissue engineering and long-term all-optical electrophysiology. *Lab Chip* 2020;20(21). Doi: 10.1039/d0lc00615g.
108. Shafaattalab S., Lin E., Christidi E., et al. Ibrutinib Displays Atrial-Specific Toxicity in Human Stem Cell-Derived Cardiomyocytes. *Stem Cell Reports* 2019;12(5):996–1006. Doi: 10.1016/j.stemcr.2019.03.011.
109. Wang A., Liew CG. Genetic manipulation of human induced pluripotent stem cells. *Curr Protoc Stem Cell Biol* 2013;1(SUPPL.23). Doi: 10.1002/9780470151808.sc05b02s23.
110. Zakrzewski W., Dobrzyński M., Szymonowicz M., Rybak Z. Stem cells: Past, present, and future. *Stem Cell Res Ther* 2019. Doi: 10.1186/s13287-019-1165-5.
111. Poliwoda S., Noor N., Downs E., et al. Stem cells: a comprehensive review of origins and emerging clinical roles in medical practice. *Orthop Rev (Pavia)* 2022;14(3). Doi: 10.52965/001C.37498.
112. Takahashi K., Yamanaka S. Induction of Pluripotent Stem Cells from Mouse Embryonic and Adult Fibroblast Cultures by Defined Factors. *Cell* 2006;126(4). Doi: 10.1016/j.cell.2006.07.024.
113. Takahashi K., Tanabe K., Ohnuki M., et al. Induction of Pluripotent Stem Cells from Adult Human Fibroblasts by Defined Factors. *Cell* 2007;131(5). Doi: 10.1016/j.cell.2007.11.019.
114. Lo B., Parham L. Ethical issues in stem cell research. *Endocr Rev* 2009. Doi: 10.1210/er.2008-0031.
115. Paik DT., Chandy M., Wu JC. Patient and disease-specific induced

- pluripotent stem cells for discovery of personalized cardiovascular drugs and therapeutics. *Pharmacol Rev* 2020;72(1). Doi: 10.1124/pr.116.013003.
116. Okita K., Ichisaka T., Yamanaka S. Generation of germline-competent induced pluripotent stem cells. *Nature* 2007;448(7151). Doi: 10.1038/nature05934.
117. Stadtfeld M., Brennand K., Hochedlinger K. Reprogramming of Pancreatic β Cells into Induced Pluripotent Stem Cells. *Curr Biol* 2008;18(12). Doi: 10.1016/j.cub.2008.05.010.
118. Mikkelsen TS., Hanna J., Zhang X., et al. Dissecting direct reprogramming through integrative genomic analysis. *Nature* 2008;454(7200). Doi: 10.1038/nature07056.
119. Brambrink T., Foreman R., Welstead GG., et al. Sequential Expression of Pluripotency Markers during Direct Reprogramming of Mouse Somatic Cells. *Cell Stem Cell* 2008;2(2). Doi: 10.1016/j.stem.2008.01.004.
120. Okita K., Nakagawa M., Hyenjong H., Ichisaka T., Yamanaka S. Generation of mouse induced pluripotent stem cells without viral vectors. *Science* (80-) 2008;322(5903). Doi: 10.1126/science.1164270.
121. Fusaki N., Ban H., Nishiyama A., Saeki K., Hasegawa M. Efficient induction of transgene-free human pluripotent stem cells using a vector based on Sendai virus, an RNA virus that does not integrate into the host genome. *Proc Japan Acad Ser B Phys Biol Sci* 2009;85(8). Doi: 10.2183/pjab.85.348.
122. Nakanishi M., Otsu M. Development of Sendai Virus Vectors and their Potential Applications in Gene Therapy and Regenerative Medicine. *Curr Gene Ther* 2012;12(5). Doi: 10.2174/156652312802762518.
123. Jia F., Wilson KD., Sun N., et al. A nonviral minicircle vector for deriving human iPS cells. *Nat Methods* 2010;7(3). Doi: 10.1038/nmeth.1426.

124. Narsinh KH., Jia F., Robbins RC., Kay MA., Longaker MT., Wu JC. Generation of adult human induced pluripotent stem cells using nonviral minicircle DNA vectors. *Nat Protoc* 2011;6(1). Doi: 10.1038/nprot.2010.173.
125. Belviso I., Romano V., Nurzynska D., Castaldo C., Di Meglio F. Non-integrating Methods to Produce Induced Pluripotent Stem Cells for Regenerative Medicine: An Overview. *Biomechanics and Functional Tissue Engineering*. 2021.
126. Warren L., Manos PD., Ahfeldt T., et al. Highly efficient reprogramming to pluripotency and directed differentiation of human cells with synthetic modified mRNA. *Cell Stem Cell* 2010;7(5). Doi: 10.1016/j.stem.2010.08.012.
127. Plews JR., Li JL., Jones M., et al. Activation of pluripotency genes in human fibroblast cells by a novel mRNA based approach. *PLoS One* 2010;5(12). Doi: 10.1371/journal.pone.0014397.
128. Miyoshi N., Ishii H., Nagano H., et al. Reprogramming of mouse and human cells to pluripotency using mature microRNAs. *Cell Stem Cell* 2011;8(6). Doi: 10.1016/j.stem.2011.05.001.
129. Kim D., Kim CH., Moon J Il., et al. Generation of Human Induced Pluripotent Stem Cells by Direct Delivery of Reprogramming Proteins. *Cell Stem Cell* 2009. Doi: 10.1016/j.stem.2009.05.005.
130. Guan J., Wang G., Wang J., et al. Chemical reprogramming of human somatic cells to pluripotent stem cells. *Nature* 2022;605(7909). Doi: 10.1038/s41586-022-04593-5.
131. Aboul-Soud MAM., Alzahrani AJ., Mahmoud A. Induced pluripotent stem cells (Ipscs)—roles in regenerative therapies, disease modelling and drug screening. *Cells* 2021. Doi: 10.3390/cells10092319.
132. Kattman SJ., Witty AD., Gagliardi M., et al. Stage-specific optimization of

- activin/nodal and BMP signaling promotes cardiac differentiation of mouse and human pluripotent stem cell lines. *Cell Stem Cell* 2011;8(2). Doi: 10.1016/j.stem.2010.12.008.
133. Willems E., Spiering S., Davidovics H., et al. Small-molecule inhibitors of the Wnt pathway potently promote cardiomyocytes from human embryonic stem cell-derived mesoderm. *Circ Res* 2011;109(4). Doi: 10.1161/CIRCRESAHA.111.249540.
134. Ren Y., Lee MY., Schliffke S., et al. Small molecule Wnt inhibitors enhance the efficiency of BMP-4-directed cardiac differentiation of human pluripotent stem cells. *J Mol Cell Cardiol* 2011;51(3). Doi: 10.1016/j.yjmcc.2011.04.012.
135. Burridge PW., Thompson S., Millrod MA., et al. A universal system for highly efficient cardiac differentiation of human induced pluripotent stem cells that eliminates interline variability. *PLoS One* 2011;6(4). Doi: 10.1371/journal.pone.0018293.
136. Rajala K., Pekkanen-Mattila M., Aalto-Setälä K. Cardiac differentiation of pluripotent stem cells. *Stem Cells Int* 2011. Doi: 10.4061/2011/383709.
137. Gessert S., Kühl M. The multiple phases and faces of Wnt signaling during cardiac differentiation and development. *Circ Res* 2010;107(2):186–99. Doi: 10.1161/CIRCRESAHA.110.221531.
138. van Wijk B., Moorman AFM., van den Hoff MJB. Role of bone morphogenetic proteins in cardiac differentiation. *Cardiovasc Res* 2007. Doi: 10.1016/j.cardiores.2006.11.022.
139. Rosenblatt-Velin N., Lepore MG., Cartoni C., Beermann F., Pedrazzini T. FGF-2 controls the differentiation of resident cardiac precursors into functional cardiomyocytes. *J Clin Invest* 2005;115(7). Doi: 10.1172/JCI23418.
140. Korol O., Gupta RW., Mercola M. A novel activity of the Dickkopf-1

- amino terminal domain promotes axial and heart development independently of canonical Wnt inhibition. *Dev Biol* 2008;324(1). Doi: 10.1016/j.ydbio.2008.09.012.
141. Fei T., Xia K., Li Z., et al. Genome-wide mapping of SMAD target genes reveals the role of BMP signaling in embryonic stem cell fate determination. *Genome Res* 2010;20(1). Doi: 10.1101/gr.092114.109.
142. Chen VC., Stull R., Joo D., Cheng X., Keller G. Notch signaling respecifies the hemangioblast to a cardiac fate. *Nat Biotechnol* 2008;26(10). Doi: 10.1038/nbt.1497.
143. Sugi Y., Lough J. Activin-A and FGF-2 mimic the inductive effects of anterior endoderm on terminal cardiac myogenesis in vitro. *Dev Biol* 1995;168(2). Doi: 10.1006/dbio.1995.1102.
144. Lyra-Leite DM., Gutiérrez-Gutiérrez Ó., Wang M., Zhou Y., Cyganek L., Burridge PW. A review of protocols for human iPSC culture, cardiac differentiation, subtype-specification, maturation, and direct reprogramming. *STAR Protoc* 2022. Doi: 10.1016/j.xpro.2022.101560.
145. Kehat I., Kenyagin-Karsenti D., Snir M., et al. Human embryonic stem cells can differentiate into myocytes with structural and functional properties of cardiomyocytes. *J Clin Invest* 2001;108(3). Doi: 10.1172/JCI200112131.
146. Takei S., Ichikawa H., Johkura K., et al. Bone morphogenetic protein-4 promotes induction of cardiomyocytes from human embryonic stem cells in serum-based embryoid body development. *Am J Physiol - Hear Circ Physiol* 2009;296(6). Doi: 10.1152/ajpheart.01288.2008.
147. Laflamme MA., Chen KY., Naumova A V., et al. Cardiomyocytes derived from human embryonic stem cells in pro-survival factors enhance function of infarcted rat hearts. *Nat Biotechnol* 2007;25(9). Doi: 10.1038/nbt1327.
148. Gonzalez R., Lee JW., Schultz PG. Stepwise chemically induced cardiomyocyte specification of human embryonic stem cells. *Angew Chemie*

- Int Ed 2011;50(47). Doi: 10.1002/anie.201103909.
149. Lian X., Hsiao C., Wilson G., et al. Robust cardiomyocyte differentiation from human pluripotent stem cells via temporal modulation of canonical Wnt signaling. *Proc Natl Acad Sci U S A* 2012;109(27). Doi: 10.1073/pnas.1200250109.
150. Mummery C., Ward-van Oostwaard D., Doevendans P., et al. Differentiation of human embryonic stem cells to cardiomyocytes: Role of coculture with visceral endoderm-like cells. *Circulation* 2003;107(21). Doi: 10.1161/01.cir.0000068356.38592.68.
151. Warkman AS., Whitman SA., Miller MK., et al. Developmental expression and cardiac transcriptional regulation of Myh7b, a third myosin heavy chain in the vertebrate heart. *Cytoskeleton* 2012;69(5). Doi: 10.1002/cm.21029.
152. Luo XL., Zhang P., Liu X., et al. Myosin light chain 2 marks differentiating ventricular cardiomyocytes derived from human embryonic stem cells. *Pflugers Arch Eur J Physiol* 2021;473(7). Doi: 10.1007/s00424-021-02578-3.
153. Nelson DO., Jin DX., Downs KM., Kamp TJ., Lyons GE. Irx4 identifies a chamber-specific cell population that contributes to ventricular myocardium development. *Dev Dyn* 2014;243(3). Doi: 10.1002/dvdy.24078.
154. Watanabe Y., Wang Y., Tanaka Y., et al. Hey2 enhancer activity defines unipotent progenitors for left ventricular cardiomyocytes in juxta-cardiac field of early mouse embryo. *Proc Natl Acad Sci U S A* 2023;120(37). Doi: 10.1073/pnas.2307658120.
155. England J., Loughna S. Heavy and light roles: Myosin in the morphogenesis of the heart. *Cell Mol Life Sci* 2013. Doi: 10.1007/s00018-012-1131-1.
156. Orr N., Arnaout R., Gula LJ., et al. A mutation in the atrial-specific myosin light chain gene (MYL4) causes familial atrial fibrillation. *Nat Commun* 2016;7. Doi: 10.1038/ncomms11303.

157. Houweling AC., Van Borren MM., Moorman AFM., Christoffels VM. Expression and regulation of the atrial natriuretic factor encoding gene *Nppa* during development and disease. *Cardiovasc Res* 2005. Doi: 10.1016/j.cardiores.2005.06.013.
158. Brandenburg S., Arakel EC., Schwappach B., Lehnart SE. The molecular and functional identities of atrial cardiomyocytes in health and disease. *Biochim Biophys Acta - Mol Cell Res* 2016. Doi: 10.1016/j.bbamcr.2015.11.025.
159. Walden AP., Dibb KM., Trafford AW. Differences in intracellular calcium homeostasis between atrial and ventricular myocytes. *J Mol Cell Cardiol* 2009;46(4). Doi: 10.1016/j.yjmcc.2008.11.003.
160. Zhang Q., Jiang J., Han P., et al. Direct differentiation of atrial and ventricular myocytes from human embryonic stem cells by alternating retinoid signals. *Cell Res* 2011;21(4):579–87. Doi: 10.1038/cr.2010.163.
161. Dohn TE., Ravisankar P., Tirera FT., et al. Nr2f-dependent allocation of ventricular cardiomyocyte and pharyngeal muscle progenitors. *PLoS Genet* 2019;15(2). Doi: 10.1371/journal.pgen.1007962.
162. Devalla HD., Schwach V., Ford JW., et al. Atrial-like cardiomyocytes from human pluripotent stem cells are a robust preclinical model for assessing atrial-selective pharmacology. *EMBO Mol Med* 2015;7(4):394–410. Doi: 10.15252/emmm.201404757.
163. Lee JH., Protze SI., Laksman Z., Backx PH., Keller GM. Human Pluripotent Stem Cell-Derived Atrial and Ventricular Cardiomyocytes Develop from Distinct Mesoderm Populations. *Cell Stem Cell* 2017;21(2):179-194.e4. Doi: 10.1016/j.stem.2017.07.003.
164. Cyganek L., Tiburcy M., Sekeres K., et al. Deep phenotyping of human induced pluripotent stem cell-derived atrial and ventricular cardiomyocytes. *JCI Insight* 2018;3(12):1–17. Doi: 10.1172/jci.insight.99941.

165. Lemme M., Ulmer BM., Lemoine MD., et al. Atrial-like Engineered Heart Tissue: An In Vitro Model of the Human Atrium. *Stem Cell Reports* 2018;11(6):1378–90. Doi: 10.1016/j.stemcr.2018.10.008.
166. Wiesinger A., Boink GJJ., Christoffels VM., Devalla HD. Retinoic acid signaling in heart development: Application in the differentiation of cardiovascular lineages from human pluripotent stem cells. *Stem Cell Reports* 2021. Doi: 10.1016/j.stemcr.2021.09.010.
167. Marczenke M., Piccini I., Mengarelli I., et al. Cardiac subtype-specific modeling of Kv1.5 ion channel deficiency using human pluripotent stem cells. *Front Physiol* 2017;8(JUL). Doi: 10.3389/fphys.2017.00469.
168. Laksman Z., Wauchop M., Lin E., et al. Modeling Atrial Fibrillation using Human Embryonic Stem Cell-Derived Atrial Tissue. *Sci Rep* 2017;7(1):1–11. Doi: 10.1038/s41598-017-05652-y.
169. Thorpe J., Perry MD., Contreras O., et al. Development of a robust induced pluripotent stem cell atrial cardiomyocyte differentiation protocol to model atrial arrhythmia. *Stem Cell Res Ther* 2023;14(1):1–17. Doi: 10.1186/s13287-023-03405-5.
170. Goldfracht I., Efraim Y., Shinnawi R., et al. Engineered heart tissue models from hiPSC-derived cardiomyocytes and cardiac ECM for disease modeling and drug testing applications. *Acta Biomater* 2019;92:145–59. Doi: 10.1016/j.actbio.2019.05.016.
171. Tiburcy M., Meyer T., Liaw NY., Zimmermann WH. Generation of Engineered Human Myocardium in a Multi-well Format. *STAR Protoc* 2020;1(1). Doi: 10.1016/j.xpro.2020.100032.
172. Nakanishi H., Lee JK., Miwa K., et al. Geometrical patterning and constituent cell heterogeneity facilitate electrical conduction disturbances in a human induced pluripotent stem cell-based platform: An in vitro disease model of atrial arrhythmias. *Front Physiol* 2019;10(JUN):1–20. Doi:

- 10.3389/fphys.2019.00818.
173. Walters T., Spence S., Larobina M., Atkinson V., Kalman J. A Study of the Electrophysiology of the PV–LA Junction During Acute Stretch in Humans: Conduction Slowing and Complex Fractionated Electrograms. *Hear Lung Circ* 2013;22. Doi: 10.1016/j.hlc.2013.05.220.
174. Seibertz F., Rubio T., Springer R., et al. Atrial fibrillation-associated electrical remodelling in human induced pluripotent stem cell-derived atrial cardiomyocytes: a novel pathway for antiarrhythmic therapy development 2023. Doi: <https://doi.org/10.1093/cvr/cvad143>.
175. Guo Y., Pu WT. Cardiomyocyte Maturation: New Phase in Development. *Circ Res* 2020. Doi: 10.1161/CIRCRESAHA.119.315862.
176. Biendarra-Tiegs SM., Secreto FJ., Nelson TJ. Addressing Variability and Heterogeneity of Induced Pluripotent Stem Cell-Derived Cardiomyocytes. *Advances in Experimental Medicine and Biology*, vol. 1212. 2020.
177. Entcheva E., Kay MW. Cardiac optogenetics: a decade of enlightenment. *Nat Rev Cardiol* 2021. Doi: 10.1038/s41569-020-00478-0.
178. Arrenberg AB., Stainier DYR., Baier H., Huisken J. Optogenetic control of cardiac function. *Science* (80-) 2010;330(6006). Doi: 10.1126/science.1195929.
179. Björk S., Ojala EA., Nordström T., et al. Evaluation of optogenetic electrophysiology tools in human stem cell-derived cardiomyocytes. *Front Physiol* 2017;8(NOV). Doi: 10.3389/fphys.2017.00884.
180. Song L., Awari DW., Han EY., et al. Dual Optical Recordings for Action Potentials and Calcium Handling in Induced Pluripotent Stem Cell Models of Cardiac Arrhythmias Using Genetically Encoded Fluorescent Indicators. *Stem Cells Transl Med* 2015;4(5). Doi: 10.5966/sctm.2014-0245.
181. Chow BY., Han X., Boyden ES. Genetically encoded molecular tools for

- light-driven silencing of targeted neurons. *Progress in Brain Research*, vol. 196. 2012.
182. Mattingly M., Weineck K., Costa J., Cooper RL. Hyperpolarization by activation of halorhodopsin results in enhanced synaptic transmission: Neuromuscular junction and CNS circuit. *PLoS One* 2018;13(7). Doi: 10.1371/journal.pone.0200107.
183. Kouyama T., Kanada S., Takeguchi Y., Narusawa A., Murakami M., Ihara K. Crystal Structure of the Light-Driven Chloride Pump Halorhodopsin from *Natronomonas pharaonis*. *J Mol Biol* 2010;396(3). Doi: 10.1016/j.jmb.2009.11.061.
184. Tønnesen J., Sørensen AT., Deisseroth K., Lundberg C., Kokaia M. Optogenetic control of epileptiform activity. *Proc Natl Acad Sci U S A* 2009;106(29). Doi: 10.1073/pnas.0901915106.
185. Han X., Chow BY., Zhou H., et al. A high-light sensitivity optical neural silencer: Development and application to optogenetic control of non-human primate cortex. *Front Syst Neurosci* 2011;(APRIL 2011). Doi: 10.3389/fnsys.2011.00018.
186. Schneider F., Gradmann D., Hegemann P. Ion selectivity and competition in channelrhodopsins. *Biophys J* 2013;105(1). Doi: 10.1016/j.bpj.2013.05.042.
187. Inaguma A., Tsukamoto H., Kato HE., et al. Chimeras of channelrhodopsin-1 and-2 from *chlamydomonas reinhardtii* exhibit distinctive light-induced structural changes from channelrhodopsin-2. *J Biol Chem* 2015;290(18). Doi: 10.1074/jbc.M115.642256.
188. Neghab HK., Soheilifar MH., Saboury AA., Goliaei B., Hong J., Djavid GE. Optogenetic Stimulation of Primary Cardiomyocytes Expressing ChR2. *J Lasers Med Sci* 2021;12. Doi: 10.34172/jlms.2021.32.
189. Nyns ECA., Kip A., Bart CI., et al. Optogenetic termination of ventricular

- arrhythmias in the whole heart: Towards biological cardiac rhythm management. *Eur Heart J* 2017;38(27). Doi: 10.1093/eurheartj/ehw574.
190. Johnston CM., Rog-Zielinska EA., Wülfers EM., et al. Optogenetic targeting of cardiac myocytes and non-myocytes: Tools, challenges and utility. *Prog Biophys Mol Biol* 2017;130. Doi: 10.1016/j.pbiomolbio.2017.09.014.
191. Wietek J., Beltramo R., Scanziani M., Hegemann P., Oertner TG., Simon Wiegert J. An improved chloride-conducting channelrhodopsin for light-induced inhibition of neuronal activity in vivo. *Sci Rep* 2015;5. Doi: 10.1038/srep14807.
192. Berndt A., Lee SY., Wietek J., et al. Structural foundations of optogenetics: Determinants of channelrhodopsin ion selectivity. *Proc Natl Acad Sci U S A* 2016;113(4). Doi: 10.1073/pnas.1523341113.
193. Govorunova EG., Sineshchekov OA., Janz R., Liu X., Spudich JL. Natural light-gated anion channels: A family of microbial rhodopsins for advanced optogenetics. *Science (80-)* 2015;349(6248). Doi: 10.1126/science.aaa7484.
194. Bernal Sierra YA., Rost BR., Pofahl M., et al. Potassium channel-based optogenetic silencing. *Nat Commun* 2018;9(1). Doi: 10.1038/s41467-018-07038-8.
195. Govorunova EG., Gou Y., Sineshchekov OA., et al. Kalium channelrhodopsins are natural light-gated potassium channels that mediate optogenetic inhibition. *Nat Neurosci* 2022;25(7). Doi: 10.1038/s41593-022-01094-6.
196. Vierock J., Peter E., Grimm C., et al. WiChR, a highly potassium-selective channelrhodopsin for low-light one- and two-photon inhibition of excitable cells. *Sci Adv* 2022;8(49). Doi: 10.1126/sciadv.add7729.
197. Floria M., Radu S., Gosav EM., et al. Cardiac optogenetics in atrial fibrillation: Current challenges and future opportunities. *Biomed Res Int*

2020. Doi: 10.1155/2020/8814092.
198. Sasse P., Funken M., Beiert T., Bruegmann T. Optogenetic termination of cardiac arrhythmia: Mechanistic enlightenment and therapeutic application? *Front Physiol* 2019. Doi: 10.3389/fphys.2019.00675.
199. Lemme M., Braren I., Prondzynski M., et al. Chronic intermittent tachypacing by an optogenetic approach induces arrhythmia vulnerability in human engineered heart tissue. *Cardiovasc Res* 2020;116(8). Doi: 10.1093/cvr/cvz245.
200. Dou W., Malhi M., Zhao Q., et al. Microengineered platforms for characterizing the contractile function of in vitro cardiac models. *Microsystems Nanoeng* 2022. Doi: 10.1038/s41378-021-00344-0.
201. Mangold KE., Brumback BD., Angsutararux P., et al. Mechanisms and models of cardiac sodium channel inactivation. *Channels* 2017. Doi: 10.1080/19336950.2017.1369637.
202. Bruegmann T., Boyle PM., Vogt CC., et al. Optogenetic defibrillation terminates ventricular arrhythmia in mouse hearts and human simulations. *J Clin Invest* 2016;126(10). Doi: 10.1172/JCI88950.
203. Crocini C., Ferrantini C., Coppini R., et al. Optogenetics design of mechanistically-based stimulation patterns for cardiac defibrillation. *Sci Rep* 2016;6. Doi: 10.1038/srep35628.
204. Bruegmann T., Beiert T., Vogt CC., Schrickel JW., Sasse P. Optogenetic termination of atrial fibrillation in mice. *Cardiovasc Res* 2018;114(5). Doi: 10.1093/cvr/cvx250.
205. Nyns ECA., Poelma RH., Volkers L., et al. An automated hybrid bioelectronic system for autogenous restoration of sinus rhythm in atrial fibrillation. *Sci Transl Med* 2019;11(481). Doi: 10.1126/scitranslmed.aau6447.

206. Biasci V., Santini L., Marchal GA., et al. Optogenetic manipulation of cardiac electrical dynamics using sub-threshold illumination: dissecting the role of cardiac alternans in terminating rapid rhythms. *Basic Res Cardiol* 2022;117(1). Doi: 10.1007/s00395-022-00933-8.
207. Yu J., Vodyanik MA., Smuga-Otto K., et al. Induced pluripotent stem cell lines derived from human somatic cells. *Science* (80-) 2007;318(5858). Doi: 10.1126/science.1151526.
208. Ontoria-Oviedo I., Földes G., Tejedor S., et al. Modeling transposition of the great arteries with patient-specific induced pluripotent stem cells. *Int J Mol Sci* 2021;22(24). Doi: 10.3390/ijms222413270.
209. Stefanovic S., Zaffran S. Mechanisms of retinoic acid signaling during cardiogenesis. *Mech Dev* 2017;143:9–19. Doi: 10.1016/j.mod.2016.12.002.
210. Kleinsorge M., Cyganek L. Subtype-Directed Differentiation of Human iPSCs into Atrial and Ventricular Cardiomyocytes. *STAR Protoc* 2020;1(1):100026. Doi: 10.1016/j.xpro.2020.100026.
211. Pfeiffer ER., Tangney JR., Omens JH., McCulloch AD. Biomechanics of cardiac electromechanical coupling and mechanoelectric feedback. *J Biomech Eng* 2014;136(2). Doi: 10.1115/1.4026221.
212. Kuo IY., Ehrlich BE. Signaling in muscle contraction. *Cold Spring Harb Perspect Biol* 2015;7(2). Doi: 10.1101/cshperspect.a006023.
213. Barth AS., Merk S., Arnoldi E., et al. Reprogramming of the human atrial transcriptome in permanent atrial fibrillation: Expression of a ventricular-like genomic signature. *Circ Res* 2005;96(9):1022–9. Doi: 10.1161/01.RES.0000165480.82737.33.
214. Zeemering S., Isaacs A., Winters J., et al. Atrial fibrillation in the presence and absence of heart failure enhances expression of genes involved in cardiomyocyte structure, conduction properties, fibrosis, inflammation, and endothelial dysfunction. *Hear Rhythm* 2022;19(12):2115–24. Doi:

- 10.1016/j.hrthm.2022.08.019.
215. Ortmann D., Brown S., Czechanski A., et al. Naive Pluripotent Stem Cells Exhibit Phenotypic Variability that Is Driven by Genetic Variation. *Cell Stem Cell* 2020;27(3). Doi: 10.1016/j.stem.2020.07.019.
216. Mimbbrero Guillamon M., Loncaric F., Loncaric F., et al. Inflammation and fibrosis biomarkers are related to atrial dysfunction in patients at risk of atrial fibrillation. *Eur Heart J* 2020;41(Supplement_2). Doi: 10.1093/ehjci/ehaa946.0130.
217. Korantzopoulos P., Letsas KP., Tse G., Fragakis N., Goudis CA., Liu T. Inflammation and atrial fibrillation: A comprehensive review. *J Arrhythmia* 2018. Doi: 10.1002/joa3.12077.
218. Gunawan MG., Sangha SS., Shafaattalab S., et al. Drug screening platform using human induced pluripotent stem cell-derived atrial cardiomyocytes and optical mapping. *Stem Cells Transl Med* 2021;10(1):68–82. Doi: 10.1002/sctm.19-0440.
219. Peyronnet R., Desai A., Edelmann JC., et al. Simultaneous assessment of radial and axial myocyte mechanics by combining atomic force microscopy and carbon fibre techniques. *Philos Trans R Soc B Biol Sci* 2022;377(1864). Doi: 10.1098/rstb.2021.0326.
220. Wu S pin., Cheng CM., Lanz RB., et al. Atrial Identity Is Determined by a COUP-TFII Regulatory Network. *Dev Cell* 2013;25(4):417–26. Doi: 10.1016/j.devcel.2013.04.017.
221. Bizy A., Guerrero-Serna G., Hu B., et al. Myosin light chain 2-based selection of human iPSC-derived early ventricular cardiac myocytes. *Stem Cell Res* 2013;11(3). Doi: 10.1016/j.scr.2013.09.003.
222. Herron TJ., Da Rocha AM., Campbell KF., et al. Extracellular matrix-mediated maturation of human pluripotent stem cell-derived cardiac monolayer structure and electrophysiological function. *Circ Arrhythmia*

- Electrophysiol 2016;9(4):1–12. Doi: 10.1161/CIRCEP.113.003638.
223. Bao ZZ., Bruneau BG., Seidman JG., Seidman CE., Cepko CL. Regulation of chamber-specific gene expression in the developing heart by *Irx4*. *Science* (80-) 1999;283(5405). Doi: 10.1126/science.283.5405.1161.
224. Duong TB., Ravisankar P., Song YC., et al. *Nr2f1a* balances atrial chamber and atrioventricular canal size via BMP signaling-independent and -dependent mechanisms. *Dev Biol* 2018;434(1). Doi: 10.1016/j.ydbio.2017.11.010.
225. Litviňuková M., Talavera-López C., Maatz H., et al. Cells of the adult human heart. *Nature* 2020;588(7838):466–72. Doi: 10.1038/s41586-020-2797-4.
226. Burashnikov A., Di Diego JM., Zygmunt AC., Belardinelli L., Antzelevitch C. Atrial-selective sodium channel block as a strategy for suppression of atrial fibrillation. *Annals of the New York Academy of Sciences*, vol. 1123. 2008.
227. Hong Y., Zhao Y., Li H., et al. Engineering the maturation of stem cell-derived cardiomyocytes. *Front Bioeng Biotechnol* 2023. Doi: 10.3389/fbioe.2023.1155052.
228. Liu YW., Chen B., Yang X., et al. Human embryonic stem cell-derived cardiomyocytes restore function in infarcted hearts of non-human primates. *Nat Biotechnol* 2018;36(7). Doi: 10.1038/nbt.4162.
229. Yue T., Park KH., Reese BE., et al. Quantifying Drug-Induced Nanomechanics and Mechanical Effects to Single Cardiomyocytes for Optimal Drug Administration to Minimize Cardiotoxicity. *Langmuir* 2016;32(7). Doi: 10.1021/acs.langmuir.5b04314.
230. Sun S., Shi H., Moore S., et al. Progressive Myofibril Reorganization of Human Cardiomyocytes on a Dynamic Nanotopographic Substrate. *ACS Appl Mater Interfaces* 2020;12(19). Doi: 10.1021/acsami.0c03464.

231. Pioner JM., Racca AW., Klaiman JM., et al. Isolation and mechanical measurements of myofibrils from human induced pluripotent stem cell-derived cardiomyocytes. *Stem Cell Reports* 2016;6(6). Doi: 10.1016/j.stemcr.2016.04.006.
232. Greiner J., Schiatti T., Kaltenbacher W., et al. Consecutive-Day Ventricular and Atrial Cardiomyocyte Isolations from the Same Heart: Shifting the Cost-Benefit Balance of Cardiac Primary Cell Research. *Cells* 2022;11(2). Doi: 10.3390/cells11020233.
233. Ahmed RE., Anzai T., Chanthra N., Uosaki H. A Brief Review of Current Maturation Methods for Human Induced Pluripotent Stem Cells-Derived Cardiomyocytes. *Front Cell Dev Biol* 2020. Doi: 10.3389/fcell.2020.00178.
234. Guillem MS., Climent AM., Rodrigo M., Fernández-Aviles F., Atienza F., Berenfeld O. Presence and stability of rotors in atrial fibrillation: Evidence and therapeutic implications. *Cardiovasc Res* 2016;109(4). Doi: 10.1093/cvr/cvw011.
235. Pandit S V., Zlochiver S., Filgueiras-Rama D., et al. Targeting atrioventricular differences in ion channel properties for terminating acute atrial fibrillation in pigs. *Cardiovasc Res* 2011;89(4). Doi: 10.1093/cvr/cvq359.
236. Martins RP., Kaur K., Hwang E., et al. Dominant frequency increase rate predicts transition from paroxysmal to long-term persistent atrial fibrillation. *Circulation* 2014;129(14). Doi: 10.1161/CIRCULATIONAHA.113.004742.
237. Heijman J., Sutanto H., Crijns HJGM., Nattel S., Trayanova NA. Computational models of atrial fibrillation: Achievements, challenges, and perspectives for improving clinical care. *Cardiovasc Res* 2021;117(7):1682–99. Doi: 10.1093/cvr/cvab138.
238. Stables CL., Curtis MJ. Development and characterization of a mouse in

- vitro model of ischaemia-induced ventricular fibrillation. *Cardiovasc Res* 2009;83(2). Doi: 10.1093/cvr/cvp068.
239. Leowattana W., Leowattana T., Leowattana P. Human-induced pluripotent stem cell-atrial-specific cardiomyocytes and atrial fibrillation. *World J Clin Cases* 2022;10(27). Doi: 10.12998/wjcc.v10.i27.9588.
240. Thorpe J., Perry MD., Contreras O., et al. Development of a robust induced pluripotent stem cell atrial cardiomyocyte differentiation protocol to model atrial arrhythmia. *Stem Cell Res Ther* 2023:1–16. Doi: 10.1186/s13287-023-03405-5.
241. Steenman M. Insight into atrial fibrillation through analysis of the coding transcriptome in humans. *Biophys Rev* 2020. Doi: 10.1007/s12551-020-00735-z.
242. Herrera-Rivero M., Gandhi S., Witten A., Ghalawinji A., Schotten U., Stoll M. Cardiac chamber-specific genetic alterations suggest candidate genes and pathways implicating the left ventricle in the pathogenesis of atrial fibrillation. *Genomics* 2022;114(2):110320. Doi: 10.1016/j.ygeno.2022.110320.
243. Thomas AM., Cabrera CP., Finlay M., et al. Differentially expressed genes for atrial fibrillation identified by rna sequencing from paired human left and right atrial appendages. *Physiol Genomics* 2019;51(8):323–32. Doi: 10.1152/physiolgenomics.00012.2019.
244. Ninh VK., Brown JH. The contribution of the cardiomyocyte to tissue inflammation in cardiomyopathies. *Curr Opin Physiol* 2021. Doi: 10.1016/j.cophys.2020.10.003.
245. Giannandrea M., Parks WC. Diverse functions of matrix metalloproteinases during fibrosis. *DMM Dis Model Mech* 2014. Doi: 10.1242/dmm.012062.
246. Kuwahara F., Kai H., Tokuda K., et al. Roles of intercellular adhesion molecule-1 in hypertensive cardiac remodeling. *Hypertension*, vol. 41. 2003.

247. Oliviero P., Chassagne C., Salichon N., et al. Expression of laminin α 2 chain during normal and pathological growth of myocardium in rat and human. *Cardiovasc Res* 2000;46(2). Doi: 10.1016/S0008-6363(00)00034-1.
248. Lindsey ML., Zamilpa R. Temporal and spatial expression of matrix metalloproteinases and tissue inhibitors of metalloproteinases following myocardial infarction. *Cardiovasc Ther* 2012. Doi: 10.1111/j.1755-5922.2010.00207.x.
249. Salvador AM., Nevers T., Velázquez F., et al. Intercellular adhesion molecule 1 regulates left ventricular leukocyte infiltration, cardiac remodeling, and function in pressure overload-induced heart failure. *J Am Heart Assoc* 2015;5(3). Doi: 10.1161/JAHA.115.003126.
250. Schafer S., Viswanathan S., Widjaja AA., et al. IL-11 is a crucial determinant of cardiovascular fibrosis. *Nature* 2017;552(7683). Doi: 10.1038/nature24676.
251. Xu J., Ren JF., Mugelli A., Belardinelli L., Keith JC., Pelleg A. Age-dependent atrial remodeling induced by recombinant human interleukin-11: Implications for atrial flutter/fibrillation. *J Cardiovasc Pharmacol* 2002;39(3). Doi: 10.1097/00005344-200203000-00015.
252. Kimura N., Itoh S., Nakae S., et al. Interleukin-16 deficiency suppresses the development of chronic rejection in murine cardiac transplantation model. *J Hear Lung Transplant* 2011;30(12). Doi: 10.1016/j.healun.2011.08.017.
253. Tamaki S., Mano T., Sakata Y., et al. Interleukin-16 Promotes Cardiac Fibrosis and Myocardial Stiffening in Heart Failure with Preserved Ejection Fraction. *PLoS One* 2013;8(7). Doi: 10.1371/journal.pone.0068893.
254. Pyo RT., Sui J., Dhume A., et al. CXCR4 modulates contractility in adult cardiac myocytes. *J Mol Cell Cardiol* 2006;41(5). Doi: 10.1016/j.yjmcc.2006.08.008.
255. Liu P., Sun H., Zhou X., et al. CXCL12/CXCR4 axis as a key mediator in

- atrial fibrillation via bioinformatics analysis and functional identification. *Cell Death Dis* 2021;12(9). Doi: 10.1038/s41419-021-04109-5.
256. Voss S., Krüger S., Scherschel K., et al. Macrophage migration inhibitory factor (MIF) Expression increases during myocardial infarction and supports pro-inflammatory signaling in cardiac fibroblasts. *Biomolecules* 2019;9(2). Doi: 10.3390/biom9020038.
257. Cheng WL., Chen YC., Li SJ., et al. Galectin-3 enhances atrial remodelling and arrhythmogenesis through CD98 signalling. *Acta Physiol* 2022;234(3). Doi: 10.1111/apha.13784.
258. Bingen BO., Neshati Z., Askar SFA., et al. Atrium-Specific Kir3.x determines inducibility, dynamics, and termination of fibrillation by regulating restitution-driven alternans. *Circulation* 2013;128(25). Doi: 10.1161/CIRCULATIONAHA.113.005019.
259. Corey S., Krapivinsky G., Krapivinsky L., Clapham DE. Number and stoichiometry of subunits in the native atrial G-protein- gated K⁺ channel, I(KACh). *J Biol Chem* 1998;273(9). Doi: 10.1074/jbc.273.9.5271.
260. Bingen BO., Askar SFA., Neshati Z., et al. Constitutively Active Acetylcholine-Dependent Potassium Current Increases Atrial Defibrillation Threshold by Favoring Post-Shock Re-Initiation. *Sci Rep* 2015;5. Doi: 10.1038/srep15187.
261. Denayer T., Stöhrn T., Van Roy M. Animal models in translational medicine: Validation and prediction. *New Horizons Transl Med* 2014;2(1). Doi: 10.1016/j.nhtm.2014.08.001.
262. Hubrecht RC., Carter E. The 3Rs and humane experimental technique: Implementing change. *Animals* 2019;9(10). Doi: 10.3390/ani9100754.
263. Brundel BJJM., Shiroshita-Takeshita A., Qi X., et al. Induction of heat shock response protects the heart against atrial fibrillation. *Circ Res* 2006;99(12). Doi: 10.1161/01.RES.0000252323.83137.fe.

-
264. Mace LC., Yermalitskaya L V., Yi Y., Yang Z., Morgan AM., Murray KT. Transcriptional remodeling of rapidly stimulated HL-1 atrial myocytes exhibits concordance with human atrial fibrillation. *J Mol Cell Cardiol* 2009;47(4). Doi: 10.1016/j.yjmcc.2009.07.006.
265. Dias P., Desplantez T., El-Harasis MA., et al. Characterisation of connexin expression and electrophysiological properties in stable clones of the hl-1 myocyte cell line. *PLoS One* 2014;9(2). Doi: 10.1371/journal.pone.0090266.
266. Liu J., Volkens L., Jangsangthong W., et al. Generation and primary characterization of iAM-1, a versatile new line of conditionally immortalized atrial myocytes with preserved cardiomyogenic differentiation capacity. *Cardiovasc Res* 2018;114(14). Doi: 10.1093/cvr/cvy134.
267. Brown KW., Gallimore PH. Malignant progression of an sv40-transformed human epidermal keratinocyte cell line. *Br J Cancer* 1987;56(5). Doi: 10.1038/bjc.1987.240.
268. Cotsiki M., Lock RL., Cheng Y., et al. Simian virus 40 large T antigen targets the spindle assembly checkpoint protein Bub1. *Proc Natl Acad Sci U S A* 2004;101(4). Doi: 10.1073/pnas.0308006100.
269. Bruegmann T., Malan D., Hesse M., et al. Optogenetic control of heart muscle in vitro and in vivo. *Nat Methods* 2010;7(11). Doi: 10.1038/nmeth.1512.
270. Chow BY., Han X., Dobry AS., et al. High-performance genetically targetable optical neural silencing by light-driven proton pumps. *Nature* 2010;463(7277). Doi: 10.1038/nature08652.
271. Inoue K., Ono H., Abe-Yoshizumi R., et al. A light-driven sodium ion pump in marine bacteria. *Nat Commun* 2013;4. Doi: 10.1038/ncomms2689.
272. Wietek J., Wiegert JS., Adeishvili N., et al. Conversion of channelrhodopsin into a light-gated chloride channel. *Science* (80-) 2014;344(6182). Doi:

10.1126/science.1249375.

273. Berndt A., Lee SY., Ramakrishnan C., Deisseroth K. Structure-guided transformation of channelrhodopsin into a light-activated chloride channel. *Science* (80-) 2014;344(6182). Doi: 10.1126/science.1252367.
274. Ravens U., Himmel HM. Drugs preventing Na⁺ and Ca²⁺ overload. *Pharmacol Res* 1999;39(3). Doi: 10.1006/phrs.1998.0416.